Available online at www.sciencedirect.com
SCIENCE DIRECT®
Physics Reports 412 (2005) 1–88
PHYSICS REPORTS
www.elsevier.com/locate/physrep

BCS–BEC crossover: From high temperature superconductors to ultracold superfluids

Qijin Chen[a,1], Jelena Stajic[b,2], Shina Tan[b], K. Levin[b,*]

[a] *Department of Physics and Astronomy, Johns Hopkins University, Baltimore, MD 21218, USA*
[b] *James Franck Institute and Department of Physics, University of Chicago, Chicago, IL 60637, USA*

Accepted 15 February 2005

editor: D.L. Mills

Abstract

We review the BCS to Bose–Einstein condensation (BEC) crossover scenario which is based on the well known crossover generalization of the BCS ground state wavefunction Ψ_0. While this ground state has been summarized extensively in the literature, this Review is devoted to less widely discussed issues: understanding the effects of finite temperature, primarily below T_c, in a manner consistent with Ψ_0. Our emphasis is on the intersection of two important problems: high T_c superconductivity and superfluidity in ultracold fermionic atomic gases. We address the "pseudogap state" in the copper oxide superconductors from the vantage point of a BCS–BEC crossover scenario, although there is no consensus on the applicability of this scheme to high T_c. We argue that it also provides a useful basis for studying atomic gases near the unitary scattering regime; they are most likely in the counterpart pseudogap phase. That is, superconductivity takes place out of a non-Fermi liquid state where preformed, metastable fermion pairs are present at the onset of their Bose condensation. As a microscopic basis for this work, we summarize a variety of T-matrix approaches, and assess their theoretical consistency. A close connection with conventional superconducting fluctuation theories is emphasized and exploited.

PACS: 03.75.−b; 74.20.−z

Keywords: Bose–Einstein condensation; BCS–BEC crossover; Fermionic superfluidity; High T_c superconductivity

* Corresponding author.
E-mail address: levin@uchicago.edu (K. Levin).
[1] Current address: James Franck Institute and Department of Physics, University of Chicago, Chicago, IL 60637, USA.
[2] Current address: Los Alamos National Laboratory, Los Alamos, NM 87545, USA.

0370-1573/$ - see front matter © 2005 Elsevier B.V. All rights reserved.
doi:10.1016/j.physrep.2005.02.005

Contents

1. Introduction to qualitative crossover picture

This review addresses an extended form of the BCS theory of superfluidity (or superconductivity) known as "BCS–Bose–Einstein condensation (BEC) crossover theory". Here we contemplate a generalization of the standard mean field description of superfluids now modified so that one allows attractive interactions of arbitrary strength. In this way one describes how the system smoothly goes from being a superfluid system of the BCS type (where the attraction is arbitrarily weak) to a Bose Einstein condensate of diatomic molecules (where the attraction is arbitrarily strong). One, thereby, sees that BCS theory is intimately connected to BEC. Attractive interactions between fermions are needed to form "bosonic-like" molecules (called Cooper pairs) which then are driven statistically to Bose condense. BCS theory is a special case in which the condensation and pair formation temperatures coincide.

The importance of obtaining a generalization of BCS theory which addresses the crossover from BCS to BEC at general temperatures $T \leqslant T_c$ cannot be overestimated. BCS theory as originally postulated can be viewed as a paradigm among theories of condensed matter systems; it is complete, in many ways generic and model independent, and well verified experimentally. The observation that a BCS-like approach goes beyond strict BCS theory, suggests that there is a larger mean field theory to be addressed. Equally exciting is the possibility that this mean field theory can be discovered and simultaneously tested in a very controlled fashion using ultracold fermionic atoms. We presume here that it may also have applicability to other short coherence length materials, such as the high temperature superconductors.

This Review is written in order to convey important new developments from one subfield of physics to another. Here it is hoped that we will communicate the recent excitement felt by the cold atom community to condensed matter physicists. Conversely we wish to communicate a comparable excitement in studies of high temperature superconductivity to atomic physicists. There has been a revolution in our understanding of ultracold fermions in traps in the last few years. The milestones in this research were the creation of a degenerate Fermi gas (1999), the formation of dimers of fermions (2003), Bose-Einstein condensation (BEC) of these dimers (late 2003) and finally superfluidity of fermionic pairs (2004).

In high temperature superconductors the BCS–BEC crossover picture has been investigated for many years now. It leads to a particular interpretation of a fascinating, but not well understood phase, known as the "pseudogap state". In the cold atom system, this crossover description is not just a scenario, but has been realized in the laboratory. This is because one has the ability (via Feshbach resonances) to apply magnetic fields in a controlled way to tune the strength of the attraction. We note, finally, that research in this field has not been limited exclusively to the two communities. One has seen the application of these crossover ideas to studies of excitons in solids (Lai et al., 2004), to nuclear physics (Baldo et al., 1995; Heiselberg, 2004a) and to particle physics (Itakura, 2003; Klinkhamer and Volovik, 2004; Kolb and Heinz, 2003) as well. There are not many problems in physics which have as great an overlap with different subfield communities as this "BCS–BEC crossover problem".

In this Review, we begin with an introduction to the qualitative picture of the BCS–BEC crossover scenario which is represented schematically in Fig. 1. We discuss this picture in the context of both high

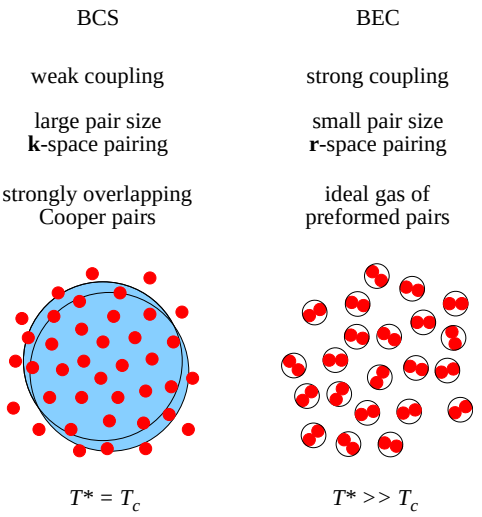

Fig. 1. Contrast between BCS- and BEC-based superfluids. Here T^* represents the temperature at which pairs form, while T_c is that at which they condense.

T_c superconductivity and ultracold atomic superfluidity, summarizing experiments in both. In Section 2, we present a more quantitative study of this crossover primarily at and below the superfluid transition temperature T_c. Section 3 contains a detailed discussion of the superfluid density and gauge invariance issues, in large part to emphasize self consistency checks for different theoretical approaches to crossover. These alternative theories are summarized and compared in Section 4. Sections 5 and 6, respectively, present the physical implications of crossover physics, in one particular rendition, in the context of ultracold fermionic superfluids and high temperature superconductors. Our conclusions are presented in Section 7 and a number of Appendices are included for clarity. A reader interested in only the broad overview may choose to omit Sections 2–4.

Our notational conventions as well as a list of abbreviations used in this Review are listed in Appendix D at the end.

1.1. Fermionic pseudogaps and meta-stable pairs: two sides of the same coin

A number of years ago Eagles (Eagles, 1969) and Leggett (Leggett, 1980) independently noted[1] that the BCS ground state wavefunction

$$\Psi_0 = \Pi_{\mathbf{k}}(u_{\mathbf{k}} + v_{\mathbf{k}} c^{\dagger}_{k,\uparrow} c^{\dagger}_{-k,\downarrow})|0\rangle \tag{1}$$

had a greater applicability than had been appreciated at the time of its original proposal by Bardeen, Cooper and Schrieffer (BCS). As the strength of the attractive pairing interaction U (< 0) between fermions is increased, this wavefunction is also capable of describing a continuous evolution from BCS like behavior to a form of Bose–Einstein condensation. What is essential is that the chemical potential μ of the fermions be self consistently computed as U varies.

[1] Through private correspondence it appears that F. Dyson may have made similar observations even earlier.

The variational parameters $v_{\mathbf{k}}$ and $u_{\mathbf{k}}$ which appear in Eq. (1) are usually represented by the two more directly accessible parameters $\Delta_{\rm sc}(0)$ and μ, which characterize the fermionic system. Here $\Delta_{\rm sc}(0)$ is the zero temperature superconducting order parameter. These fermionic parameters are uniquely determined in terms of U and the fermionic density n. The variationally determined self consistency conditions are given by two BCS-like equations which we refer to as the "gap" and "number" equations respectively.

$$\Delta_{\rm sc}(0) = -U \sum_{\mathbf{k}} \Delta_{\rm sc}(0) \frac{1}{2E_{\mathbf{k}}} , \tag{2}$$

$$n = \sum_{\mathbf{k}} \left[1 - \frac{\varepsilon_{\mathbf{k}} - \mu}{E_{\mathbf{k}}} \right] , \tag{3}$$

where[2]

$$E_{\mathbf{k}} \equiv \sqrt{(\varepsilon_{\mathbf{k}} - \mu)^2 + \Delta_{\rm sc}^2(0)} \tag{4}$$

and $\varepsilon_{\mathbf{k}} = k^2/2m$ is the fermion energy dispersion.[3] Within this ground state there have been extensive studies of collective modes (Cote and Griffin, 1993; Micnas et al., 1990; Randeria, 1995), effects of two dimensionality (Randeria, 1995), and, more recently, extensions to atomic gases (Perali et al., 2003; Viverit et al., 2004). Noziéres and Schmitt-Rink were the first (Nozières and Schmitt-Rink, 1985) to address nonzero T. We will outline some of their conclusions later in this Review. Randeria and co-workers reformulated the approach of Noziéres and Schmitt-Rink (NSR) and moreover, raised the interesting possibility that crossover physics might be relevant to high temperature superconductors (Randeria, 1995). Subsequently other workers have applied this picture to the high T_c cuprates (Chen et al., 1998; Micnas and Robaszkiewicz, 1998; Ranninger and Robin, 1996) and ultracold fermions (Milstein et al., 2002; Ohashi and Griffin, 2002) as well as formulated alternative schemes (Griffin and Ohashi, 2003; Pieri et al., 2004) for addressing $T \neq 0$. Importantly, a number of experimentalists, most notably Uemura (Uemura, 1997), have claimed evidence in support (Deutscher, 1999; Junod et al., 1999; Renner et al., 1998) of the BCS–BEC crossover picture for high T_c materials.

Compared to work on the ground state, considerably less has been written on crossover effects at nonzero temperature based on Eq. (1). Because our understanding has increased substantially since the pioneering work of NSR, and because they are the most interesting, this review is focussed on these finite T effects, at the level of a simple mean field theory. Mean field approaches are always approximate. We can ascribe the simplicity and precision of BCS theory to the fact that in conventional superconductors the coherence length ξ is extremely long. As a result, the kind of averaging procedure implicit in mean field theory becomes nearly exact. Once ξ becomes small, BCS is not expected to work at the same level of precision. Nevertheless even when they are not exact, mean field approaches are excellent ways of building up intuition. And further progress is not likely to be made without investigating first the simplest of mean field approaches, associated with Eq. (1).

---

[2] In general, the order parameter $\Delta_{\rm sc}$ and the excitation gap may have a $\mathbf{k}$-dependence, $\Delta_k = \Delta\varphi_{\mathbf{k}}$, except in the case of a contact potential. To keep the mathematical expressions simpler, however, we neglect $\varphi_{\mathbf{k}}$ for the s-wave pairing under investigation of this Review. It can be easily reinserted back when needed in actual calculations. In particular, we use $\varphi_{\mathbf{k}} = \exp(-k^2/2k_c^2)$ with a large cutoff k_c in most of our numerical calculations.

[3] Throughout this Review, we set $\hbar = 1$ and $k_{\rm B} = 1$.

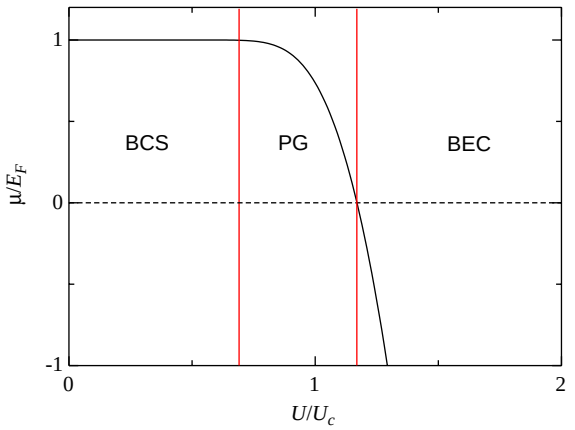

Fig. 2. Typical behavior of the $T = 0$ chemical potential in the three regimes. As the pairing strength increases from 0, the chemical potential μ starts to decrease and then becomes negative. The character of the system changes from fermionic ($\mu > 0$) to bosonic ($\mu < 0$). The PG (pseudogap) case corresponds to nonFermi liquid based superconductivity, and U_c corresponds to critical coupling for forming a two fermion bound state in vacuum, as in Eq. (17) below.

The effects of BEC–BCS crossover are most directly reflected in the behavior of the fermionic chemical potential μ. We plot the behavior of μ in Fig. 2, which indicates the BCS and BEC regimes. In the weak coupling regime $\mu = E_{\mathrm{F}}$ and ordinary BCS theory results. However at sufficiently strong coupling, μ begins to decrease, eventually crossing zero and then ultimately becoming negative in the BEC regime, with increasing $|U|$. We generally view $\mu = 0$ as a crossing point. For positive μ the system has a remnant Fermi surface, and we say that it is "fermionic". For negative μ, the Fermi surface is gone and the material is "bosonic".

The new and largely unexplored physics of this problem lies in the fact that once outside the BCS regime, but before BEC, superconductivity or superfluidity emerge out of a very exotic, non-Fermi liquid normal state. Indeed, it should be clear that Fermi liquid theory must break down somewhere in the intermediate regime, as one goes continuously from fermionic to bosonic statistics. This intermediate case has many names: "resonant superfluidity", the "unitary regime" or, as we prefer (because it is more descriptive of the many body physics) the "pseudogap (PG) regime". The PG regime plotted in Fig. 2 is drawn so that its boundary on the left coincides with the onset of an appreciable excitation gap at T_c, called $\Delta(T_c)$; its boundary on the right coincides with where $\mu = 0$. This non-Fermi liquid based superconductivity has been extensively studied (Chen et al., 1998, 2000; Jankó et al., 1997; Maly et al., 1999a).

Fermi liquid theory is inappropriate here principally because there is a gap for creating fermionic excitations. The non-Fermi liquid like behavior is reflected in that of the fermionic spectral function (Maly et al., 1999a) which has a two-peak structure in the normal state, broadened somewhat, but rather similar to its counterpart in BCS theory. Importantly, the onset of superconductivity occurs in the presence of fermion pairs, which reflect this excitation gap. Unlike their counterparts in the BEC limit, these pairs are not infinitely long lived. Their presence is apparent even in the normal state where an energy must be applied to create fermionic excitations. This energy cost derives from the breaking of the metastable pairs. Thus we say that there is a "pseudogap" at and above T_c. But pseudogap effects are not restricted to this normal state. Pre-formed pairs have a natural counterpart in the superfluid phase, as non-condensed pairs.

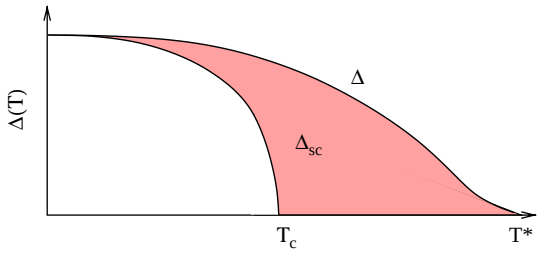

Fig. 3. Contrasting behavior of the excitation gap $\Delta(T)$ and superfluid order parameter $\Delta_{\mathrm{sc}}(T)$ versus temperature. The height of the shaded region roughly reflects the density of noncondensed pairs at each temperature.

It will be stressed throughout this Review that gaps in the fermionic spectrum and bosonic degrees of freedom are two sides of the same coin. A particularly important observation to make is that the starting point for crossover physics is based on the fermionic degrees of freedom. Bosonic degrees of freedom are deduced from these; they are not primary. A nonzero value of the excitation gap Δ is equivalent to the presence of metastable or stable fermion pairs. And it is only in this indirect fashion that we can probe the presence of these "bosons", within the framework of Eq. (1).

In many ways this crossover theory appears to represent a more generic form of superfluidity. Without doing any calculations we can anticipate some of the effects of finite temperature. Except for very weak coupling, *pairs form and condense at different temperatures*. The BCS limit might be viewed as the anomaly. Because the attractive interaction is presumed to be arbitrarily weak, in BCS the normal state is unaffected by U and superfluidity appears precipitously, that is without warning at T_c. More generally, in the presence of a moderately strong attractive interaction it pays energetically to take some advantage and to form pairs (say roughly at temperature T^*) within the normal state. Then, for statistical reasons these bosonic degrees of freedom ultimately are driven to condense at $T_c < T^*$, just as in BEC.

Just as there is a distinction between T_c and T^*, *there must be a distinction between the superconducting order parameter* Δ_{sc} *and the excitation gap* Δ. The presence of a normal state excitation gap or pseudogap for fermions is inextricably connected to this generalized BCS wavefunction. In Fig. 3, we present a schematic plot of these two energy parameters. It may be seen that the order parameter vanishes at T_c, as in a second order phase transition, while the excitation gap turns on smoothly below T^*. It should also be stressed that there is only one gap energy scale in the ground state (Leggett, 1980) of Eq. (1). Thus at zero temperature

$$\Delta_{\mathrm{sc}}(0) = \Delta(0) \ . \tag{5}$$

In addition to the distinction between Δ and Δ_{sc}, another important way in which *bosonic degrees of freedom are revealed is indirectly through the temperature dependence of* Δ. *In the BEC regime where fermion pairs are pre-formed,* Δ *is essentially constant for all* $T \leqslant T_c$ (*as is* μ). By contrast in the BCS regime it exhibits the well known temperature dependence of the superconducting order parameter. This is equivalent to the statement that bosonic degrees of freedom are only present in the condensate for this latter case. This behavior is illustrated in Fig. 4.

Again, without doing any calculations we can make one more inference about the nature of crossover physics at finite T. *The excitations of the system must smoothly evolve from fermionic in the BCS regime to bosonic in the BEC regime*. In the intermediate case, the excitations are a mix of fermions and

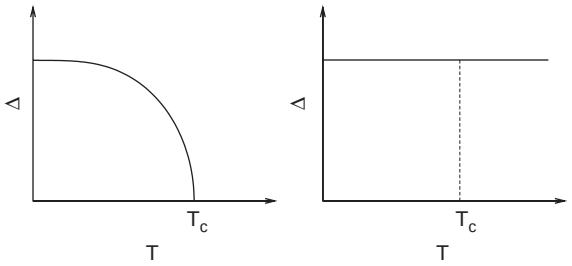

Fig. 4. Comparison of typical temperature dependences of the excitation gaps in the BCS (left) and BEC (right) limits. For the former, the gap is small and vanishes at T_c; whereas for the latter, the gap is very large and essentially temperature independent.

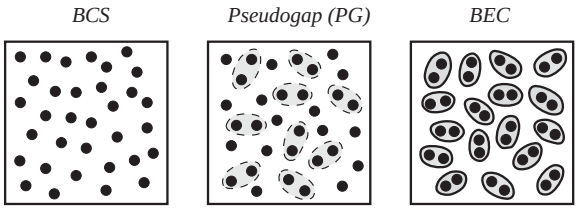

Fig. 5. The character of the excitations in the BCS–BEC crossover both above and below T_c. The excitations are primarily fermionic Bogoliubov quasiparticles in the BCS limit and bosonic pairs (or "Feshbach bosons") in the BEC limit. In the PG case the "virtual molecules" consist primarily of "Cooper" pairs of fermionic atoms.

metastable pairs. Fig. 5 characterizes the excitations out of the condensate as well as in the normal phase. This schematic figure will play an important role in our thinking throughout this review. In the BCS and BEC regimes one is led to an excitation spectrum with a single component. For the PG case it is clear that the excitations now have two distinct (albeit, strongly interacting) components.

1.2. Introduction to high T_c superconductivity: pseudogap effects

This Review deals with the intersection of two fields and two important problems: high temperature superconductors and ultracold fermionic atoms in which, through Feshbach resonance effects, the attractive interaction may be arbitrarily tuned by a magnetic field. Our focus is on the broken symmetry phase and how it evolves from the well known ground state at $T = 0$ to T_c. We begin with a brief overview (Tallon and Loram, 2001; Timusk and Statt, 1999) of pseudogap effects in the hole doped high temperature superconductors. A study of concrete data in these systems provides a rather natural way of building intuition about non-Fermi liquid based superfluidity, and this should, in turn, be useful for the cold atom community.

It has been argued by some (Chen et al., 1999; Micnas and Robaszkiewicz, 1998; Pieri and Strinati, 2000; Ranninger and Robin, 1996; Yanase et al., 2003) that a BCS–BEC crossover-induced pseudogap is the origin of the mysterious normal state gap observed in high temperature superconductors. Although, this is a highly contentious subject, a principal supporting rationale is that this above-T_c excitation gap seems to evolve smoothly into the fermionic gap within the superconducting state. This, in conjunction with a panoply of normal state anomalies which appear to represent precursor superconductivity effects,

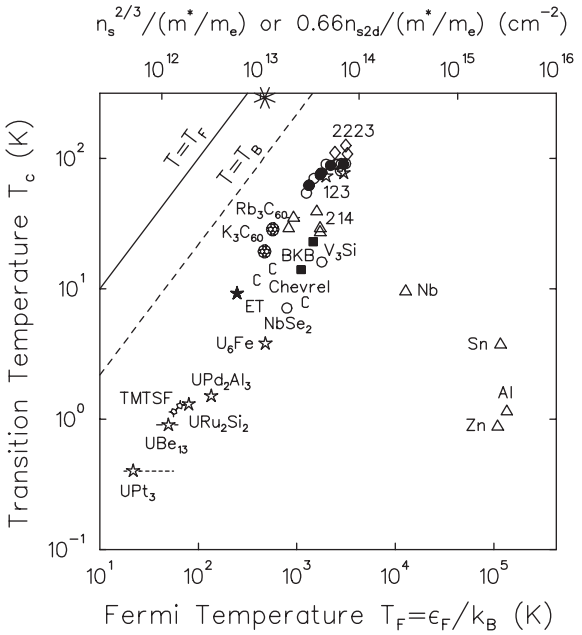

Fig. 6. Uemura plot (Uemura, 1997) of the superconducting transition temperature as a function of Fermi temperature (lower axis) and of the low T superfluid density (upper axis) for various superconductors. The plot indicates how "exotic" superconductors appear to be in a distinct category as compared with more conventional metal superconductors such as Nb, Sn, Al and Zn. Note the logarithmic scales.

suggests that the pseudogap has more in common with the superconducting phase than with the insulating magnetic phase associated with the parent compound.

The arguments in favor of this (albeit, controversial) crossover viewpoint rest on the following observations: (i) the transition temperature is anomalously high and the coherence length ξ for superconductivity anomalously short, around 10 Å as compared more typically with 1000Å. (ii) These systems are quasi-two-dimensional so that one might expect pre-formed pairs or precursor superconductivity effects to be enhanced. (iii) The normal state gap has the same d-wave symmetry as the superconducting order parameter (Campuzano et al., 2004; Damascelli et al., 2003), and (iv) to a good approximation its onset temperature, called T^*, satisfies (Kugler et al., 2001; Oda et al., 1997) $T^* \approx 2\Delta(0)/4.3$ which satisfies the BCS scaling relation. (v) There is widespread evidence for pseudogap effects both above (Tallon and Loram, 2001; Timusk and Statt, 1999) and below (Loram et al., 1994; Stajic et al., 2003b) T_c. Finally, it has also been argued that short coherence length superconductors may quite generally exhibit a distinctive form of superconductivity (Uemura, 1997). Fig. 6 shows a plot of data collected by Uemura which seems to suggest that the traditional BCS superconductors stand apart from other more exotic (and frequently short ξ) forms of superconductivity. From this plot one can infer, that, except for high T_c, there is nothing special about the high T_c superconductors; they are not alone in this distinctive class which includes the organics and heavy fermion superconductors as well. Thus, to understand them, one might want to focus on this simplest aspect (short ξ) of high T_c superconductors, rather than invoke more exotic and less generic features.

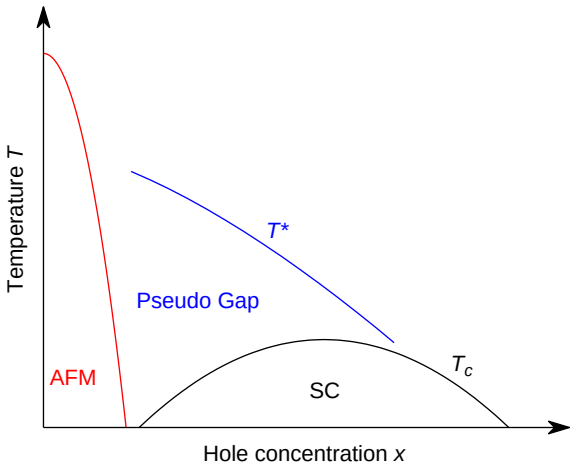

Fig. 7. Typical phase diagram of hole-doped high T_c superconductors. There exists a pseudogap phase above T_c in the underdoped regime. Here SC denotes superconductor, and T^* is the temperature at which the pseudogap smoothly turns on.

In Fig. 7 we show a sketch of the phase diagram for the copper oxide superconductors. Here x represents the concentration of holes which can be controlled by adding Sr substitutionally, say, to $La_{1-x}Sr_xCuO_4$. At zero and small x the system is an antiferromagnetic (AFM) insulator. Precisely at half filling ($x=0$) we understand this insulator to derive from Mott effects. These Mott effects may or may not be the source of the other exotic phases indicated in the diagram, as "SC" for superconductivity and the pseudogap phase. Once AFM order disappears the system remains insulating until a critical concentration (typically around a few percent Sr) when an insulator–superconductor transition is encountered. Here photoemission studies (Campuzano et al., 2004; Damascelli et al., 2003) suggest that once this line is crossed, μ appears to be positive. For $x \leqslant 0.2$, the superconducting phase has a non-Fermi liquid (or pseudogapped) normal state (Tallon and Loram, 2001). We note an important aspect of this phase diagram at low x. As the pseudogap becomes stronger (T^* increases), superconductivity as reflected in the magnitude of T_c becomes weaker. One way to think about this competition is through the effects of the pseudogap on T_c. As this gap increases, the density of fermionic states at E_F decreases, so that there are fewer fermions around to participate in the superconductivity.

Importantly, there is a clear excitation gap present at the onset of superconductivity which is called $\Delta(T_c)$ and which vanishes at $x \approx 0.2$. The magnitude of the pseudogap at T_c is shown in Fig. 8, from (Tallon and Loram, 2001). Quite remarkably, as indicated in the figure, a host of different probes seem to converge on the size of this gap.

Fig. 9 indicates the temperature dependence of the excitation gap for three different hole stoichiometries. These data were taken (Ding et al., 1996) from angle resolved photoemission spectroscopy (ARPES) measurements on single-crystal $Bi_2Sr_2CaCu_2O_{8+\delta}$ (BSCCO) samples. For one sample shown as circles, (corresponding roughly to "optimal" doping) the gap vanishes roughly at T_c as might be expected for a BCS superconductor. At the other extreme are the data indicated by inverted triangles in which an excitation gap appears to be present up to room temperature, with very little temperature dependence. This is what is referred to as a highly underdoped sample (small x), which from the phase diagram can be seen to have a rather low T_c. Moreover, T_c is not evident in these data on underdoped samples. This

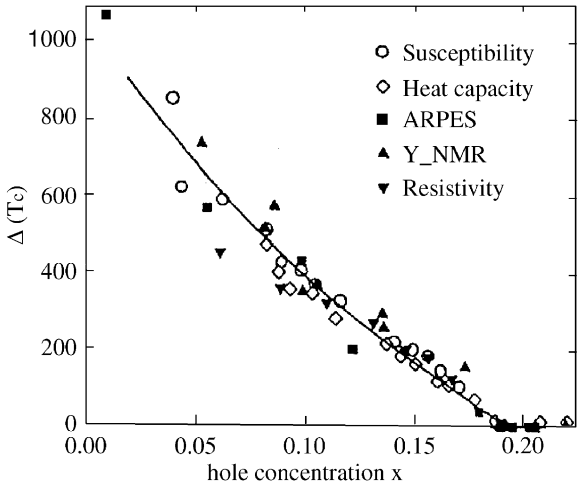

Fig. 8. Pseudogap magnitude at T_c versus doping concentration in hole doped high T_c superconductors measured with different experimental techniques (from Tallon and Loram, 2001). Units on vertical axis are temperature in degrees K.

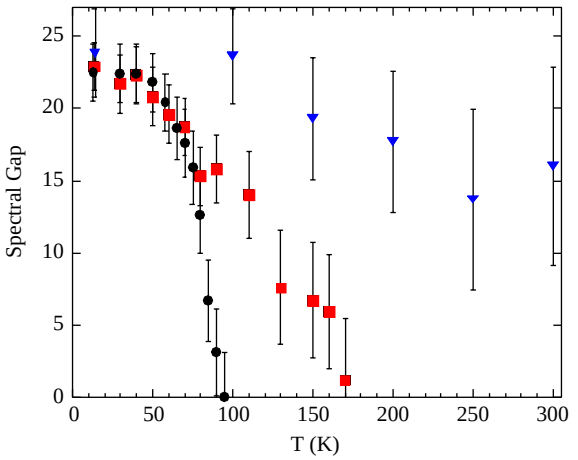

Fig. 9. (Color) Temperature dependence of the excitation gap from ARPES measurements for optimally doped (filled black circles), underdoped (red squares) and highly underdoped (blue inverted triangles) single-crystal BSCCO samples (taken from Ding et al., 1996). There exists a pseudogap phase above T_c in the underdoped regime.

is a very remarkable feature which indicates that from the fermionic perspective there appears to be no profound sensitivity to the onset of superconductivity.

While the high T_c community has focussed on pseudogap effects above T_c, there is a good case to be made that these effects also persist below. Shown in Fig. 10 are STM data (Renner et al., 1998) taken below T_c within a vortex core (solid lines) and between vortices in the bulk (dashed lines). The quantity $\mathrm{d}I/\mathrm{d}V$ may be viewed as a measure of the fermionic density of states at energy E given by the voltage V. This figure shows that there is a clear depletion of the density of states around the Fermi energy

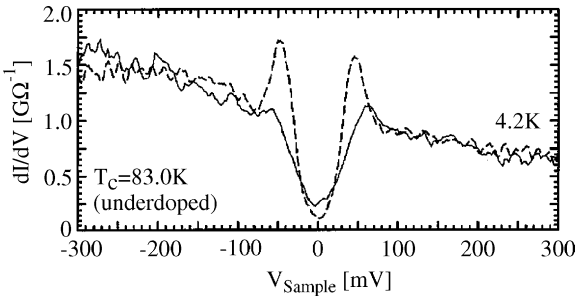

Fig. 10. STM measurements of the $\mathrm{d}I/\mathrm{d}V$ characteristics of an underdoped BSCCO sample inside (solid) and outside (dashed) a vortex core at low T from Renner et al., 1998. $\mathrm{d}I/\mathrm{d}V$ is proportional to the density of states.

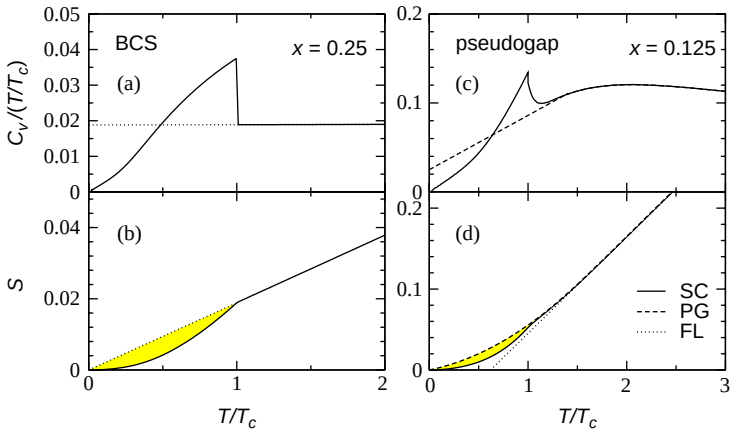

Fig. 11. Behavior of entropy S and specific heat coefficient $\gamma \equiv C_v/T$ as a function of temperature for (a)–(b) BCS and (c)–(d) pseudogapped superconductors. Dotted and dashed lines are extrapolated normal states below T_c. The shaded areas were used to determine the condensation energy.

($V = 0$) in the normal phase within the core. Indeed the size of the inferred energy gap (or pseudogap) corresponds to the energy separation between the two maxima in $\mathrm{d}I/\mathrm{d}V$; this can be seen to be the same for both the normal and superconducting regions (solid and dashed curves). This figure emphasizes the fact that the existence of an energy gap has little or nothing to do with the existence of phase coherent superconductivity. It also suggests that pseudogap effects effectively persist below T_c; the normal phase underlying superconductivity for $T \leqslant T_c$ is not a Fermi liquid.

Analysis of thermodynamical data (Loram et al., 1994; Tallon and Loram, 2001) has led to a similar inference. Fig. 11 presents a schematic plot of the entropy S and specific heat for the case of a BCS superconductor, as contrasted with a pseudogapped superconductor. Actual data are presented in Fig. 38. Fig. 11 makes it clear that in a BCS superconductor, the normal state which underlies the superconducting phase, *is* a Fermi liquid; the entropy at high temperatures extrapolates into a physically meaningful entropy below T_c. For the PG case, the Fermi liquid-extrapolated entropy becomes negative. In this way Loram et al. (1994) deduced that the normal phase underlying the superconducting state is not a Fermi liquid. Rather, they claimed to obtain proper thermodynamics, it must be assumed that this state contains

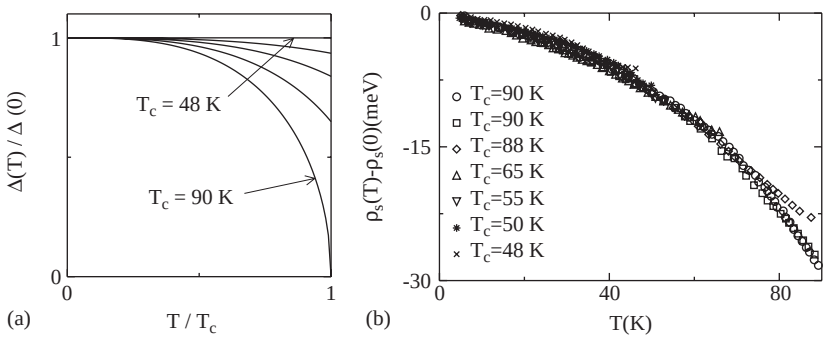

Fig. 12. Temperature dependence of (a) the fermionic excitation gap Δ and (b) superfluid density ρ_s from experiment for various doping concentrations (from (Stajic et al., 2003b)). (a) Shows a schematic plot of Δ as seen in the ARPES and STM tunneling data. When $\Delta(T_c) \neq 0$, there is little correlation between $\Delta(T)$ and $\rho_s(T)$; this figure suggests that something other than fermionic quasiparticles (e.g., bosonic excitations) may be responsible for the disappearance of superconductivity with increasing T. (b) Shows a quasi-universal behavior for the slope $\mathrm{d}\rho_s/\mathrm{d}T$ at different doping concentrations, despite the highly nonuniversal behavior for $\Delta(T)$.

a persistent pseudogap. They argued for a distinction between the excitation gap Δ and the superconducting order parameter, within the superconducting phase. To fit their data they presumed a modified fermionic dispersion

$$E_{\mathbf{k}} = \sqrt{(\varepsilon_{\mathbf{k}} - \mu)^2 + \Delta^2(T)}\ , \tag{6}$$

where

$$\Delta^2(T) = \Delta_{\mathrm{sc}}^2(T) + \Delta_{pg}^2\ . \tag{7}$$

Here Δ_{pg} is taken on phenomenological grounds to be T-independent. The authors argue that the pseudogap contribution may arise from physics unrelated to the superconductivity. While others (Chakravarty et al., 2001; Nozieres and Pistolesi, 1999) have similarly postulated that Δ_{pg} may in fact derive from another (hidden) order parameter or underlying band structure effect, in general the fermionic dispersion relation $E_{\mathbf{k}}$ will take on a different character from that assumed above, which is very specific to a superconducting origin for the pseudogap.

Finally, Fig. 12 makes the claim for a persistent pseudogap below T_c in an even more suggestive way. Fig. 12(a) represents a schematic plot of excitation gap data such as are shown in Fig. 9. Here the focus is on temperatures below T_c. Most importantly, this figure indicates that the T dependence in Δ varies dramatically as the stoichiometry changes. Thus, in the extreme underdoped regime, where PG effects are most intense, there is very little T dependence in Δ below T_c. By contrast at high x, when PG effects are less important, the behavior of Δ follows that of BCS theory. What is most impressive however, is that these wide variations in $\Delta(T)$ are *not* reflected in the superfluid density $\rho_s(T)$, which is proportional to the inverse square of the London magnetic penetration depth and can be measured by, for example, muon spin relaxation (μSR) experiments. Necessarily, $\rho_s(T)$ vanishes at T_c. What is plotted (Stajic et al., 2003b) in Fig. 12(b) is $\rho_s(T) - \rho_s(0)$ versus T. That these data all seem to sit on a rather universal curve is a key point. The envelope curve in $\rho_s(T) - \rho_s(0)$ is associated with an "optimal" sample where $\Delta(T)$ essentially follows the BCS prediction. Fig. 12 then indicates that, *despite the highly nonuniversal*

behavior for $\Delta(T)$, the superfluid density does not make large excursions from its BCS- predicted form. This is difficult to understand if the fermionic degrees of freedom through $\Delta(T)$ are dominating at all x. Rather this figure suggests that something other than fermionic excitations is responsible for the disappearance of superconductivity, particularly in the regime where $\Delta(T)$ is relatively constant in T. At the very least pseudogap effects must persist below T_c.

Driving the superconductivity away is another important way to probe the pseudogap. This occurs naturally with temperatures in excess of T_c, but it also occurs when sufficient pair breaking is present through impurities (Tallon et al., 1997; Tallon and Loram, 2001; Zhao et al., 1993) or applied magnetic fields (Ando et al., 1995). An important effect of temperature needs to be stressed. With increasing $T > T_c$, the *d*-wave shape of the excitation gap is rapidly washed out (Campuzano et al., 2004; Damascelli et al., 2003); the nodes of the order parameter, in effect, begin to spread out, just above T_c. The inverse of this effect should also be emphasized: when approached from above, *T_c is marked by the abrupt onset of long lived quasiparticles*.

One frequently, and possibly universally, sees a superconductor–insulator (SI) transition when T_c is driven to zero in the presence of a pseudogap. This suggests a simple scenario: that *the pseudogap may survive when superconductivity is suppressed*. In this way the ground state is no longer a simple metal. This SI transition is seen upon Zn doping (Tallon et al., 1997; Tallon and Loram, 2001; Zhao et al., 1993), as well as in the presence of applied magnetic fields (Ando et al., 1995). Moreover, the intrinsic change in stoichiometry illustrated in the phase diagram of Fig. 7 also leads to an SI transition. One can thus deduce that the effects of pair-breaking on T_c and T^* are very different, with the former being far more sensitive than the latter.

It is clear that pseudogapped fermions are in evidence in a multiplicity of experiments. Are there indications of bosonic degrees of freedom in the normal state of high T_c superconductors? The answer is unequivocally yes: *meta-stable bosons are observable as superconducting fluctuations*. These bosons are intimately connected to the pseudogap; in effect they are the other side of the same coin. These bosonic effects are enhanced in the presence of the quasi-two dimensional lattice structure of these materials. Very detailed analyses (Larkin and Varlamov, 2001) of thermodynamic and transport properties of the highest T_c or "optimal" samples reveal clearly these pre-formed pairs. Moreover they are responsible (Kwon and Dorsey, 1999) for divergences at T_c in the dc conductivity σ and in the transverse thermoelectric (Ussishkin et al., 2002) response α_{xy}. These transport coefficients are defined more generally in terms of the electrical and heat currents by

$$\mathbf{J}^{\mathbf{elec}} = \sigma\mathbf{E} + \alpha(-\nabla T) \ , \tag{8}$$

$$\mathbf{J}^{\mathbf{heat}} = \tilde{\alpha}\mathbf{E} + \kappa(-\nabla T) \ . \tag{9}$$

Here σ is the conductivity tensor, κ the thermal conductivity tensor, and α, $\tilde{\alpha}$ are thermoelectric tensors. Other coefficients, while not divergent, exhibit precursor effects, all of which are found to be in good agreement (Larkin and Varlamov, 2001) with fluctuation theory. As pseudogap effects become more pronounced with underdoping much of the fluctuation behavior appears to set in at a higher temperature scale associated with T^*, but often some fraction thereof (Tan and Levin, 2004; Xu et al., 2000).

Figs. 13 and 14 make the important point that precursor effects in the transverse thermoelectric response (α_{xy}) and conductivity σ appear at higher temperatures ($\propto T^*$) as pseudogap effects become progressively more important; the dotted lines which have the strongest pseudogap continue to the highest temperatures in both the figures. Moreover, both transport coefficients evolve smoothly from a regime where they are

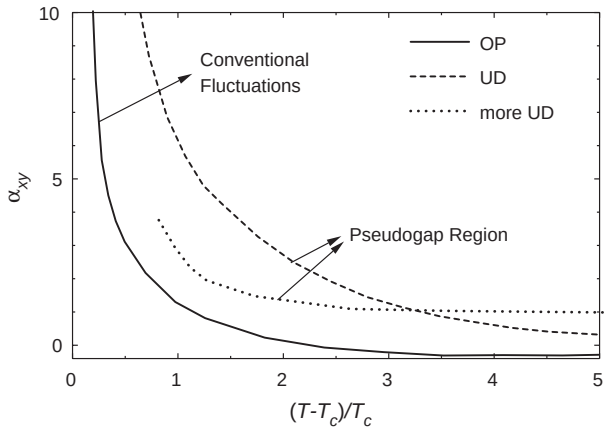

Fig. 13. Transverse thermoelectric response (which relates to the Nernst coefficient) plotted here in fluctuation regime above T_c. Here OP and UD correspond to optimal and underdoping, respectively. Data were taken from Xu et al. (2000).

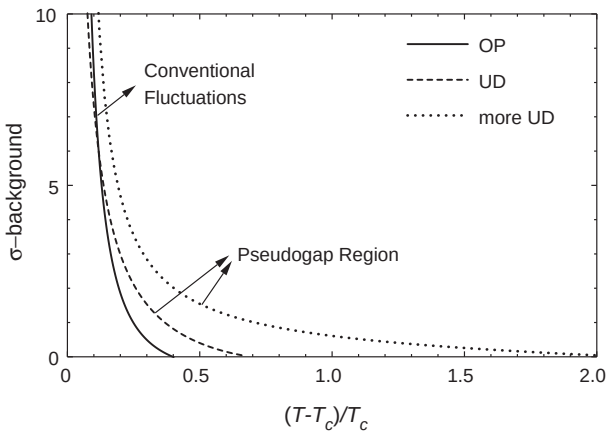

Fig. 14. Conductivity in fluctuation regime for optimally (OP) and underdoped (UD) cuprate superconductors. Data from Watanabe et al. (1997).

presumed to be described by conventional fluctuations (Larkin and Varlamov, 2001; Ussishkin et al., 2002) as shown by the solid lines in the figures into a regime where their behavior is associated with a pseudogap. A number of people have argued (Corson et al., 1999; Xu et al., 2000) that normal state vortices are responsible for the so called anomalous transport behavior of the pseudogap regime. We will argue in this Review that these figures may alternatively be interpreted as suggesting that bosonic degrees of freedom, not vortices, are responsible for these anomalous transport effects.

1.3. Introduction to high T_c superconductivity: Mott physics and possible ordered states

Most workers in the field of high T_c superconductivity would agree that we have made enormous progress in characterizing these materials and in identifying key theoretical questions and constructs.

Experimental progress, in large part, comes from transport studies (Tallon and Loram, 2001; Timusk and Statt, 1999) in addition to three powerful spectroscopies: photoemission (Campuzano et al., 2004; Damascelli et al., 2003), neutron (Aeppli et al., 1997a, b; Cheong et al., 1991; Fong et al., 1995; Kastner et al., 1998; Mook et al., 1998; Rossat-Mignod et al., 1991; Tranquada et al., 1992) and Josephson interferometry (Wollman et al., 1995; Tsuei et al., 1994; Mathai et al., 1995). These data have provided us with important clues to address related theoretical challenges. Among the outstanding theoretical issues in the cuprates are (i) understanding the attractive "mechanism" that binds electrons into Cooper pairs, (ii) understanding the evolution of the normal phase from Fermi liquid (in the "overdoped" regime) to marginal Fermi liquid (at "optimal" doping) to the pseudogap state, which is presumed to occur as doping concentration x decreases, and (iii) understanding the nature of that superconducting phase which evolves from each of these three normal states.

The theoretical community has concentrated rather extensively on special regions and x-dependences in the phase diagram which are presumed to be controlled by "Mott physics". There are different viewpoints on precisely what constitutes Mott physics in the metallic phases, and, for example, whether or not this is necessarily associated with spin-charge separation. For the most part, one presumes here that the insulating phase of the parent compound introduces strong Coulomb correlations into the doped metallic states which may or may not also be associated with strong antiferromagnetic correlations. There is a recent, rather complete review (Lee et al., 2004) of Mott physics within the scenario of spin-charge separation, which clarifies the physics it entails.

Concrete experimental signatures of Mott physics are the observations that the superfluid density $\rho_s(T = 0, x) \to 0$ as $x \to 0$, as if it were reflecting an order parameter for a metal insulator transition. More precisely it is deduced that $\rho_s(0, x) \propto x$, at low x. Unusual effects associated with this linear- in- x dependence also show up in other experiments, such as the weight of coherence features in photoemission data (Campuzano et al., 2004; Damascelli et al., 2003), as well as in thermodynamical signatures (Tallon and Loram, 2001).

While there is no single line of reasoning associated with these Mott constraints, the low value of the superfluid density has been argued (Emery and Kivelson, 1995) to be responsible for soft phase fluctuations of the order parameter, which may be an important contributor to the pseudogap. However, recent concerns about this "phase fluctuation scenario" for the origin of the pseudogap have been raised (Lee, 2004). It is now presumed by a number of groups that phase fluctuations alone may not be adequate and an additional static or fluctuating order of one form or another needs to be incorporated. Related to a competing or co-existing order are conjectures (Chakravarty et al., 2001) that the disappearance of pseudogap effects around $x \approx 0.2$ is an indication of a "quantum critical point" associated with a hidden order parameter which may be responsible for the pseudogap. Others have associated small (Vojta et al., 2000) x or alternatively optimal (Varma, 1999) x with quantum critical points of a different origin. The nature of the other competing or fluctuating order has been conjectured to be RVB (Anderson et al., 2004), "d-density wave" (Chakravarty et al., 2001), stripes (Castellani et al., 1995; Zachar et al., 1997) or possibly antiferromagnetic spin fluctuations (Chubukov et al., 1996; Demler and Zhang, 1995; Pines, 1997). The latter is another residue of the insulating phase.

What is known about the "pairing mechanism"? Some would argue that this is an ill-defined question, and that superconductivity has to be understood through condensation energy arguments based for example on the data generated from the extrapolated normal state entropy (Loram et al., 1994; Tallon and Loram, 2001) discussed above in the context of Fig. 11. These condensation arguments are often built around the nontrivial assumption that there is a thermodynamically well behaved but meta-stable normal

phase which coexists with the superconductivity. Others would argue that Coulomb effects are responsible for *d*-wave pairing, either directly (Leggett, 1999; Liu and Levin, 1997), or indirectly via magnetic fluctuations (Pines, 1997; Scalapino et al., 1986). Moreover, the extent to which the magnetism is presumed to persist into the metallic phase near optimal doping is controversial. Initially, NMR measurements were interpreted as suggesting (Millis et al., 1990) strong antiferromagnetic fluctuations, while neutron measurements, which are generally viewed as the more conclusive, do not provide compelling evidence (Si et al., 1993) for their presence in the normal phase. Nevertheless, there are interesting neutron-measured magnetic signatures (Kao et al., 2000; Liu et al., 1995; Zha et al., 1993) below T_c associated with *d*-wave superconductivity. There are also analogous STM effects which are currently of interest (Wang and Lee, 2003).

1.4. Overview of the BCS–BEC picture of high T_c superconductors in the underdoped regime

We summarize here the physical picture associated with the more controversial BCS–BEC crossover approach to high T_c superconductors, based on the standard ground state of Eq. (1). One presumes that the normal state (pseudo)gap arises from pre-formed pairs. This gap $\Delta(T)$ is thus present at the onset of superconductivity, and reflects the fact that Cooper pairs form before they Bose condense, as a result of sufficiently strong attraction. Below T_c, Δ evolves smoothly into the excitation gap of the superconducting phase.

This behavior reflects the fact that T_c corresponds to the condensation of the $q = 0$ pairs, while finite momentum pairs persist into the ordered phase as excitations of the condensate. As the temperature is progressively lowered below T_c, there are fewer and fewer such bosonic excitations. Their number vanishes precisely at $T = 0$, at which point the system reaches the ground state of Eq. (1). Here the superconducting order parameter and the excitation gap become precisely equal. This approach is based on a mean field scheme and is thus not equivalent to treating phase fluctuations of the order parameter. In general, below T_c, the superconducting order parameter $\Delta_{\rm sc}$ and the pseudogap contributions add in quadrature in the dispersion of Eq. (6) as

$$\Delta^2(T) = \Delta_{\rm sc}^2(T) + \Delta_{pg}^2(T) \ , \tag{10}$$

where $\Delta_{pg} \to 0$ as $T \to 0$; this behavior should be contrasted with that in Eq. (7).

Transport and thermodynamics in the normal and superconducting phases are determined by two types of quasiparticles: fermionic excitations which exhibit a gap $\Delta(T)$, and noncondensed pairs or bosonic excitations. Contributions from the former are rather similar to their (low T) counterparts in BCS theory, except that they are present well above T_c as well, with substantially larger Δ than in strict BCS theory. In this way, experiments which probe the opening of an excitation gap (such as Pauli susceptibility in the spin channel, and resistivity in the charge channel) will exhibit precursor effects, that is, the gradual onset of superconductivity from around T^* to below T_c.

The contributions to transport and thermodynamics of the bosonic excitations are rather similar to those deduced from the time dependent Ginsburg–Landau theory of superconducting fluctuations, provided that one properly extends this theory, in a quantum fashion, away from the critical regime. It is these contributions which often exhibit divergences at T_c, but unlike conventional superconductors, bosonic contributions (pre-formed pairs) are present, up to high temperatures of the order of $T^*/2$, providing the boson density is sufficiently high. Again, these bosons do not represent fluctuations of the order parameter, but they obey a generically similar dynamical equation of motion, and, in the more general case which

goes beyond Eq. (1), they will be coupled to order parameter fluctuations. Here, in an oversimplified sense there is a form of spin-charge separation. The bosons are spin-less (singlet) with charge $2e$, while the fermions carry both spin and charge, but are non-Fermi-liquid like, as a consequence of their energy gap.

In the years following the discovery of high T_c superconductors, attention focused on the so-called marginal Fermi liquid behavior of the cuprates. This phase is associated with near-optimal doping. The most salient signature of this marginality is the dramatically linear in temperature dependence of the resistivity from just above T_c to very high temperatures, well above room temperature. Today, we know that pseudogap effects are present at optimal doping, so that the precise boundary between the marginal and pseudogap phases is not clear. As a consequence, addressing this normal state resistivity in the BCS–BEC crossover approach has not been done in detail, although it is unlikely to yield a strictly linear T dependence at a particular doping. Nevertheless, the bosonic contributions lead to a *decrease* in resistivity as temperature is lowered, while the opening of a d-wave gap associated with the fermionic terms leads to an *increase*, which tends to compensate. These are somewhat analogous to Aslamazov–Larkin and Maki–Thompson fluctuation contributions (Larkin and Varlamov, 2001). The bosons generally dominate in the vicinity of T_c, but at higher T, in the vicinity of T^*, the gapped fermions will be the more important.

The vanishing of T_c with sufficiently large T^* (extreme underdoping) occurs in an interesting way in this crossover theory. This effect is associated with the localization of the bosonic degrees of freedom. Pauli principle effects in conjunction with the extended size of d-wave pairs inhibit pair hopping, and thus destroy superconductivity. One can speculate that, just as in conventional Bose systems, once the bosons are localized, they will exhibit an alternative form of long range order. Indeed, "pair density wave" models have been invoked (Chen et al., 2004) to explain recent STM data (Fu et al., 2004; Vershinin et al., 2004). In contrast to the cold atom systems, for the d-wave case the BEC regime is never accessed. This superconductor-insulator transition takes place in the fermionic regime where $\mu \approx 0.8E_F$.

In the context of BCS–BEC crossover physics, it is not essential to establish the source of the attractive interaction. For the most part we skirt this issue in this Review by taking the pairing onset temperature $T^*(x)$ as a phenomenological input parameter. At the simplest level one may argue that as the system approaches the Mott insulating limit ($x \to 0$) fermions become less mobile; this serves to increase the effectiveness of the attractive interaction at low doping levels.

The variable x in the high T_c problem should be viewed then, as a counterpart to the magnetic field variable in the cold atom problem which tunes the system through a Feshbach resonance; both x and field strength modulate the size of the attraction. However, for the cuprates, in contrast to the cold atom systems, one never reaches the BEC limit of the crossover theory.

It is reasonable to presume based on the evidence to date, that pairing ultimately derives from Coulombic effects, not phonons, which are associated with $l=0$ pairing. While the widely used Hubbard model ignores these effects, longer ranged screened Coulomb interactions have been found (Liu and Levin, 1997) to be attractive for electrons in a d-wave channel. In this context, it is useful to note that, similarly, in He^3 short range repulsion destroys s-wave pairing, but leads to attraction in a higher ($l = 1$) channel (Anderson and Brinkman, 1973). There is, however, no indication of pseudogap phenomena in He^3, so that an Eliashberg extended form of BCS theory appears to be adequate. Eliashberg theory is a very different form of "strong coupling" theory from crossover physics, which treats in detail the dynamics of the mediating boson. Interestingly, there is an upper bound to T_c in both schemes. For Eliashberg theory this arises from the induced effective mass corrections (Levin and Valls, 1983), whereas in the crossover problem this occurs because of the presence of a pseudogap at T_c.

Other analogies have also been invoked in comparing the cuprates with superfluid He^3, based on the propensity towards magnetism. In the case of the quantum liquid, however, there is a positive correlation between short range magnetic ordering (Levin and Valls, 1983) and superconductivity while the correlation appears negative for the cuprates (and some of their heavy fermion "cousins") where magnetism and superconductivity appear to compete.

1.4.1. Searching for the definitive high T_c theory

In no sense should one argue that the BCS–BEC crossover approach precludes consideration of Mott physics. Nor should it be viewed as superior. Indeed, many of the experiments we will address in this Review have alternatively been addressed within the Mott scenario. Presumably both components are important in any ultimate theory. We have chosen in this Review to focus on one component only, and it is hoped that a comparably detailed review of Mott physics will be forthcoming. In this way one could compare the strengths and weaknesses of both schemes. A summary (Carlson et al., 2002) of some aspects of the Mott picture with emphasis on one dimensional stripe states should be referred to as a very useful starting point. Also available now is a new Review (Lee et al., 2004) of Mott physics, based on spin charge separation.

Besides those discussed in this Review, there is a litany of other experiments which are viewed as requiring explanation in order for a high T_c theory to be taken seriously. Among these are the important linear resistivity in the normal state (at optimal doping) and unusual temperature and x dependences in Hall data. While there has been little insight offered from the crossover scheme to explain the former, aspects of the latter have been successfully addressed within pre-formed pair scenarios (Geshkenbein et al., 1997). Using fermiology based schemes the major features of photoemission (Norman and Pepin, 2003) and of neutron scattering and NMR data were studied theoretically and rather early on (Kao et al., 2000; Si et al., 1993; Zha et al., 1993), along with a focus on the now famous 41 meV feature (Liu et al., 1995). These and other related approaches to the magnetic data, make use of a microscopically derived (Si et al., 1992) random phase approximation scheme which incorporates the details of the Fermi surface shape and d-wave gap. Among remaining experiments in this litany is the origin of incoherent transport along the c-axis (Rojo and Levin, 1993).

On the basis of the above cited literature which addressed magnetic and c-axis[4] data we are led to conclude that pseudogap effects and related crossover physics are not central to their understanding. The presence of a normal state gap will lead to some degree of precursor behavior above T_c, but d-wave nesting related effects such as reflected in neutron data (Kao et al., 2000; Liu et al., 1995; Zha et al., 1993) will be greatly weakened above T_c by the blurring out of the d-wave gap nodes (Campuzano et al., 2004; Damascelli et al., 2003). It should be said, however, that c-axis optical data do appear to reflect pseudogap effects (Ioffe and Millis, 1999) above T_c. (The ab-plane counterparts are discussed in Section 6.3). In summary, we are far from the definitive high T_c theory and the field has much to gain by establishing a collaboration with the cold atom community where BCS–BEC crossover as well as Mott physics (Hofstetter et al., 2002) can be further elucidated and explored.

[4] Here the ab-plane refers to the crystal plane in parallel with the layers of the cuprate compounds, and the c-axis refers to the axis normal to the layers.

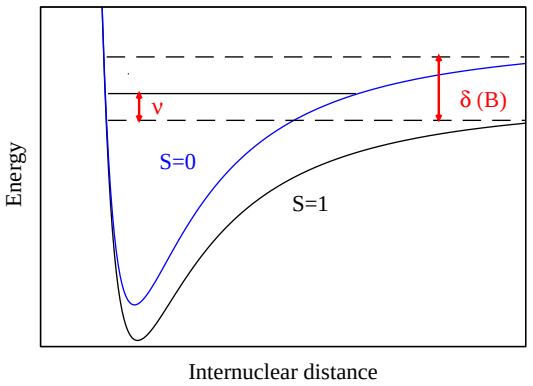

Fig. 15. A schematic representation of the Feshbach resonance for ^{6}Li. The effective interaction between the scattering of atoms in the triplet state is greatly enhanced, when the energy level of the singlet bound state approaches the continuum of the $S = 1$ channel.

1.5. Many body Hamiltonian and two body scattering theory: mostly cold atoms

The existence of Feshbach resonances in a gas of ultracold fermionic atoms allows the attractive interaction between atoms to be tuned arbitrarily, via application of a magnetic field. Fig. 15 presents a characteristic plot of the two body interaction potentials which are responsible for this resonance. These interaction potentials represent an effective description of all Coulomb interactions between the electrons and nuclei. For definiteness, we consider the case of ^{6}Li here. In the region of magnetic fields near the "wide" Feshbach resonance, ≈ 837 G, we may focus on the two lowest atomic levels characterized by states $|F, m_F\rangle$, where the two quantum numbers correspond to the total spin and its z component. We specify the two $|1\rangle \equiv |\frac{1}{2}, \frac{1}{2}\rangle$ and $|2\rangle \equiv |\frac{1}{2}, -\frac{1}{2}\rangle$. In place of these quantum numbers one can alternatively characterize the two states in terms of the projections of the electronic (m_s) and nuclear (m_i) spins along the magnetic field. In this way the states 1 and 2 have $m_s = -\frac{1}{2}$ and $m_i = 1$ and 0, respectively.

The curve in Fig. 15 labelled $S = 1$ represents the (attractive) interaction between these two states. This corresponds to the so-called "open" channel and is associated with a triplet (electronic) spin state. A Feshbach resonance requires that there be an otherwise unspecified near-by state which we refer to as in the "closed" channel. The potential which gives rise to this singlet (electronic) spin state is shown by the $S = 0$ curve in Fig. 15. A Feshbach resonance arises when this bound state lies near the zero of energy corresponding to the continuum of scattering states in the triplet or open channel. The electronic Zeeman coupling to the triplet state makes is possible to shift the relative position of the two potentials by application of a magnetic field. This shift is indicated by δ in Fig. 15. In this way, the resonance is magnetically tunable and the scattering length of the system will vary continuously with field, diverging at that magnetic field which corresponds to the Feshbach resonance. We represent the deviation of this field from the resonance condition by the "detuning parameter" ν. When ν is large and positive, the singlet state is substantially raised relative to the triplet—and it plays relatively little role. By contrast when the magnitude of ν is large, but with negative sign, then the physics is dominated by the singlet or closed channel.

The most general form for the Hamiltonian contains two types of particles: fermions which represent the open channel and "molecular bosons" which represent the two fermion bound state of the closed channel. We will also refer to the latter as "Feshbach bosons". These, in turn, lead to two types of interaction effects: those associated with the direct attraction between fermions, parameterized by U, and those associated with "fermion–boson" interactions, whose strength is governed by g. The latter may be viewed as deriving from hyperfine interactions which couple the (total) nuclear and electronic spins. In the high T_c applications, one generally, but not always, ignores the bosonic degrees of freedom. Otherwise the Hamiltonians are the same, and can be written as

$$\begin{aligned} H - \mu N = & \sum_{\mathbf{k},\sigma} (\varepsilon_{\mathbf{k}} - \mu) a^{\dagger}_{\mathbf{k},\sigma} a_{\mathbf{k},\sigma} + \sum_{\mathbf{q}} (\varepsilon^{mb}_{\mathbf{q}} + v - 2\mu) b^{\dagger}_{\mathbf{q}} b_{\mathbf{q}} \\ & + \sum_{\mathbf{q},\mathbf{k},\mathbf{k}'} U(\mathbf{k},\mathbf{k}') a^{\dagger}_{\mathbf{q}/2+\mathbf{k},\uparrow} a^{\dagger}_{\mathbf{q}/2-\mathbf{k},\downarrow} a_{\mathbf{q}/2-\mathbf{k}',\downarrow} a_{\mathbf{q}/2+\mathbf{k}',\uparrow} \\ & + \sum_{\mathbf{q},\mathbf{k}} (g(\mathbf{k}) b^{\dagger}_{\mathbf{q}} a_{\mathbf{q}/2-\mathbf{k},\downarrow} a_{\mathbf{q}/2+\mathbf{k},\uparrow} + h.c.) \ . \end{aligned} \tag{11}$$

Here the fermion and boson kinetic energies are given by $\varepsilon_{\mathbf{k}} = k^2/(2m)$, and $\varepsilon^{mb}_{\mathbf{q}} = q^2/(2M)$, and v is an important parameter which represents the magnetic field "detuning". $M = 2m$ is the bare mass of the Feshbach bosons. For the cold atom problem $\sigma = \uparrow, \downarrow$ represents the two different hyperfine states ($|1\rangle$ and $|2\rangle$). One may ignore (Timmermans et al., 2001) the nondegeneracy of these two states, since there is no known way for state 2 to decay into state 1. In the two channel problem the ground state wavefunction is slightly modified and given by

$$\bar{\Psi}_0 = \Psi_0 \otimes \Psi^{\mathrm{B}}_0 \ , \tag{12}$$

where the normalized molecular boson contribution Ψ^{B}_0 is

$$\Psi^{\mathrm{B}}_0 = \mathrm{e}^{-\lambda^2/2 + \lambda b^{\dagger}_0} |0\rangle \ . \tag{13}$$

as discussed originally by Kostyrko and Ranninger, 1996. Here λ is a variational parameter. We present the resulting variational conditions for the ground state in Appendix A.

Whether both forms of interactions are needed in either the high T_c or cold atom systems is still under debate. The bosons ($b^{\dagger}_{\mathbf{k}}$) of the cold atom problem (Holland et al., 2001; Timmermans et al., 2001) will be referred to as Feshbach bosons. These represent a separate species, not to be confused with the fermion pair ($a^{\dagger}_{\mathbf{k}} a^{\dagger}_{-\mathbf{k}}$) operators. Thus we call this a "two channel" model. In this review we will discuss the behavior of crossover physics both with and without these Feshbach bosons (FB). Previous studies of high T_c superconductors have invoked a similar bosonic term (Geshkenbein et al., 1997; Micnas et al., 1990; Ranninger and Robin, 1996) as well, although less is known about its microscopic origin. This fermion–boson coupling is not to be confused with the coupling between fermions and a "pairing-mechanism"-related boson ($[b + b^{\dagger}]a^{\dagger}a$) such as phonons. The coupling $b^{\dagger}aa$ and its conjugate represents a form of sink and source for creating fermion pairs, inducing superconductivity in some ways, as a by-product of Bose condensation. We will emphasize throughout that crossover theory proceeds in a similar fashion with and without Feshbach bosons.

It is useful at this stage to introduce the s-wave scattering length, a_s, defined by the low energy limit of two body scattering in vacuum. This scattering length can, in principle, be deduced from Fig. 15. It

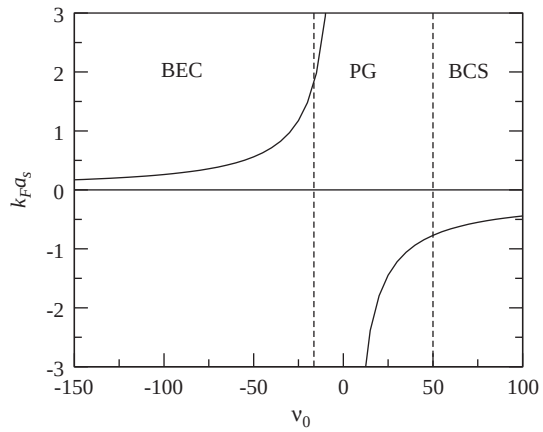

Fig. 16. Characteristic behavior of the scattering length a_s in the three regimes. a_s diverges when $\nu_0 = 2\mu$. Here, and in subsequent figures ν_0 is always in units of E_F and we estimate for the magnetic field detuning, $1\,\mathrm{G} \approx 60 E_F$ for a typical $E_F = 2\,\mu$K, for either ^{6}Li or ^{40}K.

follows that a_s is negative when there is no bound state, it tends to $-\infty$ at the onset of the bound state and to $+\infty$ just as the bound state stabilizes. It remains positive but decreases in value as the interaction becomes increasingly strong. The magnitude of a_s is arbitrarily small in both the extreme BEC and BCS limits, but with opposite sign (see Fig. 16). *The fundamental postulate of crossover theory is that even though the two-body scattering length changes abruptly at the unitary scattering condition* ($|a_s| = \infty$), *in the N-body problem the superconductivity varies smoothly through this point*. Throughout this Review, we presume an equivalence between the "pseudogap" and unitary scattering regimes.

An important goal is to understand how to incorporate all the constraints of the two body physics into the superfluid gap equation. As a by-product, one avoids implicit divergences which would also appear in the problem. To begin we ignore Feshbach effects. The way in which the two body interaction U enters to characterize the scattering (in vacuum) is different from the way in which it enters to characterize the N-body processes leading to superfluidity. In each case, however, one uses a T-matrix formulation to sum an appropriately selected but infinite series of terms in U. For the two-body problem in vacuum, we introduce the scattering length, a_s,

$$\frac{m}{4\pi a_s} \equiv \frac{1}{U_0}\,, \tag{14}$$

which is related to U via the Lippmann–Schwinger equation

$$\frac{m}{4\pi a_s} \equiv \frac{1}{U} + \sum_{\mathbf{k}} \frac{1}{2\varepsilon_{\mathbf{k}}}\,. \tag{15}$$

In this way one may solve for the unknown U in terms of a_s or U_0. The two-body T-matrix equation [Eq. (15)] can be rewritten as

$$U = \Gamma U_0, \quad \Gamma = \left(1 + \frac{U_0}{U_c}\right)^{-1}, \tag{16}$$

where we define the quantity U_c as

$$U_c^{-1} = -\sum_{\mathbf{k}} \frac{1}{2\varepsilon_{\mathbf{k}}} \ . \tag{17}$$

Here U_c is the critical value of the potential associated with the binding of a two particle state in vacuum. Specific evaluation of U_c requires that there be a cut-off imposed on the above summation, associated with the range of the potential.

Now let us turn to the Feshbach problem, where the superfluidity is constrained by a more extended set of parameters U, g, v and also μ. Provided we redefine the appropriate "two body" scattering length, Eq. (15) holds even in the presence of Feshbach effects (Milstein et al., 2002; Ohashi and Griffin, 2002). It has been shown that U in the above equations is replaced by $U_{\rm eff}$ and a_s by a_s^*

$$\frac{m}{4\pi a_s^*} \equiv \frac{1}{U_{\rm eff}} + \sum_{\mathbf{k}} \frac{1}{2\varepsilon_{\mathbf{k}}} \ . \tag{18}$$

Here it is important to stress that many body effects, via the fermionic chemical potential μ enter into a_s^*.

More precisely the effective interaction between two fermions is Q dependent. It arises from a second order process involving emission and absorption of a molecular boson. The net effect of the direct plus indirect interactions is given by

$$U_{\rm eff}(Q) \equiv U + g^2 D_0(Q) \ , \tag{19}$$

where

$$D_0(Q) \equiv 1/[\mathrm{i}\Omega_n - \varepsilon_{\mathbf{q}}^{mb} - v + 2\mu] \tag{20}$$

is the noninteracting molecular boson propagator. What appears in the gap equation, however, is

$$U_{\rm eff}(Q=0) \equiv U_{\rm eff} = U - \frac{g^2}{v - 2\mu} \ . \tag{21}$$

Experimentally, the two body scattering length a_s^* varies with magnetic field B. Near resonance, it can be parameterized (Kokkelmans et al., 2002) in terms of three parameters of the two body problem U_0, g_0 and the magnetic field which at resonance is given by B_0. One fits the scattering length to $a_{bg}(1-(w/(B-B_0))$ so that the width w is related to g_0 and the background scattering length a_{bg} is related to U_0. Away from resonance, the crossover picture requires that the scattering length vanish asymptotically as

$$a_s^* \approx 0 \quad \text{in extreme BEC limit} \ , \tag{22}$$

so that the system represents an ideal Bose gas. Here it should be noted that this BEC limit corresponds to $v \to \mu^+$. The counterpart of Eq. (22) also holds for the one channel problem. Note that the actual resonance of the many body problem will be somewhat shifted from the atomic-fitted resonance parameter B_0.

It is convenient to define the parameter v_0 which is directly related to the difference in the applied magnetic field B and B_0

$$v_0 = (B - B_0)\Delta\mu^0 \ , \tag{23}$$

where $\Delta\mu^0$ is the difference in the magnetic moment of the singlet and triplet paired states. *We will use the parameter ν_0 as a measure of magnetic field strength throughout this Review*. The counterpart of Eq. (14) is then

$$\frac{m}{4\pi a_s^*} \equiv \frac{1}{U_0 - \frac{g_0^2}{\nu_0 - 2\mu}} \equiv \frac{1}{U^*} , \tag{24}$$

where $U_0 = 4\pi a_{bg}/m$ and $g_0^2 = U_0 \Delta\mu^0 w$. For the purposes of this Review we will use the scattering length a_s^*, although for simplicity we often drop the asterisk and write it as a_s.

We can again invert the Lippmann–Schwinger or T-matrix scattering equation (Bruun and Pethick, 2004; Kokkelmans et al., 2002) to arrive at the appropriate parameters g and ν which enter into the Hamiltonian and thus into the gap equation. Just as in Eq. (16), one finds a connection between measurable parameters (with subscript 0) and their counterparts in the Hamiltonian (without the subscript):

$$U = \Gamma U_0, \quad g = \Gamma g_0, \quad \nu - \nu_0 = -\Gamma \frac{g_0^2}{U_c} . \tag{25}$$

To connect the various energy scales, which appear in the problem, typically $1\mathrm{G} \approx 60 E_\mathrm{F}$ for both ^{6}Li and ^{40}K. Here it is assumed that the Fermi energy is $E_\mathrm{F} \approx 2\,\mu\mathrm{K}$.

In Fig. 16 and using Eq. (18), we plot a prototypical scattering length $k_\mathrm{F} a_s \equiv k_\mathrm{F} a_s^*$ as a function of the magnetic field dependent parameter, ν_0. This figure indicates the BEC, BCS and PG regimes. Here, as earlier, the PG regime is bounded on the left by $\mu = 0$ and on the right by $\Delta(T_c) \approx 0$.

A key finding associated with this plot is that *the PG regime begins on the so-called "BEC side of resonance", independent of whether Feshbach effects are included or not*. That is, the fermionic chemical potential reaches zero while the scattering length is positive. This generic effect of the ground state self consistent equations arises from the Pauli principle. For an isolated system, two particle resonant scattering occurs at $U = U_c$, where U_c is defined in Eq. (17). In the many body context, because of Pauli principle repulsion between fermions, it requires an effectively stronger attraction to bind particles into molecules. Stated alternatively, the onset of the fermionic regime ($\mu > 0$) occurs for more strongly attractive interactions, than those required for two body resonant scattering. As a consequence of $\mu > 0$, *there is very little condensate weight in the Feshbach boson channel near the unitary limit, for values of the coupling parameter g_0, appropriate to currently studied* (*and rather wide*) *Feshbach resonances*.

Finally, it is useful to compare the two interaction terms which we have defined above, (U_eff and U^*), and to contrast their behavior in the BEC and unitary limits. The quantity U^* is proportional to the scattering length; it reflects the two body physics and necessarily diverges at unitarity, where $U_\mathrm{eff} = U_c$. By contrast, in the BEC regime, U^*, or a_s^* approaches zero, (under the usual presumption that the interaction is a contact interaction). This vanishing of U^* should be compared with the observation that the quantity U_eff, which reflects the many body physics, must diverge in this BEC limit.

1.5.1. Differences between one and two channel models: physics of Feshbach bosons

The main effects associated with including the explicit Feshbach resonance are twofold. These Feshbach bosons provide a physical mechanism for tuning the scattering length to be arbitrarily large, and in the BEC limit, they lead to different physics from the one channel problem. As will be illustrated later via a comparison of Figs. 23 and 25, in an artificial way one can capture most of the salient physics of the unitary regime via a one channel approach in which one drops all molecular boson related terms in the

Hamiltonian, but takes the interaction U to be arbitrary. In this way there is very little difference between fermion-only and fermion–boson models. There is an important proviso, though, that one is not dealing with narrow resonances which behave rather differently near unitarity, as will be seen in Fig. 32. In addition, as in the one channel model a form of universality (Ho, 2004) is found in the ground state at the unitary limit, provided g is sufficiently large. This is discussed later in the context of Fig. 30.

We emphasize that, within the BEC regime there are three important effects associated with the Feshbach coupling g. As will become clear later, (i) in the extreme BEC limit when g is nonzero, there are no occupied fermionic states. The number constraint can be satisfied entirely in terms of Feshbach bosons. (ii) The absence of fermions will, moreover, greatly weaken the inter-boson interactions which are presumed to be mediated by the fermions. In addition, as one decreases $|U_{\rm eff}|$ from very attractive to moderately attractive (i.e., increases a_s^* on the BEC side) the nature of the condensed pairs changes. Even in the absence of Feshbach bosons (FB), the size of the pairs increases. But in their presence the admixture of bosonic (i.e., molecular bosons) and fermionic (i.e., Cooper pair) components in the condensate is continuously varied from fully bosonic to fully fermionic. Finally (iii) the role of the condensate enters in two very different ways into the self consistent gap and number equations, depending on whether or not there are FB. The molecular boson condensate appears principally in the number equation, while the Cooper pair condensate appears principally in the gap equation. To make this point clearer we can refer ahead to Eq. (81) which contains the FB condensate contribution n_b^0. By contrast the Cooper condensate contribution $\Delta_{\rm sc}$ enters into the total excitation gap Δ as in Eq. (10) and Δ is, in turn, constrained via Eq. (69). Points (i) and (iii), which may appear somewhat technical, have essential physical implications, among the most important of these is point (ii) above.

We stress, however, that *for the PG and BCS regimes the differences with and without FB are, however, considerably less pronounced.*

1.6. Current summary of cold atom experiments: crossover in the presence of Feshbach resonances

There has been an exciting string of developments over the past few years in studies of ultracold fermionic atoms, in particular, ^{6}Li and ^{40}K, which have been trapped and cooled via magnetic and optical means. Typically these traps contain $\sim 10^5$ atoms at very low densities $\approx 10^{13}$ cm^{-3} when cooled to very low T. Here the Fermi temperature $E_{\rm F}$ in a trap can be estimated to be of the order of a micro-Kelvin. It was argued on the basis of BCS theory alone (Houbiers et al., 1997), and rather early on (1997), that the temperatures associated with the superfluid phases may be attainable in these trapped gases. This set off a search for the "holy grail" of fermionic superfluidity. That a Fermi degenerate state could be reached at all is itself quite remarkable; this was first reported by DeMarco and Jin (1999). By late 2002 reports of unusual hydrodynamics in a degenerate Fermi gas indicated that strong interactions were present (O'Hara et al., 2002). This strongly interacting Fermi gas (associated with the unitary scattering regime) has attracted widespread attention independent of the search for superfluidity, because it appears to be a prototype for analogous systems in nuclear physics (Baker, 1999; Heiselberg, 2004a) and in quark–gluon plasmas (Itakura, 2003; Kolb and Heinz, 2003). Moreover, there has been a fairly extensive body of analytic work on the ground state properties of this regime (Carlson et al., 1999; Heiselberg, 2001), which goes beyond the simple mean field wave function ansatz.

As a consequence of attractive s-wave interactions between fermionic atoms in different hyperfine states, it was anticipated that dimers could also be made. Indeed, these molecules formed rather efficiently (Cubizolles et al., 2003; Regal et al., 2003; Strecker et al., 2003) as reported in mid-2003 either via

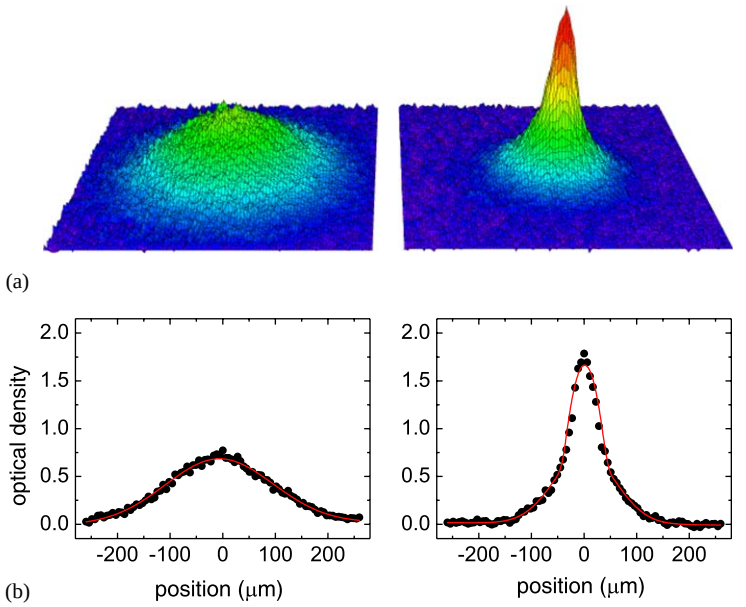

Fig. 17. (Color) Spatial density profiles of a molecular cloud of trapped ^{40}K atoms in the BEC regime in the transverse directions after 20 ms of free expansion (from Greiner et al., 2003), showing thermal molecular cloud above T_c (left) and a molecular condensate (right) below T_c. (a) Shows the surface plots, and (b) shows the cross-sections through images (dots) with bimodal fits (lines).

three body recombination (Jochim et al., 2003a) or by sweeping the magnetic field across a Feshbach resonance. Moreover, they are extremely long lived (Strecker et al., 2003). From this work it was relatively straightforward to anticipate that a Bose condensate would also be achieved. Credit goes to theorists such as Holland (Holland et al., 2001) and to Timmermans (Timmermans et al., 2001) and their co-workers for recognizing that the superfluidity need not be only associated with condensation of long lived bosons, but in fact could also derive, as in BCS, from fermion pairs. In this way, it was argued that a suitable tuning of the attractive interaction via Feshbach resonance effects, would lead to a realization of a BCS–BEC crossover.

By late 2003 to early 2004, four groups (Bourdel et al., 2004; Greiner et al., 2003; Jochim et al., 2003b; Zwierlein et al., 2003) had observed the "condensation of weakly bound molecules" (that is, on the $a_s > 0$ side of resonance), and shortly thereafter a number had also reported evidence for superfluidity on the BCS side (Regal et al., 2004; Zwierlein et al., 2004; Kinast et al., 2004; Chin et al., 2004). The BEC side is the more straightforward since the presence of the superfluid is reflected in a bi-modal distribution in the density profile. This is shown in Fig. 17 from Greiner et al. (2003), and is conceptually similar to the behavior for condensed Bose atoms (Dalfovo et al., 1999). On the BEC side but near resonance, the estimated T_c is of the order of 500 nK, with condensate fractions varying from 20% or so, to nearly 100%. The condensate lifetimes are relatively long in the vicinity of resonance, and fall off rapidly as one goes deeper into the BEC. However, for $a_s < 0$ there is no clear expectation that the density profile will provide a signature of the superfluid phase.

These claims that superfluidity may have been achieved on the BCS side ($a_s < 0$) of resonance were viewed as particularly exciting. The atomic community, for the most part, felt the previous counterpart

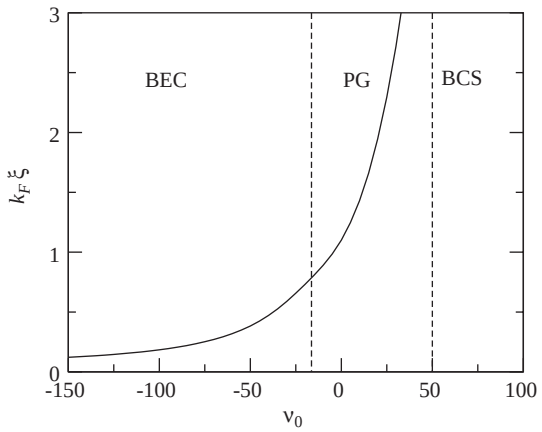

Fig. 18. Characteristic behavior of Cooper pair size ξ in the condensate in the three regimes. The dotted vertical lines are not sharp transitions but indicate where $\mu = 0$ (left line) and where $\Delta(T_c) \approx 0$ (right line). The dimensionless $k_F\xi$ gives the ratio between pair size ξ and the mean inter-particle spacing $1/k_F$. Pairs shrink and become tightly bound in the deep BEC regime.

observations on the BEC side were expected and not significantly different from condensation in Bose atoms. The evidence for this new form of "fermionic superfluidity" rests on studies (Regal et al., 2004; Zwierlein et al., 2004) that perform fast sweeps from negative a_s to positive a_s across the resonance. The field sweeps allow, in principle, a pairwise projection of fermionic atoms (on the BCS side) onto molecules (on the BEC side). It is presumed that in this way one measures the momentum distribution of fermionic atom pairs. The existence of a condensate was thus inferred. Other experiments which sweep across the Feshbach resonance adiabatically, measure the size of the cloud after release (Bourdel et al., 2004) or within a trap (Bartenstein et al., 2004b). Evidence for superfluidity on the BCS side, which does not rely on the sweep experiments, has also been deduced from collective excitations of a fermionic gas (Bartenstein et al., 2004a; Kinast et al., 2004). Pairing gap measurements with radio frequency (RF) probes (Chin et al., 2004) have similarly been interpreted (Kinnunen et al., 2004a) as evidence for superfluidity, although it appears more likely that these experiments establish only the existence of fermionic pairs. Quite recently, evidence for a phase transition has been presented via thermodynamic measurements and accompanying theory (Kinast et al., 2005). The latter, like the theory (Kinnunen et al., 2004a) of RF experiments (Chin et al., 2004), is based on the formalism presented in this Review.

Precisely what goes on during the sweep is not entirely understood. It should be stressed again that where the scattering length changes sign is not particularly important to the *N*-body physics. *Thus starting on the "BCS side of resonance" and ending on the "BEC side of resonance" involves a very continuous sweep in which the physics is not qualitatively changed*. It has been speculated that for this sweep procedure to work a large percentage of the Cooper pair partners must be closer than the inter-atomic spacing. Others have alternatively viewed the sweep as having little to do with the large Cooper pairs of BCS superconductivity.

It is useful to establish the various pair sizes here. In the PG regime the normal state consists of a significant number of small (compared to BCS) pre-formed pairs. Below T_c, the condensate pair size is also small. Finally, there are excited pair states in the superfluid phase, with characteristic size ξ_{pg}. The Cooper pair size ξ as plotted in Fig. 18 was deduced from the condensate (Randeria, 1995) at $T = 0$,

but this can be shown to be rather similar to ξ_{pg}, corresponding to the size of excited pair states (Chen, 2000; Chen et al., 1998) both above and below T_c. It seems plausible that during the sweep there is some rearrangement of excited states (both fermionic and bosonic) and condensate. In addition, all pairs (excited and condensate) contract in size. When, at the end of a sweep, they are sufficiently small, then they are more "visible". What appears to be essential, however, is that the sweep time scales are rapid enough so that the existence of a condensate at the initial starting point is a necessary and sufficient condition for observing a condensate at the end of a sweep.

1.7. T-matrix-based approaches to BCS–BEC crossover in the absence of Feshbach effects

In this subsection we introduce the concept of a *T*-matrix within the pairing channel. This is defined in Eq. (26) below and it represents an effectively screened interaction in which the appropriate polarizability (χ) is associated with the particle–particle rather than the particle–hole channel, as in the more conventional dielectric susceptibility. The *T*-matrix thus appears as an infinite series of two particle "ladder" diagrams.

Away from zero temperature, a variety of different many body approaches have been invoked to address the physics of BCS–BEC crossover. For the most part, these revolve around *T*-matrix schemes. Here one solves self consistently for the single fermion propagator (G) and the pair propagator (t). That one stops at this level without introducing higher order Green's functions (involving three, and four particles, etc) is believed to be adequate for addressing a leading order mean field theory such as that represented by Eq. (1). One can see that pair–pair (boson–boson) interactions are only treated in a mean field averaging procedure; they arise exclusively from the fermions and are presumed to be sufficiently weak so as not to lead to any incomplete condensation in the ground state, as is compatible with Eq. (1).

One can view this approach as the first step beyond BCS in a hierarchy of mean field theories. In BCS, above T_c one includes only the bare fermion propagator G_0. Below T_c, pairs play a role but only through the condensate. At the next level one accounts for the interaction between particles and noncondensed pairs in both the normal and superconducting states. The pairs introduce a self energy Σ into the particles, which represents a correction to BCS theory. The pairs are treated at an effective mean field level. By truncating the equations of motion in this way, the effects of all higher order Green's functions are subsumed into t in an averaged way.

Below we demonstrate that at this *T*-matrix level there are a number of distinct schemes which can be implemented to address BCS–BEC crossover physics. These same alternatives have also entered into a discussion of pre-formed pairs as they appear in treatments of superconducting fluctuations. Above T_c, quite generally one writes for the *T*-matrix

$$t(Q) = \frac{U}{1 + U\chi(Q)} \tag{26}$$

and theories differ only on what is the nature of the pair susceptibility $\chi(Q)$, and the associated self energy of the fermions. Here and throughout we use Q to denote a four-vector and write $\sum_Q \equiv T \sum_{i\Omega_n} \sum_{\mathbf{q}}$, where Ω_n is a Matsubara frequency. Below T_c one can also consider a *T*-matrix approach to describe the particles and pairs in the condensate. For the most part we will defer extensions to the broken symmetry phase to Section 2.2.

1.7.1. Review of BCS theory using the T-matrix approach

In order to assess alternative schemes, it is useful to review BCS theory within a T-matrix formalism. In BCS theory, pairs explicitly enter into the problem below T_c, but only through the condensate. These condensed pairs are associated with a T-matrix given by

$$t_{\rm sc}(Q) = -\Delta_{\rm sc}^2 \delta(Q)/T \tag{27}$$

with fermionic self energy

$$\Sigma_{\rm sc}(K) = \sum_Q t_{\rm sc}(Q) G_0(Q-K) \tag{28}$$

so that $\Sigma_{\rm sc}(K) = -\Delta_{\rm sc}^2 G_0(-K)$. Here, and throughout, G_0 is the Green's function of the noninteracting system. The number of fermions in a BCS superconductor is given by

$$n = 2\sum_K G(K) \tag{29}$$

and

$$G(K) = [G_0^{-1}(K) - \Sigma_{\rm sc}(K)]^{-1} \tag{30}$$

Doing the Matsubara summation in Eq. (29), one can then deduce the usual BCS expression for the number of particles, which determines the fermionic chemical potential

$$n = \sum_{\mathbf{k}} \left[1 - \frac{\varepsilon_{\mathbf{k}} - \mu}{E_{\mathbf{k}}} + 2\frac{\varepsilon_{\mathbf{k}} - \mu}{E_{\mathbf{k}}} f(E_{\mathbf{k}}) \right] , \tag{31}$$

where

$$E_{\mathbf{k}} = \sqrt{(\varepsilon_{\mathbf{k}} - \mu)^2 + \Delta_{\rm sc}^2(T)} \tag{32}$$

We need, however, an additional equation to determine $\Delta_{\rm sc}(T)$. The BCS gap equation can be written as

$$1 + U\chi_{\rm BCS}(0) = 0, \quad T \leqslant T_c , \tag{33}$$

where

$$\chi_{\rm BCS}(Q) = \sum_K G(K) G_0(Q-K) . \tag{34}$$

This suggests that one consider the uncondensed or normal state pair propagator to be of the form

$$t(Q) = \frac{U}{1 + U\chi_{\rm BCS}(Q)} \tag{35}$$

then in the superconducting state we have a BEC like condition on the pair chemical potential $\mu_{\rm pair}$ defined by

$$t^{-1}(Q=0) = \mu_{\rm pair} \times \text{const} . \tag{36}$$

where the overall constant is unimportant for the present purposes. Thus we say that the pair chemical potential satisfies

$$\mu_{\text{pair}} = 0, \quad T \leqslant T_c \ . \tag{37}$$

That μ_{pair} vanishes at *all* $T \leqslant T_c$ is a stronger condition than the usual Thouless condition for T_c. Moreover, it should be stressed that *BCS theory is associated with a particular asymmetric form for the pair susceptibility*. These uncondensed pairs play virtually no role in BCS superconductors but the structure of this theory points to a particular choice for a pair susceptibility. We can then write the self consistent condition on Δ_{sc} which follows from Eq. (33). Using Eqs. (27)–(34), we find the expected form for the BCS gap equation. This represents a constraint on the order parameter Δ_{sc}:

$$\Delta_{\text{sc}}(T) = -U \sum_{\mathbf{k}} \Delta_{\text{sc}}(T) \frac{1 - 2f(E_{\mathbf{k}})}{2E_{\mathbf{k}}} \ . \tag{38}$$

The above discussion was presented in a somewhat different way in a paper by Kadanoff and Martin (1961).

1.7.2. Three choices for the T-matrix of the normal state: problems with the Nozieres Schmitt-Rink approach

On general grounds we can say that there are three obvious choices for $\chi(Q)$ which appears in the general definition of the T-matrix in Eq. (26). Each of these has been studied rather extensively in the literature. All of these introduce corrections to BCS theory and all were motivated by attempts to extend the crossover ground state to finite T, or to understand widespread pseudogap effects in the high T_c superconductors. In analogy with Gaussian fluctuations, one can consider

$$\chi_0(Q) = \sum_K G_0(K) G_0(Q - K) \tag{39}$$

with self energy

$$\Sigma_0(K) = \sum_Q t(Q) G_0(Q - K) \ , \tag{40}$$

which appears in G in the analogue of Eq. (30). The number equation is then deduced by using Eq. (29).

This scheme was adopted by Nozieres and Schmitt-Rink (NSR), although these authors (Nozières and Schmitt-Rink, 1985; Randeria, 1995) approximated the number equation (Serene, 1989) by using a leading order series for G in Eq. (30) with

$$G = G_0 + G_0 \Sigma_0 G_0 \ . \tag{41}$$

It is straightforward, however, to avoid this approximation in Dyson's equation, and a number of groups (Jankó et al., 1997; Pieri et al., 2004) have extended NSR in this way.

Similarly one can consider

$$\bar{\chi}(Q) = \sum_K G(K) G(Q - K) \tag{42}$$

with self energy

$$\bar{\Sigma}(K) = \sum_{Q} t(Q) G(Q - K) \ . \tag{43}$$

This latter scheme (sometimes known as fluctuation-exchange or FLEX) has been also extensively discussed in the literature, by among others, Haussmann (1993), Tchernyshyov (1997), Micnas et al. (1995) and Yanase et al. (2003).

Finally, we can contemplate the asymmetric form (Chen et al., 1998; Giovannini and Berthod, 2001) for the T-matrix, so that the coupled equations for $t(Q)$ and $G(K)$ are based on

$$\chi(Q) = \sum_{K} G(K) G_0(Q - K) \tag{44}$$

with self energy

$$\Sigma(K) = \sum_{Q} t(Q) G_0(Q - K) \ . \tag{45}$$

Each of these three schemes determines the superfluid transition temperature via the Thouless condition. Thus $\mu_{\text{pair}} = 0$ leads to a slightly different expression for T_c, based on the differences in the choice of T-matrix which appears in Eq. (36).

A central problem with the NSR scheme ($\chi \approx G_0 G_0$) is that it incorporates self energy effects only through the number equation. The absence of self energy effects in the gap equation is equivalent to the statement that pseudogap effects only indirectly affect T_c: the particles acquire a self energy from the pairs but these self energy effects are not fed back into the propagator for the pairs. On physical grounds one anticipates that the pseudogap must have a direct effect on T_c as a consequence of the associated reduction in the density of states. Other problems related to the thermodynamics were pointed out (Sofo and Balseiro, 1992) when NSR was applied to a two dimensional system. Finally, because only the number equation contains self energy effects, it is not clear if one can arrive at a proper vanishing of the superfluid density ρ_s at T_c within this approach. This requires a precise cancellation between the diamagnetic current contributions (which depend on the number equation) and the paramagnetic terms (which reflect the gap equation).

One might be inclined, then, to prefer (Serene, 1989) the FLEX ($\chi \approx GG$) scheme since it is ϕ-derivable, in the sense of Baym (1962). This means that it is possible to write down a closed form expression for the thermodynamical potential, from which one derives other physical quantities via functional derivatives of this potential. Theoretical consistency issues in this approach have been rather exhaustively discussed by Haussmann (1993) above T_c. We are not aware of a fully self consistent calculation of ρ_s below T_c, at the same level of completeness as Haussmann's normal state analysis (or, for that matter, of the counterpart discussion to Section 3.1 and accompanying Appendix B). However, in principle, it should be possible to arrive at a proper expression for the superfluid density, providing Ward identities are imposed. There is some ambiguity (Benard et al., 1993; Micnas et al., 1995; Tchernyshyov, 1997) about whether pseudogap effects are present in the FLEX approach; a consensus has not been reached at this time. Numerical work based on FLEX is more extensive (Benard et al., 1993; Deisz et al., 1998) than for the other two alternative schemes.

It will be made clear in what follows that, if one's goal is to extend the usual crossover ground state of Eq. (1) *to finite temperatures, then one must choose the asymmetric form for the pair susceptibility.*

Here $\chi \approx GG_0$. This is different from the approach of Nozieres and Schmitt-Rink in which there is no evident consistency between their finite T treatment and the presumed ground state. Some have claimed (Randeria, 1995) that an NSR-based approach, when extended below T_c, reproduces Eqs. (69) and (70). But elsewhere in the literature it has been shown that these ground state self consistency conditions are derived from a lower level theory (Kostyrko and Ranninger, 1996). They arise from a $T = 0$ limit of what is called the saddle point approximation, or mean field approach. When pairing fluctuations beyond the saddle point (Nozières and Schmitt-Rink, 1985) are included, the number equation is changed. Then the ground state is no longer that of Eq. (1) (Pieri et al., 2004). In the cold atom literature, the distinction between the NSR-extrapolated ground state and the ground state of Eq. (1) has been pointed out in the context of atomic density profiles (Perali et al., 2004b) within traps.

It should be evident from Eq. (34) and the surrounding discussion that the asymmetric form is uniquely associated with the BCS-like behavior implicit in Eq. (1). The other two T-matrix approaches lead to different ground states which should, however, be very interesting in their own right. These will need to be characterized in future.

Additional support for the asymmetric form, which will be advocated here, was provided by Kadanoff and Martin. In their famous paper they noted that several people had surmised that the form for $\chi(Q)$ involving GG would be more accurate. However, as claimed in (Kadanoff and Martin, 1961), "This surmise is not correct." Aside from theoretical counter-arguments which they present, the more symmetric combination of Green's functions "can also be rejected experimentally since they give rise to a T^2 specific heat." Similar arguments in support of the asymmetric form were introduced (Hassing and Wilkins, 1973) into the literature in the context of addressing specific heat jumps.

1.8. Superconducting fluctuations: a type of pre-formed pairs

While there are no indications of bosonic degrees of freedom, (other than in the condensate), within strict BCS theory, it has been possible to access these bosons via probes of superconducting fluctuations. Quasi-one dimensional, or quasi-2D superconductors in the presence of significant disorder exhibit fluctuation effects (Larkin and Varlamov, 2001) or precursor pairing as seen in "paraconductivity", fluctuation diamagnetism, as well as other unusual behavior, often consisting of divergent contributions to transport. One frequently computes (Kwon and Dorsey, 1999) these bosonic contributions to transport by use of a time dependent Ginzburg Landau (TDGL) equation of motion. This is rather similar to a Gross Pitaevskii formalism except that the "bosons" here are highly damped by the fermions.

Alternatively T-matrix based approaches (involving all three choices of $\chi(Q)$) have been extensively used to discuss conventional superconducting fluctuations. The advantage of these latter schemes is that one can address both the anomalous bosonic and fermionic contributions to transport through the famous Aslamazov–Larkin and Maki–Thompson diagrams (Larkin and Varlamov, 2001). We defer a discussion of these issues until Appendix B.

It is useful to demonstrate first how conventional superconducting fluctuations behave at the lowest level of self consistency, called the Hartree approximation. This scheme is closely associated (Stajic et al., 2003a) with a GG_0 T-matrix, as is discussed in more detail in Appendix C. It is also closely associated with BCS theory, for one can show that, in the spirit of Eq. (1), at this Hartree level the excitation gap $\Delta(T_c)$ and T_c lie on a specific BCS curve (specified by n and U). What is different from strict BCS theory is that the onset of superconductivity takes place in the presence of a finite excitation gap (i.e., pseudogap), just as shown in Fig. 3. This, then, reflects the fact that there are pre-formed pairs at T_c.

By contrast with high T_c superconductors, however, in conventional fluctuation effects, the temperature T^* at which pairs start to form is always extremely close to their condensation temperature T_c. We thus say that there is a very narrow critical region.

In Hartree approximated Ginzburg Landau theory (Hassing and Wilkins, 1973) the free energy functional is given by

$$F[\Psi] = a_0(T - T^*)|\Psi|^2 + b|\Psi|^4 \approx a_0(T - T^*)|\Psi|^2 + 2b\Delta^2|\Psi|^2 \ . \tag{46}$$

Here Δ^2 plays the role of a pseudogap in the normal state. It is responsible for a lowering of T_c relative to the mean field value T^*. Collecting the quadratic terms in the above equation, it follows that

$$T_c = T^* - \frac{2b}{a_0}\Delta^2(T_c) \ . \tag{47}$$

Moreover, self consistency imposes a constraint on the magnitude of $\Delta(T_c)$ via

$$\Delta^2(T) = \int D\Psi \mathrm{e}^{-\beta_{\mathrm{F}}[\Psi]}\Psi^2 \Big/ \int D\Psi \mathrm{e}^{-\beta_{\mathrm{F}}[\Psi]} \ . \tag{48}$$

It should be noted that Eq. (47) is consistent with the statement that $\Delta(T_c)$ and T_c lie on the BCS curve, since for small separation between T_c and T^*, this curve is, below T_c, defined by

$$\Delta^2_{\mathrm{BCS}}(T) \approx \frac{a_0}{2b}(T^* - T) \ . \tag{49}$$

The primary effect of fluctuations at the Hartree level is that pairing takes place in the presence of a finite excitation gap, reflecting the presence of very short lived, but pre-formed pairs. It should be clear that Δ is not to be confused with the superconducting order parameter Δ_{sc}, as should be evident from Fig. 3. We refer the reader to a more detailed discussion which is presented in Appendix C.

Fig. 19 illustrates how this pseudogap appears experimentally, via a plot of the normalized density of states (Cohen et al., 1969) $v_1 \equiv N(E)$ in the normal state. This figure derives from tunneling measurements on Al-based films. Note the depression of $N(E_{\mathrm{F}})$ at low energies. This is among the first indications for a pseudogap reported in the literature.

Alternatively, fluctuations have also been discussed at the Gaussian (G_0G_0) level in which there is no need for self consistency, in contrast to the above picture. Here because the calculations are so much more tractable there have been very detailed applications (Larkin and Varlamov, 2001) of essentially all transport and thermodynamic measurements. This Gaussian analysis led to unexpected divergences in the para-conductivity from the so-called Maki–Thompson term which then provided a motivation to go beyond leading order theory. Patton (1971a, b) showed how this divergence could be removed within a more self consistent GG_0 scheme, equivalent to self consistent Hartree theory. Others argued (Schmid, 1969; Tucker and Halperin, 1971) that Hartree-Fock (GG) was more appropriate, although in this weak coupling, narrow fluctuation regime, the differences between these latter two schemes are only associated with factors of 2. Nevertheless with this factor of 2, $\Delta(T_c)$ and T_c are no longer on the BCS curve. It should be noted that a consensus was never fully reached (Hassing and Wilkins, 1973) by the community on this point.

1.8.1. Dynamics of pre-formed pairs above T_c: time dependent Ginzburg–Landau theory

We turn again to Fig. 5 which provides a useful starting point for addressing bosonic degrees of freedom and their implications for experiment. It is clear that transport in the unusual normal state, associated

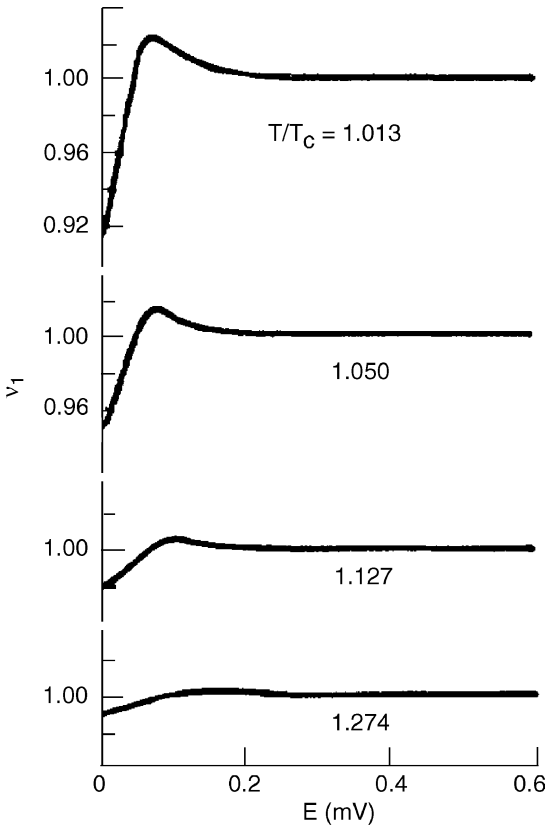

Fig. 19. Pseudogap in the density of states above T_c in conventional superconductors, from Cohen et al. (1969). $v_1 \equiv N(E)$ is the normalized density of states.

with the pseudogap (PG) phase (as well as thermodynamics) contains contributions from both fermionic and bosonic excitations. The bosons are not infinitely long lived; their lifetime is governed by their interactions with the fermions. In some instances (Larkin and Varlamov, 2001), the bosonic contributions to transport become dominant or even singular at T_c. Under these circumstances one can ignore the fermionic contributions except insofar as they lead to a lifetime for the pairs.

To address the transport properties of these more well established pre-formed pairs, one appeals to a standard way of characterizing the dynamics of bosons—a phenomenological scheme known as time dependent Ginsburg–Landau (TDGL) theory. This theory has some microscopic foundations in diagrammatic T-matrix approaches in which one considers only the Aslamazov–Larkin terms (which are introduced in Appendix B). At the Gaussian level both TDGL and the T-matrix approaches are tractable. At the Hartree level things rapidly become more complicated, and it is far easier to approach the problem (Tan and Levin, 2004) by adopting a strictly phenomenological TDGL.

The generic Hartree-TDGL equation of motion for classical charged bosons interacting with electromagnetic fields (ϕ, $\mathbf{A}$) is given by

$$\gamma\left(\mathrm{i}\frac{\partial}{\partial t} - \mathrm{e}^{*}\phi(\mathbf{x},t)\right)\psi(\mathbf{x},t) = \frac{(-\mathrm{i}\nabla - e^{*}\mathbf{A}(\mathbf{x},t))^{2}}{2M^{*}}\psi(\mathbf{x},t) - \mu_{\mathrm{pair}}(T)\psi(\mathbf{x},t) + D(\mathbf{x},t)\ . \qquad (50)$$

Here $\psi(\mathbf{x}, t)$ is a classical field variable representing the bosons which have vanishing chemical potential μ_{pair} at T_c. The function $D(\mathbf{x}, t)$ introduces a noise variable into the equation of motion. Generally γ is complex.

We will explore the implications of this equation in our more quantitative discussion of Section 6.5.

2. Quantitative details of crossover

2.1. $T = 0$, BEC limit without Feshbach bosons

We begin by reviewing $T = 0$ crossover theory in the BEC limit. Our starting point is the ground state wavefunction Ψ_0 of Eq. (1), along with the self consistency conditions of Eq. (2). For positive chemical potential μ, the quantity $\Delta_{\text{sc}}(0)$ also corresponds to the energy gap for fermionic excitations. In the ground state the two energy scales $\Delta(0)$ and $\Delta_{\text{sc}}(0)$ are degenerate, just as they are (at all temperatures) in strict BCS theory.

It is convenient to rewrite these equations[5] in terms of the inter-fermion scattering length a_s

$$\frac{m}{4\pi a_s} = \sum_{\mathbf{k}} \left[\frac{1}{2\varepsilon_{\mathbf{k}}} - \frac{1}{2E_{\mathbf{k}}} \right] , \tag{51}$$

$$n = \sum_{\mathbf{k}} \left[1 - \frac{\varepsilon_{\mathbf{k}} - \mu}{E_{\mathbf{k}}} \right] , \quad T = 0 . \tag{52}$$

In the fermionic regime ($\mu > 0$) these equations are essentially equivalent to those of BCS theory, although at weak coupling appropriate to strict BCS, little attention is paid to the number equation since $\mu = E_{\text{F}}$ is always satisfied. The more interesting regime corresponds to $\mu \leqslant 0$ where these equations take on a new interpretation. Deep inside the BEC regime it can be seen that

$$n = \Delta_{\text{sc}}^2(0) \frac{m^2}{4\pi\sqrt{2m|\mu|}} , \tag{53}$$

which, in conjunction with Eq. (51) (expanded in powers of $\Delta_{\text{sc}}^2(0)/\mu^2$):

$$\frac{m}{4\pi a_s} = (2m)^{3/2} \frac{\sqrt{|\mu|}}{8\pi} \left[1 + \frac{1}{16} \frac{\Delta_{\text{sc}}^2(0)}{\mu^2} \right] , \tag{54}$$

yields

$$\mu = -\frac{1}{2ma_s^2} + \frac{a_s \pi n}{m} . \tag{55}$$

---

[5] To make the equations simpler, in much of what we present in this review we will consider a contact potential interaction. The momentum sums are assumed to run to infinity. More generally, one can include a cutoff function $\varphi_{\mathbf{k}}$ for the momentum integrals. The gap function thus becomes $\Delta_{\mathbf{k}} = \Delta\varphi_{\mathbf{k}}$. For the cuprate d-wave cuprate superconductors, $\varphi_{\mathbf{k}} = \cos k_x a - \cos k_y a$. For our numerical work on atomic gases we use a Gaussian cutoff $\varphi_{\mathbf{k}}^2 = \mathrm{e}^{-k^2/k_0^2}$ with k_0 taken to be as large as is numerically feasible.

This last equation is equivalent (Perali et al., 2003; Viverit et al., 2004) to its counterpart in Gross–Pitaevskii (GP) theory. This theory describes true bosons, and is associated with the well known equation of state

$$n_{\rm pairs} = \frac{m_{\rm B}}{4\pi a_{\rm B}}\,\mu_{\rm B}\ . \tag{56}$$

To see the equivalence we associate the number of bosons $n_{\rm pairs} = n/2$, the boson mass $m_{\rm B} = 2m$ and the bosonic scattering length $a_{\rm B} = 2a_s$. Here the bosonic chemical potential $\mu_{\rm B} = 2\mu + \varepsilon_0$ and we define $\varepsilon_0 = 1/(2ma_s^2)$. This factor of 2 in $a_{\rm B}/a_s$ has received a fair amount of attention in the literature. Although it will be discussed later in the Review, it should be noted now that this particular numerical value is particular to the one channel description (Stajic et al., 2005b), and different from what is observed experimentally (Petrov et al., 2004).

Despite these similarities with GP theory, the fundamental parameters are the fermionic $\Delta_{\rm sc}(0)$ and chemical potential μ. It can be shown that in this deep BEC regime the number of pairs is directly proportional to the superconducting order parameter

$$n_{\rm pairs} = \frac{n}{2} = Z_0\Delta_{\rm sc}^2(0) \tag{57}$$

where

$$Z_0 \approx \frac{m^2 a_s}{8\pi}\ . \tag{58}$$

One may note from Eq. (57) that the "gap equation" now corresponds to a number equation (for bosons). Similarly the number equation, or constraint on the fermionic chemical potential defines the excitation gap for fermions, once the chemical potential is negative. In this way the roles of the two constraints are inverted (Randeria, 1995) relative to the BCS regime.

That a Gross–Pitaevskii approach captures the leading order physics at $T = 0$ can also be simply seen by rewriting the ground state wavefunction, as pointed out by Randeria (1995). Define $v_{\mathbf{k}}/u_{\mathbf{k}} \equiv \eta_{\mathbf{k}}$,

$$\begin{aligned}\Psi_0 &= const\,\Pi_k(1 + \eta_{\mathbf{k}} c_k^\dagger c_{-k}^\dagger)|0\rangle \\ &= const\,\exp\left(\sum_k \eta_{\mathbf{k}} c_k^\dagger c_{-k}^\dagger\right)|0\rangle\ .\end{aligned} \tag{59}$$

Projecting onto a state with fixed particle number N yields

$$\Psi_0 = const\left(\sum_{\mathbf{k}} \eta_{\mathbf{k}} c_k^\dagger c_{-k}^\dagger\right)^{N/2}|0\rangle\ . \tag{60}$$

This is a GP wavefunction of composite bosons with the important proviso: that the characteristic size associated with the internal wavefunction $\eta_{\mathbf{k}}$ is smaller than the inter-particle spacing. It should be stressed that, except in the BEC asymptotic limit, (where the "bosons" are noninteracting) there are essential differences between Eq. (60) and the Gross Pitaevskii wavefunction. Away from this extreme limit, pair-pair interactions (arising indirectly via the fermions and the Pauli principle), as well as the finite size of the pairs, will differentiate this system from that of true interacting bosons. This same issue arises more concretely in the context of the collective mode spectrum of ultracold gases, as discussed in Section 5.3.

2.2. Extending conventional crossover ground state to $T \neq 0$: BEC limit without Feshbach bosons

How do we extend (Chen et al., 1998) this picture to finite T? In the BEC limit, as shown in Fig. 4, fermion pairs are well established or "pre-formed" within the entire range of superconducting temperatures. The fundamental constraint associated with the BEC regime is that: *for all $T \leqslant T_c$, there should, thus, be no temperature dependence in fermionic energy scales. In this way Eqs.* (51) *and* (52) *must be imposed at all temperatures T.*

$$\frac{m}{4\pi a_s} = \sum_{\mathbf{k}} \left[\frac{1}{2\varepsilon_{\mathbf{k}}} - \frac{1}{2E_{\mathbf{k}}} \right] , \tag{61}$$

$$n = \sum_{\mathbf{k}} \left[1 - \frac{\varepsilon_{\mathbf{k}} - \mu}{E_{\mathbf{k}}} \right] , \quad T \leqslant T_c . \tag{62}$$

It follows that the number of pairs at $T = 0$ should be equal to the number of pairs at $T = T_c$. However, all pairs are condensed at $T = 0$. Clearly, the character of these pairs changes so that at T_c, all pairs are noncondensed. To implement these physical constraints (and to anticipate the results of a more microscopic theory) we write

$$n_{\text{pairs}} = \frac{n}{2} = Z_0 \Delta^2 \tag{63}$$

$$n_{\text{pairs}} = n_{\text{pairs}}^{\text{condensed}}(T) + n_{\text{pairs}}^{\text{noncondensed}}(T) \tag{64}$$

so that we may decompose the excitation gap into two contributions

$$\Delta^2 = \Delta_{\text{sc}}^2(T) + \Delta_{pg}^2(T) \tag{65}$$

where $\Delta_{\text{sc}}(T)$ corresponds to condensed and $\Delta_{pg}(T)$ to the noncondensed gap component. Each of these are proportional to the respective number of condensed and noncondensed pairs with proportionality constant Z_0. At T_c,

$$n_{\text{pairs}}^{\text{noncondensed}} = \frac{n}{2} = \sum_{\mathbf{q}} b(\Omega_q, T_c) , \tag{66}$$

where $b(x)$ is the usual Bose–Einstein function and Ω_q is the unknown dispersion of the noncondensed pairs. Thus

$$\Delta_{pg}^2(T_c) = Z_0^{-1} \sum b(\Omega_q, T_c) = \frac{n}{2} Z_0^{-1} . \tag{67}$$

We may deduce directly from Eq. (67) that $\Delta_{pg}^2 = -\sum_Q t(Q)$, if we presume that below T_c, the noncondensed pairs have propagator

$$t(Q) = \frac{Z_0^{-1}}{\Omega - \Omega_q} . \tag{68}$$

It is important to stress that the dispersion of the pairs Ω_q cannot be put in by hand. It is not known a priori. Rather, it has be to *derived* according to the constraints imposed by Eqs. (61) and (62). We can

only arrive at an evaluation of Ω_q after establishing the nature of the appropriate T-matrix theory. In what follows we derive this dispersion using the two channel model. We state the one channel results here for completeness. In the absence of FB, $\Omega_q \equiv B_0 q^2$, where $B_0 \equiv 1/(2M_0^*)$. As a consequence of a "bosonic" self energy, which arises from fermion–boson (as distinguished from boson-boson) interactions, the bosonic dispersion is found to be quadratic. This quadratic dependence persists for the two channel case as well.

2.3. Extending conventional crossover ground state to $T \neq 0$: T-matrix scheme in the presence of Feshbach bosons

To arrive at the pair dispersion for the noncondensed pairs, Ω_q, we need to formulate a generalized T-matrix based scheme which is consistent with the ground state conditions, and with the T dependence of strict BCS theory. It is useful from a pedagogical point to now include the effects of Feshbach bosons (Stajic et al., 2004). Our intuition concerning how true bosons condense is much better than our intuition concerning the condensation of fermion pairs, except in the very limited BCS regime. We may assume that Δ and μ evolve with temperature in such a way as to be compatible *with both the temperature dependences of BCS and with the above discussion for the BEC limit*. We thus take

$$\Delta(T) = -U_{\rm eff} \sum_{\mathbf{k}} \Delta(T) \frac{1 - 2f(E_{\mathbf{k}})}{2E_{\mathbf{k}}} , \tag{69}$$

$$n = \sum_{\mathbf{k}} \left[1 - \frac{\varepsilon_{\mathbf{k}} - \mu}{E_{\mathbf{k}}} + 2 \frac{\varepsilon_{\mathbf{k}} - \mu}{E_{\mathbf{k}}} f(E_{\mathbf{k}}) \right] , \tag{70}$$

where $E_{\mathbf{k}} = \sqrt{(\varepsilon_{\mathbf{k}} - \mu)^2 + \Delta^2(T)}$. Note that in the presence of Feshbach bosons, we use n to denote the density of fermionic atoms which is to be distinguished from the constituents of the Feshbach bosons. The total density of particles will be denoted by $n^{\rm tot}$. *Eqs.* (69) *and* (70) *will play a central role in this review. They have been frequently invoked in the literature, albeit under the presumption that there is no distinction between* $\Delta(T)$ *and* $\Delta_{\rm sc}(T)$.

Alternatively one can rewrite Eq. (69) as

$$\frac{m}{4\pi a_s^*} = \sum_{\mathbf{k}} \left[\frac{1}{2\varepsilon_{\mathbf{k}}} - \frac{1 - 2f(E_{\mathbf{k}})}{2E_{\mathbf{k}}} \right] . \tag{71}$$

Clearly Eqs. (69) and (70) are consistent with Eqs. (61) and (62) since Fermi functions are effectively zero in the BEC limit. Our task is to find a T-matrix formalism which is compatible with (69) and (70), and to do this we focus first on the *noncondensed* molecular bosons. Their propagator may be written as

$$D(Q) \equiv \frac{1}{{\rm i}\Omega_n - \varepsilon_q^{mb} - \nu + 2\mu - \Sigma_{\rm B}(Q)} . \tag{72}$$

We presume that the self energy of these molecules can be written in the form

$$\Sigma_{\rm B}(Q) \equiv -g^2 \chi(Q)/[1 + U\chi(Q)] , \tag{73}$$

where $\chi(Q)$ is as yet unspecified. This RPA-like self energy arises from interactions between the molecular bosons and the fermion pairs, and this particular form is required for self-consistency.

Noncondensed bosons in equilibrium with a condensate must necessarily have zero chemical potential.

$$\mu_{\text{boson}}(T) = 0, \quad T \leqslant T_c \ . \tag{74}$$

This is equivalent to the Hugenholtz–Pines condition that

$$D^{-1}(0) = 0, \quad T \leqslant T_c \ . \tag{75}$$

Using Eqs. (73) and (75) it can be seen that

$$U_{\text{eff}}^{-1}(0) + \chi(0) = 0, \quad T \leqslant T_c \ . \tag{76}$$

This equation can be made compatible with our fundamental constraint in Eq. (69) provided we take

$$\chi(Q) = \sum_K G(K) G_0(Q - K) \ , \tag{77}$$

where $G(K)$

$$G(K) \equiv [G_0^{-1}(K) - \Sigma(K)]^{-1} \tag{78}$$

includes a self energy given by the BCS-form

$$\Sigma(K) = -G_0(-K)\Delta^2 \ , \tag{79}$$

which now involves the quantity Δ to be distinguished from the order parameter Δ_{sc}. Note that with this form for $\Sigma(K)$, the number of fermions is indeed given by Eq. (70).

More generally, we may write the constraint on the total number of particles as follows. The number of noncondensed molecular bosons is given directly by

$$n_b(T) = -\sum_Q D(Q) \ . \tag{80}$$

For $T \leqslant T_c$, the number of fermions is given via Eq. (70). The *total* number (n^{tot}) of particles is then

$$n + 2n_b + 2n_b^0 = n^{\text{tot}} \ , \tag{81}$$

where $n_b^0 = \phi_m^2$ is the number of molecular bosons in the condensate, and ϕ_m is the order parameter for the molecular condensate.

Thus far, we have shown that the condition that noncondensed molecular bosons have zero chemical potential, can be made consistent with Eqs. (69) and (70) provided we constrain $\chi(Q)$ and $\Sigma(K)$ as above. We now want to examine the counterpart condition on the fermions and their condensate contribution. The analysis leading up to this point should make it clear *that we have both condensed and noncondensed fermion pairs, just as we have both condensed and noncondensed molecular bosons*. Moreover, these fermion pairs and Feshbach bosons are strongly admixed, except in the very extreme BCS and BEC limits. Because of noncondensed pairs, we will see that the excitation gap is distinct from the superconducting order parameter, although in the literature this distinction has not been widely recognized.

Just as the noncondensed molecular bosons have zero chemical potential below T_c we have the same constraint on the noncondensed fermion pairs which are in chemical equilibrium with the noncondensed bosons

$$\mu_{\text{pair}} = 0, \quad T \leqslant T_c \ . \tag{82}$$

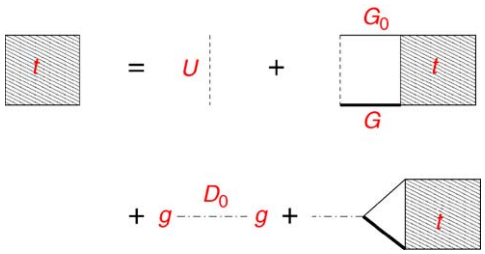

Fig. 20. Diagrammatic scheme for present T-matrix theory. Here U is the open-channel interaction, g is the coupling between open and closed channels. G_0, G and D_0 are bare fermion, full fermion, and bare Feshbach boson Green's functions, respectively. U and $g_0^2 D_0$ yield an effective pairing interaction, $U_{\rm eff}$.

The T-matrix scheme in the presence of the Feshbach bosons is shown in Fig. 20. Quite generally, the T-matrix consists of two contributions: from the condensed (*sc*) and noncondensed or "pseudogap"-associated (*pg*) pairs,

$$t = t_{pg} + t_{\rm sc} \ , \tag{83}$$

$$t_{pg}(Q) = \frac{U_{\rm eff}(Q)}{1 + U_{\rm eff}(Q)\chi(Q)}, \quad Q \neq 0 \ , \tag{84}$$

$$t_{\rm sc}(Q) = -\frac{\tilde{\Delta}_{\rm sc}^2}{T}\,\delta(Q) \ , \tag{85}$$

where we write $\tilde{\Delta}_{\rm sc} = \Delta_{\rm sc} - g\phi_m$, with $\Delta_{\rm sc} = -U\sum_{\mathbf{k}} \langle a_{-\mathbf{k}\downarrow} a_{\mathbf{k}\uparrow}\rangle$ and $\phi_m = \langle b_{\mathbf{q}=0}\rangle$. Here, the order parameter is a linear combination of both paired fermions and condensed molecules. Similarly, we have two contributions for the fermion self energy

$$\Sigma(K) = \Sigma_{\rm sc}(K) + \Sigma_{pg}(K) = \sum_{Q} t(Q) G_0(Q - K) \ , \tag{86}$$

where, as in BCS theory,

$$\Sigma_{\rm sc}(K) = \sum_{Q} t_{\rm sc}(Q) G_0(Q - K) \ . \tag{87}$$

Without loss of generality, we choose order parameters $\tilde{\Delta}_{\rm sc}$ and ϕ_m to be real and positive with $g < 0$. Importantly, these two components are connected (Kokkelmans et al., 2002) by the relation $\phi_m = g\Delta_{\rm sc}/[(\nu - 2\mu)U]$.

The vanishing of the pair chemical potential implies that

$$t_{pg}^{-1}(0) = U_{\rm eff}^{-1}(0) + \chi(0) = 0, \quad T \leqslant T_c \ . \tag{88}$$

This same equation was derived from consideration of the bosonic chemical potential. Most importantly, we argued above that this was consistent with Eq. (69) provided the fermion self energy assumes the BCS form. We now verify the assumption in Eq. (79). A vanishing chemical potential means that $t_{pg}(Q)$ is

strongly peaked around $Q = 0$. Thus, we may approximate (Maly et al., 1999a) Eq. (86) to yield

$$\Sigma(K) \approx -G_0(-K)\Delta^2 \ , \tag{89}$$

where

$$\Delta^2(T) \equiv \tilde{\Delta}^2_{\rm sc}(T) + \Delta^2_{pg}(T) \ , \tag{90}$$

and we define the pseudogap Δ_{pg}

$$\Delta^2_{pg} \equiv -\sum_{Q\neq 0} t_{pg}(Q) \ . \tag{91}$$

This bears a close resemblance to Eq. (80), if we write the number of noncondensed fermion pairs and molecular bosons as

$$n_p(T) = Z\Delta^2_{pg}(T) \ . \tag{92}$$

Note that in the normal state (where $\mu_{\rm pair}$ is nonzero) one cannot make the approximation of Eq. (89). Referring back to our discussion of Hartree-approximated TDGL, a strong analogy between Eqs. (91) and (48) should be observed. There is a similar analogy between Eqs. (69) and (49); more details are provided in Appendix C. We thus have that Eqs. (51) and (89) with Eq. (78) are alternative ways of writing Eqs. (69) and (70). Along with Eq. (91) we now have a closed set of equations for addressing the ordered phase. Moreover the propagator for noncondensed pairs can now be quantified, using the self consistently determined pair susceptibility. At moderately strong coupling and at small four-vector Q, we may expand to obtain

$$t_{pg}(Q) = \frac{Z^{-1}}{\Omega - \Omega_q + \mu_{\rm pair} + {\rm i}\Gamma_Q} \ , \tag{93}$$

Consequently, one can rewrite Eq. (91) as

$$\Delta^2_{pg}(T) = Z^{-1}\sum b(\Omega_q, T) \ . \tag{94}$$

Here we introduce a simple notation for the small Q expansions:

$$\chi(Q) - \chi(0) = Z_0({\rm i}\Omega_n - B_0 q^2) \ ,$$
$$U^{-1}_{\rm eff}(Q) - U^{-1}_{\rm eff}(0) = Z_g({\rm i}\Omega_n - B_g q^2)$$

with

$$Z_0 = \frac{1}{2\Delta^2}\left[n - 2\sum_{\mathbf{k}} f(\varepsilon_{\mathbf{k}} - \mu)\right] \ ,$$

$$Z_g = \frac{g^2}{[(2\mu - v)U + g^2]^2} \ .$$

We have that $Z = Z_0 + Z_g$, $Z_b = (Z_0 + Z_g)/Z_0$, and the q^2 coefficient $B \equiv 1/(2M^*)$ in $\Omega_q \equiv Bq^2$ is such that

$$B = \frac{B_0 Z_0 + 1/2MZ_g}{Z} \ .$$

The strong hybridization between the molecular bosons and fermion pairs should be stressed. Indeed, there is just one branch Ω_q for bosonic-like excitations, so that at small Q

$$D(Q) = \frac{Z_b^{-1}}{\Omega - \Omega_q + \mu_{\rm boson} + {\rm i}\Gamma_Q} \ , \tag{95}$$

where below T_c, $\mu_{\rm pair} = \mu_{\rm boson} = 0$. Here Γ_Q contains all the imaginary parts of the inverse T-matrix and it vanishes rapidly as $Q \to 0$. As the coupling is decreased from the BEC limit towards BCS, the character of the pairs changes from pre-dominantly molecular-boson like to (noncondensed) Cooper pairs, composed only of the fermionic atoms.

2.4. Nature of the pair dispersion: size and lifetime of noncondensed pairs below T_c

We may rewrite the pair susceptibility (Chen et al., 1998, 1999) of Eq. (77) (after performing the Matsubara sum and analytically continuing to the real axis) in a relatively simple form as

$$\chi(Q) = \sum_{\mathbf{k}} \left[\frac{1 - f(E_{\mathbf{k}}) - f(\xi_{\mathbf{k}-\mathbf{q}})}{E_{\mathbf{k}} + \xi_{\mathbf{k}-\mathbf{q}} - \Omega - {\rm i}0^+} u_{\mathbf{k}}^2 - \frac{f(E_{\mathbf{k}}) - f(\xi_{\mathbf{k}-\mathbf{q}})}{E_{\mathbf{k}} - \xi_{\mathbf{k}-\mathbf{q}} + \Omega + {\rm i}0^+} v_{\mathbf{k}}^2 \right] \ , \tag{96}$$

where $u_{\mathbf{k}}^2$ and $v_{\mathbf{k}}^2$ are given by their usual BCS expressions in terms of Δ and $\xi_{\mathbf{k}} \equiv \varepsilon_{\mathbf{k}} - \mu$. In the long wavelength, low frequency limit, the inverse of t_{pg} can be written as

$$a_1 \Omega^2 + Z_0 \left(\Omega - \frac{q^2}{2M^*} + \mu_{\rm pair} + {\rm i}\Gamma_Q \right) \ . \tag{97}$$

We are interested in the moderate and strong coupling cases, where we can drop the $a_1\Omega^2$ term in Eq. (97), and hence we have Eq. (93) with

$$\Omega_{\mathbf{q}} \equiv \frac{q^2}{2M^*} = \frac{q^2 \xi_{pg}^2}{Z_0} \ . \tag{98}$$

This establishes a quadratic dispersion and defines the effective pair mass, M^*. Analytical expressions for this mass are possible via a small $\mathbf{q}$ expansion of χ, in Eq. (96). It is important to note that the pair mass reflects the effective *size* ξ_{pg} of noncondensed pairs. This serves to emphasize the fact that the q^2 dispersion derives from the compositeness of the "bosons", in the sense of their finite spatial extent. A description of the system away from the BEC limit must accommodate the fact that the pairs have an underlying fermionic character. This pair mass has a different origin from the mass renormalization associated with real interacting bosons. There one finds a mass shift which comes from a Hartree approximate treatment of their q-dependent interactions. Finally, we note that ξ_{pg} is comparable to the size ξ of pairs in the condensate. In the weak coupling BCS limit, a small Q expansion of χ_0 shows that, because the leading order term in Ω is purely imaginary, the Ω^2 contribution cannot be neglected. The T-matrix, then, does not have the propagating q^2 dispersion, discussed above.

It follows from Eq. (96) that the pair lifetime

$$\begin{aligned} \Gamma_Q = \frac{\pi}{Z_0} \sum_{\mathbf{k}} & [1 - f(E_{\mathbf{k}}) - f(\xi_{\mathbf{k}-\mathbf{q}})] u_{\mathbf{k}}^2 \delta(E_{\mathbf{k}} + \xi_{\mathbf{k}-\mathbf{q}} - \Omega) \\ & + [f(E_{\mathbf{k}}) - f(\xi_{\mathbf{k}-\mathbf{q}})] v_{\mathbf{k}}^2 \delta(E_{\mathbf{k}} - \xi_{\mathbf{k}-\mathbf{q}} + \Omega) \ . \end{aligned} \tag{99}$$

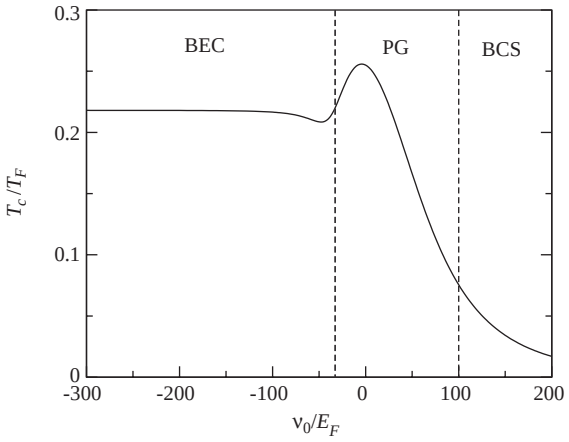

Fig. 21. Typical behavior of T_c in the homogeneous case. For the purposes of illustration, this calculation includes Feshbach effects. T_c follows BCS for large magnetic detuning parameter ν_0 and approaches the BEC asymptote 0.218 for large negative ν_0. It reaches a maximum at unitarity, and has a minimum when the fermionic chemical potential μ changes sign.

Here Γ_Q reflects the rate of decay of noncondensed bosons into a bare and dressed fermion. Note that the excitation gap in $E_{\mathbf{k}}$ significantly restricts the contribution from the δ functions. Thus, *the decay rate of pair excitations is greatly suppressed, due to the excitation gap* (*for fermions*) *in the superconducting phase*. Even in the normal phase pairs live longer than one might have anticipated from "Pauli blocking" arguments which are based on evaluating Γ_Q in a Fermi liquid state. However, the same equations are not strictly valid above T_c, because Eq. (89) no longer holds. To compute the pair lifetime in the normal state requires a more extensive calculation involving the full T-matrix self consistent equations and their numerical solution (Jankó et al., 1997; Maly et al., 1999a, b).

2.5. T_c calculations: analytics and numerics

Calculations of T_c can be performed using Eqs. (69) and (70) along with Eq. (91). The T-matrix is written in the expanded form of Eq. (93), which is based on the pair dispersion as derived in the previous section. For the most part the calculations proceed numerically.

A typical curve is plotted in Fig. 21, where the three regimes BCS, BEC and PG are indicated. For positive, but decreasing magnetic detuning ν_0, T_c follows the BCS curve until the "pseudogap" or $\Delta(T_c)$ becomes appreciable. After its maximum (near the unitary limit, at slightly negative ν_0), T_c decreases, (as does μ), to reach a minimum at $\mu \approx 0$. This decrease in T_c reflects the decreasing number of low energy fermions due to the opening of a pseudogap. Beyond this point, towards negative ν_0, the system is effectively bosonic, and the superconductivity is no longer hampered by pseudogap effects. In the presence of FB, the condensate consists of two contributions, although the weight of the fermion pair component rapidly disappears. Similarly T_c rises, although slowly, towards the ideal BEC asymptote, following the inverse effective boson mass. The corresponding curve based on the NSR approach (Nozières and Schmitt-Rink, 1985) has only one extremum, but nevertheless the overall magnitudes are not so different (Milstein et al., 2002; Ohashi and Griffin, 2002).

Analytic results are obtainable in the near-BEC limit only. The general expression for the effective mass $1/M_0^*$ in this limit is given by

$$\frac{1}{M_0^*} = \frac{1}{Z_0 \Delta^2} \sum_{\mathbf{k}} \left[\frac{1}{m} v_{\mathbf{k}}^2 - \frac{4E_{\mathbf{k}} k^2}{3m^2 \Delta^2} v_{\mathbf{k}}^4 \right] , \tag{100}$$

where here FB effects have been dropped for simplicity. In what follows, we expand Eq. (100) in powers of na_s^3 and obtain after some algebra

$$M_0^* \approx 2m \left(1 + \frac{\pi a_s^3 n}{2} \right) . \tag{101}$$

We now invoke an important constraint, derived earlier in Eq. (66) which corresponds to the fact that at T_c all fermions are constituents of uncondensed pairs

$$\frac{n}{2} = \sum_{\mathbf{q}} b(\Omega_{\mathbf{q}}, T_c) . \tag{102}$$

From the above equation it follows that $(M^* T_c)^{3/2} \propto n = const.$ which, in conjunction with Eq. (101) implies

$$\frac{T_c - T_c^0}{T_c^0} = -\frac{\pi a_s^3 n}{2} . \tag{103}$$

Here T_c^0 is the transition temperature of the ideal Bose gas with $M_0 = 2m$. This downward shift of T_c follows the effective mass renormalization, much as expected in a Hartree treatment of GP theory at T_c. Here, however, in contrast to GP theory for a homogeneous system with a contact potential (Dalfovo et al., 1999), there is a nonvanishing renormalization of the effective mass. This is a key point which underlines the importance in this approach of the fermionic degrees of freedom, even at very strong coupling.

3. Self consistency tests

All T-matrix approaches to the BCS–BEC crossover problem must be subject to self consistency tests. Among these, one should demonstrate that *normal state* self energy effects within a T-matrix scheme are not associated with superfluidity or superconductivity (Kosztin et al., 1998). While this seems at first sight straightforward, all theories should be put to this test. Thus for a charged system, a meaningful result for the superfluid density ρ_s requires that there be an exact cancellation between diamagnetic and paramagnetic current contributions at T_c. In this way self energy effects in the number equation and gap equation must be treated in a consistent fashion. In the following we address some of these self consistency issues in the context of the asymmetric ($\chi \approx GG_0$) BCS–BEC crossover scheme. Other crossover theories with different forms for the pair susceptibility should also be subjected to these tests. We begin with a summary of calculations (Kosztin et al., 2000; Stajic et al., 2003a) of the Meissner effect, followed by a treatment of the collective mode spectrum. Our discussion in this section is presented for the one channel problem, in the absence of Feshbach effects.

3.1. Important check: behavior of ρ_s

The superfluid density may be expressed in terms of the local (static) electromagnetic response kernel $K(0)$

$$n_s = \frac{m}{e^2} K(0) = n - \frac{m}{3e^2} P_{\alpha\alpha}(0) \ , \tag{104}$$

with the current–current correlation function given by

$$P_{\alpha\beta}(Q) = -2e^2 \sum_K \lambda_\alpha(K, K+Q) G(K+Q) \Lambda_\beta^{\rm EM}(K+Q, K)\, G(K) \ . \tag{105}$$

Here the bare vertex $\lambda(K, K+Q) = 1/m(\mathbf{k} + \mathbf{q}/2)$ and we consider $Q = (\mathbf{q}, 0)$, with $\mathbf{q} \to 0$. We write $\boldsymbol{\Lambda}^{\rm EM} = \lambda + \delta\boldsymbol{\Lambda}_{pg} + \delta\boldsymbol{\Lambda}_{\rm sc}$, where the pseudogap contribution $\delta\boldsymbol{\Lambda}_{pg}$ to the vertex correction will be shown in Appendix B to satisfy a Ward identity below T_c

$$\delta\boldsymbol{\Lambda}_{pg}(K, K) = \frac{\partial\Sigma_{pg}(K)}{\partial\mathbf{k}} \ . \tag{106}$$

By contrast for the superconducting contributions, one has

$$\delta\boldsymbol{\Lambda}_{\rm sc}(K, K) = -\frac{\partial\Sigma_{\rm sc}(K)}{\partial\mathbf{k}} \ . \tag{107}$$

This important difference in sign is responsible for the fact that the Meissner effect is associated with superconductivity, and not with a normal state self energy.

The particle density n, after partial integration can be rewritten as $n = -(2/3)\sum_K \mathbf{k}\cdot\partial_{\mathbf{k}} G(K)$. Then, as a result of Dyson's equation, one arrives at the following general expression which relates to the diamagnetic contribution

$$n = -\frac{2}{3}\sum_K G^2(K)\left[\frac{k^2}{m} + \mathbf{k}\cdot\frac{\partial\Sigma_{pg}(K)}{\partial\mathbf{k}} + \mathbf{k}\cdot\frac{\partial\Sigma_{\rm sc}(K)}{\partial\mathbf{k}}\right] \ . \tag{108}$$

Now, inserting Eqs. (108) and (105) into Eq. (104) one can see that the pseudogap contribution to n_s drops out by virtue of Eq. (106); we find

$$n_s = \frac{2}{3}\sum_K G^2(K)\mathbf{k}\cdot\left(\delta\boldsymbol{\Lambda}_{\rm sc} - \frac{\partial\Sigma_{\rm sc}}{\partial\mathbf{k}}\right) \ . \tag{109}$$

We emphasize that the cancellation of this pseudogap contribution to the Meissner effect is the central physics of this analysis, and it depends on treating self energy effects in a Ward-identity-consistent fashion.

We also have that

$$\delta\boldsymbol{\Lambda}_{\rm sc}(K+Q, K) = \Delta_{\rm sc}^2 G_0(-K-Q) G_0(-K)\lambda(K+Q, K) \ . \tag{110}$$

Inserting Eqs. (87), (89), and (110) into Eq. (109), after calculating the Matsubara sum, one arrives at

$$n_s = \frac{4}{3}\sum_{\mathbf{k}} \frac{\Delta_{\rm sc}^2}{E_{\mathbf{k}}^2}\varepsilon_{\mathbf{k}}\left[\frac{1-2f(E_{\mathbf{k}})}{2E_{\mathbf{k}}} + f'(E_{\mathbf{k}})\right] \ . \tag{111}$$

This expression can be simply rewritten in terms of the BCS result for the superfluid density

$$\left(\frac{n_s}{m}\right) = \frac{\Delta_{sc}^2}{\Delta^2}\left(\frac{n_s}{m}\right)^{\mathrm{BCS}} . \tag{112}$$

Here $(n_s/m)^{\mathrm{BCS}}$ is just (n_s/m) with the overall prefactor Δ_{sc}^2 replaced with Δ^2.

Finally we can rewrite Eq. (112) using Eq. (90) as

$$\left(\frac{n_s}{m}\right) = \left[1 - \frac{\Delta_{pg}^2}{\Delta^2}\right]\left(\frac{n_s}{m}\right)^{\mathrm{BCS}} . \tag{113}$$

In this form it is evident that (via Δ_{pg}^2) *pair excitations out of the condensate are responsible for a suppression of the superfluid density relative to that obtained from fermionic excitations only* (Stajic et al., 2003b).

3.2. Collective modes and gauge invariance

The presence of pseudogap self energy effects greatly complicates the computation of collective modes (Kosztin et al., 2000). This is particularly apparent at nonzero temperature. Once dressed Green's functions G enter into the calculational schemes, the collective mode polarizabilities and the electromagnetic (EM) response tensor must necessarily include vertex corrections dictated by the form of the self-energy Σ, which depends on the T-matrix which, in turn depends on the form of the pair susceptibility χ. These necessary vertex corrections are associated with gauge invariance in the same way, as was seen for ρ_s, and discussed in Appendix B. Collective modes are important in their own right, particularly in neutral superfluids, where they can be directly detected as signatures of long range order. They also must be invoked to arrive at a gauge invariant formulation of electrodynamics. It is relatively straightforward to introduce these collective mode effects into the electromagnetic response in a completely general fashion that is required by gauge invariance. The difficulty is in the implementation.

In the presence of a weak externally applied EM field, with four-vector potential $A^\mu = (\phi, \mathbf{A})$, the four-current density $J^\mu = (\rho, \mathbf{J})$ is given by

$$J^\mu(Q) = K^{\mu\nu}(Q)A_\nu(Q) , \tag{114}$$

where $K^{\mu\nu}(Q)$ is the EM response kernel.

The incorporation of gauge invariance into a general microscopic theory may be implemented in several ways. Here we do so via a generalized matrix Kubo formula (Kulik et al., 1981) in which the perturbation of the condensate is included as additional contributions $\Delta_1 + \mathrm{i}\Delta_2$ to the applied external field. These contributions are self consistently obtained (by using the gap equation) and then eliminated from the final expression for $K^{\mu\nu}$. We now implement this procedure. Let $\eta_{1,2}$ denote the change in the expectation value of the pairing field $\hat{\eta}_{1,2}$ corresponding to $\Delta_{1,2}$. For the case of an s-wave pairing interaction $U < 0$, the self-consistency condition $\Delta_{1,2} = U\eta_{1,2}/2$ leads to the following equations:

$$J^\mu = K^{\mu\nu}A_\nu = K_0^{\mu\nu}A_\nu + R^{\mu 1}\Delta_1 + R^{\mu 2}\Delta_2 , \tag{115a}$$

$$\eta_1 = -\frac{2\Delta_1}{|U|} = R^{1\nu}A_\nu + Q_{11}\Delta_1 + Q_{12}\Delta_2 , \tag{115b}$$

$$\eta_2 = -\frac{2\Delta_2}{|U|} = R^{2\nu}A_\nu + Q_{21}\Delta_1 + Q_{22}\Delta_2 \ , \tag{115c}$$

where

$$K_0^{\mu\nu}(\omega, \mathbf{q}) = P^{\mu\nu}(\omega, \mathbf{q}) + \frac{ne^2}{m} g^{\mu\nu}(1 - g^{\mu 0}) \tag{116}$$

is the usual Kubo expression for the electromagnetic response. We define the current–current correlation function $P^{\mu\nu}(\tau, \mathbf{q}) = -\mathrm{i}\theta(\tau)\langle[j^\mu(\tau, \mathbf{q}), j^\nu(0, -\mathbf{q})]\rangle$. In the above equation, $g^{\mu\nu}$ is a (diagonal) metric tensor with elements $(1, -1, -1, -1)$. We define

$$R^{\mu i}(\tau, \mathbf{q}) = -\mathrm{i}\theta(\tau)\langle[j^\mu(\tau, \mathbf{q}), \hat{\eta}_i(0, -\mathbf{q})]\rangle \tag{117}$$

with $\mu = 0, \ldots, 3$, and $i, j = 1, 2$; and

$$Q_{ij}(\tau, \mathbf{q}) = -\mathrm{i}\theta(\tau)\langle[\hat{\eta}_i(\tau, \mathbf{q}), \hat{\eta}_j(0, -\mathbf{q})]\rangle \ . \tag{118}$$

Finally, it is convenient to define

$$\tilde{Q}_{ii} = 2/U + Q_{ii} \ . \tag{119}$$

In order to demonstrate gauge invariance and reduce the number of component polarizabilities, we first rewrite $K^{\mu\nu}$ in a way which incorporates the effects of the amplitude contributions via a renormalization of the relevant generalized polarizabilities,

$$K_0'^{\mu\nu} = K_0^{\mu\nu} - \frac{R^{\mu 1}R^{1\nu}}{\tilde{Q}_{11}} \ , \tag{120}$$

It can be shown, after some analysis, that the gauge invariant form for the response tensor is given by

$$K^{\mu\nu} = K_0'^{\mu\nu} - \frac{(K_0'^{\mu\nu'}q_{\nu'})(q_{\nu''}K_0'^{\nu''\nu})}{q_{\mu'}K_0'^{\mu'\nu'}q_{\nu'}} \ . \tag{121}$$

The above equation satisfies two important requirements: it is manifestly gauge invariant and, moreover, it has been reduced to a form that depends principally on the four-current–current correlation functions. (The word "principally" appears because in the absence of particle–hole symmetry, there are effects associated with the order parameter amplitude contributions that add to the complexity of the calculations).

The EM response kernel of a superconductor contains a pole structure that is related to the underlying Goldstone boson of the system. Unlike the phase mode component of the collective mode spectrum, this Anderson–Bogoliubov (AB) mode is independent of Coulomb effects. The dispersion of this amplitude renormalized AB mode is given by

$$q_\mu K_0'^{\mu\nu}q_\nu = 0 \ . \tag{122}$$

For an isotropic system $K_0'^{\alpha\beta} = K_0'^{11}\delta_{\alpha\beta}$, and Eq. (122) can be rewritten as

$$\omega^2 K_0'^{00} + \mathbf{q}^2 K_0'^{11} - 2\omega q_\alpha K_0'^{0\alpha} = 0 \ , \tag{123}$$

with $\alpha = 1, 2, 3$, and in the last term on the left hand side of Eq. (123) a summation over repeated Greek indices is assumed.

It might seem surprising that from an analysis which incorporates a complicated matrix linearized response approach, the dispersion of the AB mode ultimately involves only the amplitude renormalized four-current correlation functions, namely the density–density, current–current and density–current correlation functions. The simplicity of this result is, nevertheless, a consequence of gauge invariance.

At zero temperature $K_0'^{0\alpha}$ vanishes, and the sound-like AB mode has the usual linear dispersion $\omega = \omega_{\mathbf{q}} = c|\mathbf{q}|$ with the "sound velocity" given by

$$c^2 = K_0'^{11}/K_0'^{00} \ . \tag{124}$$

We may, thus, interpret the AB mode as a special type of collective mode which is associated with $A_\nu = 0$. This mode corresponds to free oscillations of $\Delta_{1,2}$ with a dispersion $\omega = cq$ given by the solution to the equation

$$\det |Q_{ij}| = \tilde{Q}_{11}\tilde{Q}_{22} - Q_{12}Q_{21} = 0 \ . \tag{125}$$

The other collective modes of this system are derived by including the coupling to electromagnetic fields. Within self-consistent linear response theory the field $\delta\phi$ must be treated on an equal footing with $\Delta_{1,2}$ and formally can be incorporated into the linear response of the system by adding an extra term $K_0^{\mu 0}\delta\phi$ to the right hand side of Eqs. (115a)–(115c). Note that, quite generally, the effect of the "external field" $\delta\phi$ amounts to replacing the scalar potential $A^0 = \phi$ by $\bar{A}^0 = \bar{\phi} = \phi + \delta\phi$. In this way one arrives at the following set of three linear, homogeneous equations for the unknowns $\delta\phi$, Δ_1, and Δ_2

$$0 = R^{10}\delta\phi + \tilde{Q}_{11}\Delta_1 + Q_{12}\Delta_2 \ , \tag{126a}$$

$$0 = R^{20}\delta\phi + Q_{21}\Delta_1 + \tilde{Q}_{22}\Delta_2 \ , \tag{126b}$$

$$\delta\rho = \frac{\delta\phi}{V} = K_0^{00}\delta\phi + R^{01}\Delta_1 + R^{02}\Delta_2 \ , \tag{126c}$$

where V is an effective particle–hole interaction which may derive from the pairing channel or, in a charged superconductor, from the Coulomb interaction. The dispersion of the collective modes of the system is given by the condition that the above equations have a nontrivial solution

$$\begin{vmatrix} Q_{11} + 1/U & Q_{12} & R^{10} \\ Q_{21} & Q_{22} + 1/U & R^{20} \\ R^{01} & R^{02} & K_0^{00} - 1/V \end{vmatrix} = 0 \ . \tag{127}$$

In the BCS limit where there is particle–hole symmetry $Q_{12} = Q_{21} = R^{10} = R^{01} = 0$ and, the amplitude mode decouples from the phase and density modes; the latter two are, however, in general coupled.

The above formalism (or its equivalent RPA variations (Belkhir and Randeria, 1992; Cote and Griffin, 1993) has been applied to address collective modes in the crossover scenario. The most extensive studies have been at $T = 0$ based on the ground state of Eq. (1). There one finds a smooth change in the character of the Anderson–Bogoliubov (AB) mode. At weak coupling one obtains the usual BCS value $c = v_F/\sqrt{3}$. By contrast at strong coupling, the collective mode spectrum reflects (Belkhir and Randeria, 1992) an effective boson-boson interaction deriving from the Pauli statistics of the constituent fermions. This is most clearly seen in jellium models (Griffin and Ohashi, 2003; Kosztin et al., 2000) where the AB sound

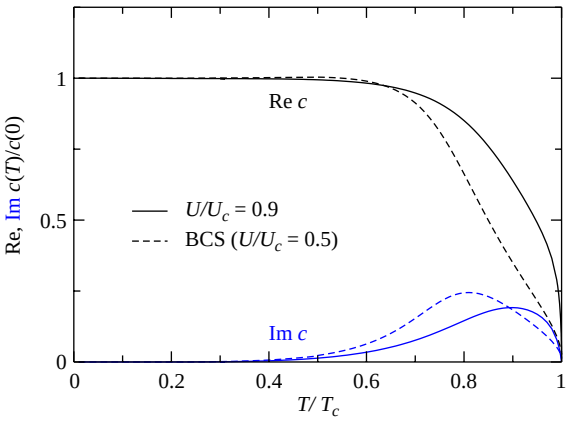

Fig. 22. Temperature dependence of the real and imaginary parts of the AB collective mode velocity for moderate (solid lines) and weak (dashed lines) coupling. The velocity vanishes at T_c for both cases.

velocity is equivalent to that predicted for a 3D interacting Bose gas $c = [4\pi n a_B/m_B^2]^{1/2}$. Here, as earlier, the inter-boson scattering length is twice that of the inter-fermionic counterpart, at strong coupling.[6]

The effects of finite temperature on the AB mode have been studied in (Kosztin et al., 2000), by making the approximation that the temperature dependence of the order parameter amplitude contribution is negligible. Then the calculation of this dispersion reduces to calculations of the electromagnetic response, as discussed, for example in ρ_s. See also Appendix B. At finite T, the AB mode becomes damped and the real and imaginary parts of the sound velocity have to be calculated numerically. Here one finds, as expected, that the complex $c \to 0$ as $T \to T_c$. The results are plotted in Fig. 22 for both moderate and weak coupling. Because the real and imaginary parts are comparable there, the mode is highly damped near T_c.

3.3. *Investigating the applicability of a Nambu matrix Green's function formulation*

Diagrammatic schemes appropriate to BCS superconductors are based on a Nambu matrix Green's function approach. The off-diagonal or anomalous Green's functions in this matrix are given by

$$F(K) \equiv \Delta_{sc} G(K) G_0(-K) \tag{128}$$

as well as its Hermitian conjugate. This Nambu formalism was designed to allow study of perturbations to the BCS state, due to, for example, external fields or impurities. For these perturbations the central assumption is that they act on both the "normal" (with BCS Green's function $G(K)$ from Eq. (30)) and anomalous channels in a symmetrical way.

Understanding as we now do that BCS theory is a very special case of superconductivity, this raises the caution that once one goes beyond BCS, some care should be taken to justify this Nambu approach. At

[6] In the neutral case, for the full collective modes of Eq. (127), there are numerical differences (of order unity) in the prefactors of the mode frequency, so that the collective modes of the crossover theory are not strictly the same as in GP theory. In these calculations V in Eq. (127) should be associated with the pairing interaction, which enters in the context of fermionic density–density correlation effects within the particle–hole channel.

the very least the distinction between the order parameter Δ_{sc} and the excitation gap Δ raises ambiguity about applying a diagrammatic theory based on Nambu–Gor'kov Green's functions.

More importantly, in treating the effects of the pseudogap self energy Σ_{pg} as we do here, it should be clear that this self energy does *not* play a symmetric role in the anomalous and normal channels. It is viewed here as an entirely normal state effect. However this theory accommodates the equivalent (Kosztin et al., 2000) of the Nambu–Gor'kov "F"-function in general response functions such as in the Maki–Thompson diagrams of Appendix B through the asymmetric combination GG_0 which always arises in pairs (for example, as the *FF* combinations of BCS theory). In this regard the GG_0 formalism appears to differ from all other *T*-matrix schemes which are designed to go below T_c, in that the Nambu scheme is not assumed at the start. Nevertheless, many features of this formalism seem to naturally arise in large part because of Eq. (128), which demonstrates an intimate connection between GG_0 and the conventional diagrams of BCS theory.

4. Other theoretical approaches to the crossover problem

4.1. $T \neq 0$ theories

We have noted in Section 1.7 that there are three main theoretical approaches to the crossover problem based on *T*-matrix theories. Their differences are associated with different forms for the pair susceptibility χ. The resulting calculations of T_c show similar variations. When two full Green's functions are present in χ (as in the FLEX approach), T_c varies monotonically (Haussmann, 1993) with increasing attractive coupling, approaching the ideal gas Bose–Einstein asymptote from below. When two bare Green's functions are present in χ, as in the work of Nozieres and Schmitt-Rink, and of Randeria and co-workers, then T_c overshoots (Sá de Melo et al., 1993; Nozières and Schmitt-Rink, 1985; Randeria, 1995) the BEC asymptote and ultimately approaches it from above. Finally when there is one bare and one dressed Green's function, T_c first overshoots and then decreases to a minimum around $\mu = 0$, eventually approaching the asymptote from below (Maly et al., 1999b). This last appears to be a combination of the other two approaches. Overall the magnitudes are relatively similar and the quantitative differences are small. There is, finally, another body of work (Giovannini and Berthod, 2001) based on the GG_0 scheme which should be noted here. The approach by the Swiss group seeks to make contact with the phase fluctuation scenario for high T_c superconductors and addresses STM and ARPES data.

Bigger differences appear when these *T*-matrix theories are extended below T_c. Detailed studies are most extensive for the NSR approach. Below T_c one presumes that the *T*-matrix (or χ) contains only bare Green's functions, but these functions are now taken to correspond to their Nambu matrix form, with the order parameter Δ_{sc} appearing in the dispersion relation for excited fermions (Pieri et al., 2004; Randeria, 1995). A motivation for generalizing the below- T_c *T*-matrix in this way is that one wants to connect to the collective mode spectrum of the superconductor, so that the dispersion relation for pair excitations is $\Omega_q \approx cq$. In this way the system would be more directly analogous to a true Bose system.

Self energy effects are also incorporated below T_c but only in the number equation, either in the approximate manner of NSR (Griffin and Ohashi, 2003; Randeria, 1995) or through use of the full Dyson resummation (Pieri et al., 2004) of the diagonal Nambu-matrix component $G(\Sigma_0)$. For the latter scheme, Strinati's group has addressed pseudogap effects in some detail with emphasis on the experimentally observed fermionic spectral function. Some concern can be raised that the fermionic excitations in the

gap equation do not incorporate this pseudogap, although these pairs are presumed to emerge out of a normal state which has a pseudogap. Indeed, this issue goes back to the original formulation of NSR, which includes self energy effects in the number equation, and not in the gap equation.

Tchernyshyov (Tchernyshyov, 1997) presented one of the first discussions below T_c for the FLEX-based T-matrix scheme. He also addressed pseudogap effects and found a suppression of the fermion density of states at low energy which allows for long-lived pair excitations inside this gap. At low momenta and frequencies, their dispersion is that of a Bogoliubov-sound-like mode with a nonzero mass. Some of these ideas have been recently extended (Domanski and Ranninger, 2003) to apply to the boson–fermion model.

The work of Micnas and collaborators (Micnas et al., 1995) which is also based on the FLEX scheme predates the work of Tchernyshyov, although their initial focus was above T_c in two dimensional Hubbard models. Here the fermionic spectral functions were studied in detail, using a numerically generated solution of the T-matrix equations. A nice review of their large body of work on "real space pairing" in the cuprates was presented based on a variety of different model Hamiltonians (Micnas and Robaszkiewicz, 1998).

An extensive body of work on the FLEX scheme has been contributed by Yamada and Yanatse (Yanase et al., 2003) both above and below T_c. They point out important distinctions between their approach and that of NSR. The effects of the broken symmetry are treated in a generalized Nambu formalism, much as assumed by Pieri et al. (2004) and by Griffin and Ohashi (2003), but here the calculations involve self energy effects in both the number and gap equations. Their work has emphasized the effects of the pseudogap on magnetic properties, but they have discussed a wide variety of experiments in high T_c and other exotic superconductors.

The nature of the ground states which result from these two alternatives ($\chi \approx GG$ and $\chi \approx G_0G_0$) has yet to be clearly established. It should be noted that, despite the extensive body of work based on the NSR or G_0G_0 scheme, no detailed picture has been presented in the literature of the nature of the ground state which results when their calculations at T_c are extrapolated (Pieri et al., 2004) down to $T = 0$. In large part, the differences between other work in the literature and that summarized in Sections 2.3 are due to the whether (as in NSR-based papers) or not (as here) the superconducting order parameter $\Delta_{\rm sc}$ alone characterizes the fermionic dispersion below T_c.

One might well ask the question: because the underlying Hamiltonian [Eq. (11)] is associated with inter-fermionic, not inter-bosonic interactions, will this be reflected in the near-BEC limit of the crossover problem? The precise BEC limit is, of course, a noninteracting, or ideal Bose gas, but away from this limit, fermionic degrees of freedom would seem to be relevant in ways that may not be accounted for by the analogue treatment of the weakly interacting Bose gas. The most extensive study (albeit, above T_c) of this issue is due to Pieri and Strinati (2000). Their work, importantly, points out the inadequacies of T-matrix schemes, particularly at strong coupling. While the ground state in their calculations is unknown, it is necessarily different from the conventional crossover state of Eq. (1). There is much intuition to be gained by studying this simplest of all ground states, as outlined in this Review, but it will clearly be of great value in future to consider states, in which, for example, there is less than full condensation.

Finally, we note that studies of non-s wave orbital pairing states in the context of the BCS–BEC crossover problem have rapidly proliferated in the literature. This is, in large part because of the observed d-wave pairing in the cuprates. Indeed, Leggett's initial work (1980), addressed p-wave pairing in ^3He. Randeria (1995) also considered non-s wave pairing. Studies (Andrenacci et al., 1999; den Hertog, 1999) of this crossover for a d-wave lattice case are plentiful at $T = 0$. Even earlier work was done (Chen et al.,

1999) on extensions of this ground state to include nonzero temperature. Moreover, a *d*-wave continuum model has also been considered (Quintanilla et al., 2002). It is expected that in the near future cold atom experiments will begin to address $l \neq 0$ pairing via appropriate choices of the Feshbach resonances (Ho and Zahariev, 2004).

4.2. Boson–Fermion models for high T_c superconductors

The notion that it might be appropriate to include bosonic degrees of freedom in high T_c superconductors goes back to Lee and Friedberg who introduced (Friedberg and Lee, 1998a, b) the "boson–fermion" model within three years of the discovery of cuprate superconductivity. The work of Lee and colleagues is based on the Hamiltonian of Eq. (11) without the direct fermion–fermion interaction U. To our knowledge this is the first study which argues for something akin to "real space pairing" in these materials. Interestingly, this work was motivated only by the observed short coherence length. Pseudogap effects, which make this case much stronger, had not yet been properly characterized. The analogies with He^4 and a more BEC-like picture of superconductivity were discussed, as well as the superfluid density, and energy gap structure, albeit for *s*-wave pairing.

Subsequent work on this model Hamiltonian in the context of the high T_c copper oxides was pursued by Ranninger and Micnas and their collaborators. Indeed, Ranninger and Robaszkiewicz (1985) were the first to write down the boson–fermion model, although initially, in an entirely different context, the bosons were associated with phonons rather than electron pairs, and they were presumed to be localized. In this context they addressed mean field theoretic solutions below T_c as well as more recently (Domanski and Ranninger, 2003) an approach based on renormalization group techniques. The physical picture which emerges leads to two gap structures below T_c, one associated with a pseudogap and another with the superconductivity. In this way it appears to be very different from approaches based on Eq. (1).

5. Physical implications: ultracold atom superfluidity

5.1. Homogeneous case

In this section we summarize the key characteristics of fermionic superfluidity in ultracold gases, in the homogeneous situation, without introducing the trap potential. Our results are based on numerical solution of the coupled Eqs. (69), (70) and (91). The upper left panel of Fig. 23 plots the fermionic chemical potential, the Feshbach boson condensate ratio and the inverse scattering length as a function of v_0. Here we have chosen what we believe is the physically appropriate value for the Feshbach coupling $g_0 = -40E_F/k_F^3$ for ^{40}K, as determined from the experimentally measured scattering length data and resonance width.[7] This parameter is roughly an order of magnitude larger for ^{6}Li. Here v_0, the gaps and μ are all in units of E_F, and the plots, unless indicated otherwise, are at zero temperature.

[7] We note that the precise values of g_0 and U_0 are not critical for either ^{6}Li or ^{40}K as long as they give roughly the right (large) resonance width ΔB and background scatter length a_{bg}. In fact, these parameters usually change during experiment since the total particle number N (and hence E_F and k_F) decreases in the process of evaporative cooling. In order to compare with experiment, one needs to compare at the correct value of $k_F a_s$.

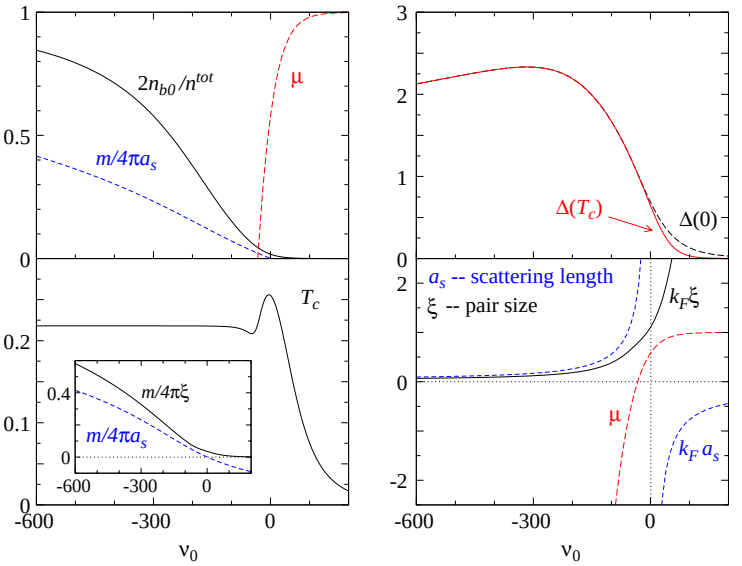

Fig. 23. (Color) Characteristics of the ground state and T_c as a function of the magnetic detuning v_0 in a homogeneous case. Shown are the chemical potential μ, fraction of molecular condensate $2n_{b0}/n^{\mathrm{tot}}$, inverse scattering length $m/4\pi a_s$, gap $\Delta(0)$, inverse pair size $m/4\pi\xi$, dimensionless relative pair size $k_{\mathrm{F}}\xi$ at $T=0$ as well as T_c and $\Delta(T_c)$. The pair size is roughly the same as inter-particle spacing, $k_{\mathrm{F}}\xi=1$, at unitarity. As v_0 decreases, the gap Δ increases and reaches a maximum, and then decreases slowly and approaches its BEC asymptote (not shown) from above. Here we take $g_0=-40E_{\mathrm{F}}/k_{\mathrm{F}}^{3/2}$ and $U_0=-3E_{\mathrm{F}}/k_{\mathrm{F}}^3$, and we use the convention for units $E_{\mathrm{F}}=k_{\mathrm{F}}=\hbar=k_{\mathrm{B}}=2m=1$. A large exponential momentum cutoff, $k_c/k_{\mathrm{F}}=80$ is assumed in the calculations.

The upper right panel plots the excitation gap at T_c as well as the gap at $T=0$. The lower left hand panel indicates T_c along with the inverse pair size ξ^{-1} in the condensate. Finally the lower right panel plots ξ itself, along with a_s.

One can glean from the figure that the Feshbach boson fraction decreases, becoming negligible when the chemical potential passes through zero. This latter point marks the onset of the PG regime, and in this regime the condensate consists almost entirely of fermionic pairs. The upper limit of the PG regime, that is, the boundary line with the BCS phase, is reached once the pseudogap, $\Delta(T_c)$ is essentially zero. This happens when μ is close to its saturation value at E_{F}. At this point the pair size rapidly increases.

These results can be compared with those derived from a smaller value of the Feshbach coupling constant $g_0=-10E_{\mathrm{F}}/k_{\mathrm{F}}^{3/2}$ shown in Fig. 24. Now the resonance is effectively narrower. Other qualitative features remain the same as in the previous figure.

One can plot the analogous figures in the absence of Feshbach effects. Here the horizontal axis is the inter-fermionic interaction strength $|U|$, as is shown in Fig. 25. Three essential differences can be observed. Note, first the obvious absence of the Feshbach boson or molecular condensate n_{b0}. There is, of course, a condensate associated with pairs of fermions (Δ_{sc}) and these pairs will become bound into "fermionic molecules" for sufficiently strong attraction. Secondly, note that the excitation gap $\Delta(0)$ is monotonically increasing as $|U|$ increases towards the BEC limit. By contrast, from the upper right panels of Fig. 24 one can see that when Feshbach effects are present $\Delta(0)\approx\Delta(T_c)$ decreases towards zero in the extreme BEC limit. It can also be seen that the shape of the scattering length curve vs. U is different from

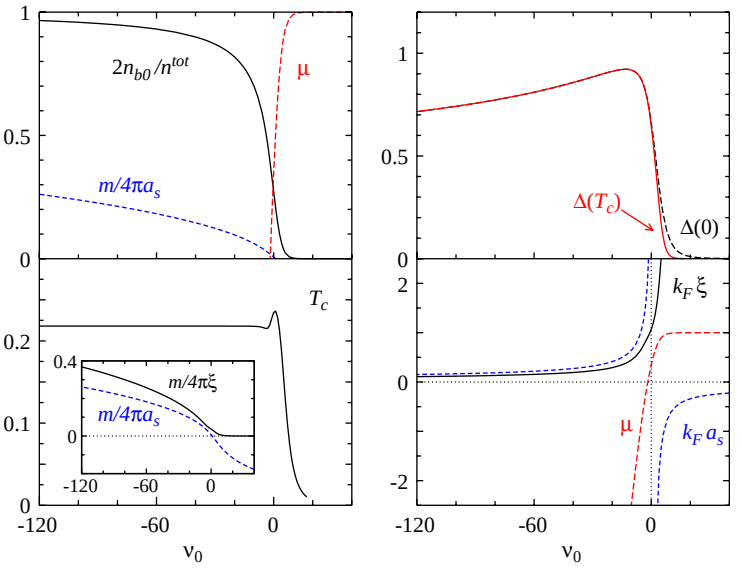

Fig. 24. (Color) Characteristics of the ground state and T_c, as in Fig. 23 except for a smaller g_0. In comparison with Fig. 23, the Feshbach resonance becomes much narrower. Here $g_0 = -10E_F/k_F^{3/2}$ and $U_0 = -3E_F/k_F^3$.

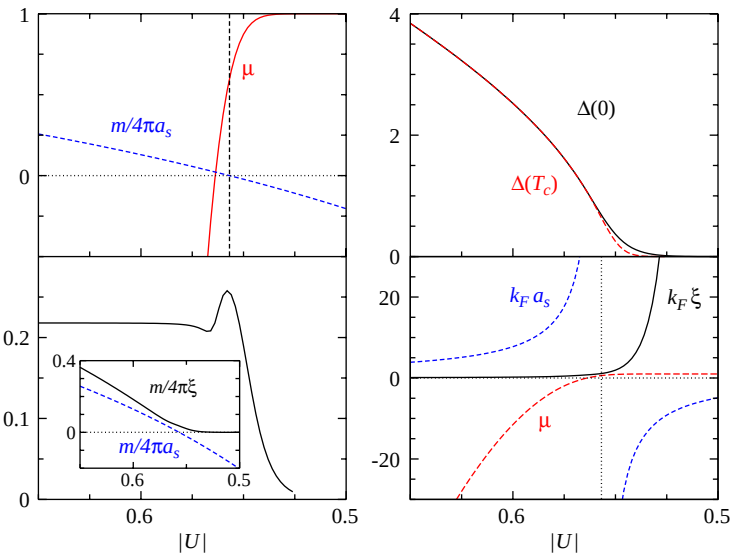

Fig. 25. (Color) Characteristics of the ground state and T_c in the one-channel model, as in Fig. 23 but as a function of the attraction strength U. Here $g_0 = 0$. Different from the two-channel shown in Figs. 23–24 case, the gap Δ increases indefinitely with $|U|$. The units for U are E_F/k_F^3. Note that $|U|$ increases to the left.

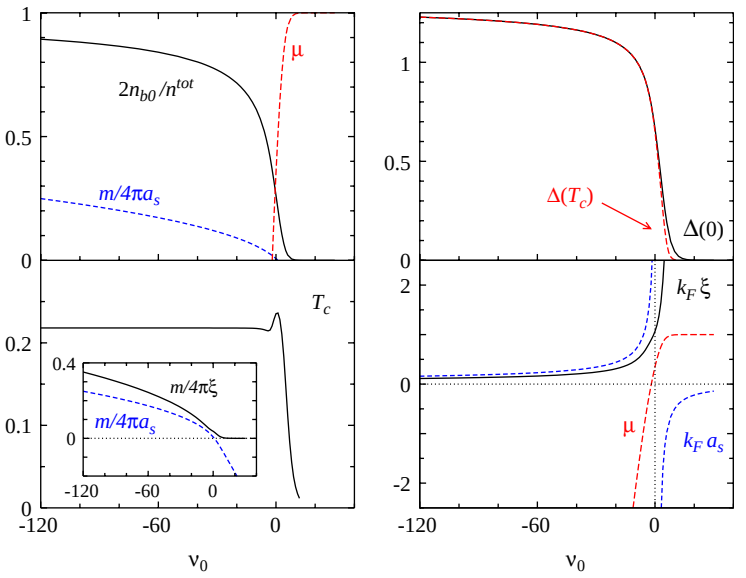

Fig. 26. (Color) Characteristics of the ground state and T_c, as in Fig. 24, except now $U_0 = 0$. As a consequence of the vanishing of U_0, the gap Δ is monotonic and approaches its BEC asymptote from below as ν_0 decreases. Here $g_0 = -10E_F/K_F^{3/2}$.

the plots in the previous two figures. Here a_s more rapidly increases in magnitude on either side of the unitary limit. Nevertheless it is important to stress that, *except for the nature of the Bose condensate in the BEC limit, the physics of the Feshbach resonance-induced superfluidity is not so qualitatively different from that associated with a direct inter-fermionic attraction.*

Fig. 26 presents the analogous plots for the case when the direct attraction between fermions U vanishes. Here the coupling constant g_0 is the same as in Fig. 24, and pseudogap effects are present here just as in all other cases. The most notable difference in the physics is that the formation of the Cooper condensate is driven exclusively by coupling to the molecular bosons. A contrast between the two figures is in the behavior of $\Delta(T_c)$ and $\Delta(0)$. For the $U = 0$ case and in the BEC limit, $\Delta(0)$ approaches the asymptotic value $(|g|\sqrt{n_b^0})$ from below. When the system is the fermionic regime ($\mu > 0$), aside from quantitative details, there is very little to distinguish the effects of U from those of g, except when these parameters are taken to very extreme limits.

Finally, in Fig. 27 we plot T_c vs. ν_0 in the presence of Feshbach effects with variable U_0, from weak to strong background coupling. The lower inset shows the behavior of the excitation gap at T_c. With very strong direct fermion attraction U, we see that T_c has a very different dependence on ν_0. In this limit there is a molecular BEC to PG crossover (which may be inaccessible in actual experiments, since U is not sufficiently high). Nevertheless, it is useful for completeness to illustrate the entire range of theoretical behavior.

Figs. 28(a)–(c) show the fermionic density of states for the BEC, PG and BCS limits. These figures are important in establishing a precise visual picture of a "pseudogap". The temperatures shown are just above T_c, and for $T = 0.75T_c$ and $T = 0.5T_c$. The methodology for arriving at these plots will be discussed in the following section, in the context of high T_c superconductors. Only in the BCS case is there a clear

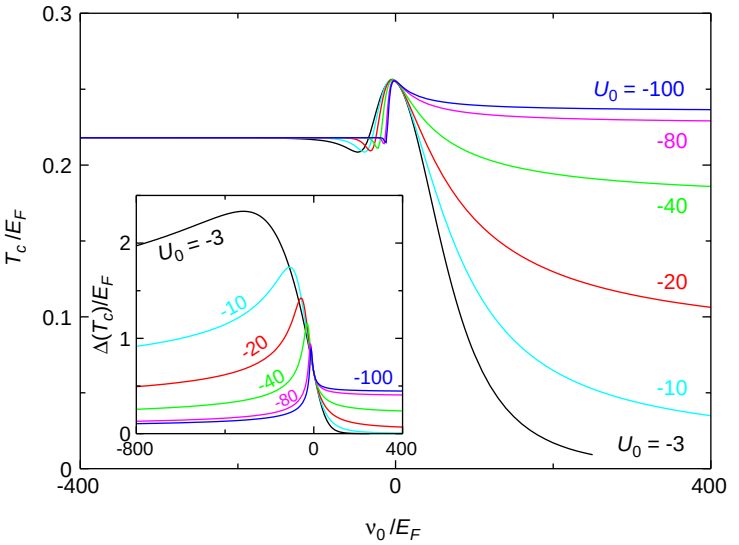

Fig. 27. (Color) Behavior of T_c (main figure) and $\Delta(T_c)$ (inset) at fixed $g_0 = -40E_F/k_F^{3/2}$ with variable U_0. As $U_0 \to -\infty$, unitarity is approached from the BCS side at large positive ν_0. At the same time, $\Delta \propto |g|$ also decreases.

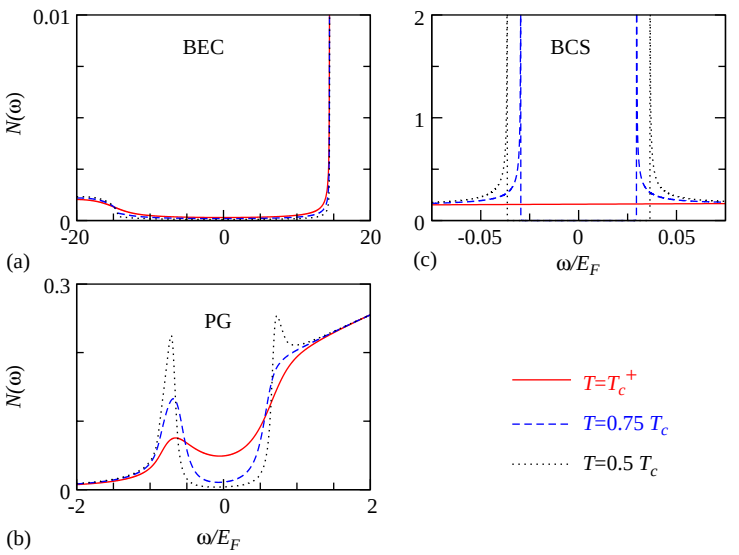

Fig. 28. Typical density of states (DOS) $N(\omega)$ *vs* energy ω in the three regimes at indicated temperatures. There is no depletion of the DOS at T_c in the BCS case. By contrast, in the BEC case, there is a large gap in DOS at T_c, roughly determined by $|\mu|$. In the intermediate, i.e., pseudogap, regime, there is a strong depletion of the DOS already at T_c. Once T decreases below T_c, the DOS decreases rapidly, signalling the superfluid phase transition.

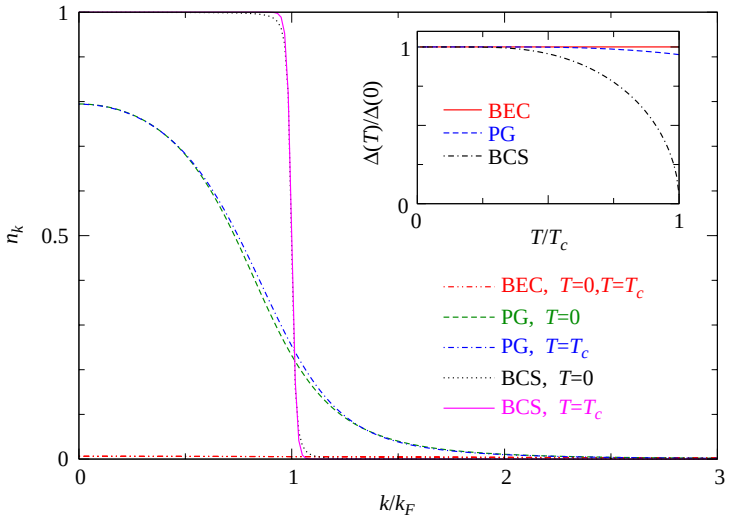

Fig. 29. Typical behavior of the fermionic momentum distribution function n_k at $T = 0$ and T_c in the three regimes for a homogeneous system. The inset indicates the corresponding normalized gaps as a function of T/T_c. In all three regimes, n_k barely changes between $T = T_c$ and 0.

signature of T_c in the density of states, but the gap is so small and T_c is so low, that this is unlikely to be experimentally detectable. Since the fermionic gap is well established in the BEC case, very little temperature dependence is seen as the system goes from the normal to the superfluid states. Only the PG case, where T_c is maximal, indicates the presence of superfluidity, not so much at T_c but once superfluid order is well established at $T = 0.5T_c$, through the presence of sharper coherence features, much as seen in the cuprates.

The inset of Fig. 29 plots the temperature dependence of $\Delta(T)$. It should be stressed that T_c is only apparent in $\Delta(T)$ in the BCS case. To underline this point, in the main body of Fig. 29 we plot the fermionic momentum distribution function n_k, which is the summand in the number equation, Eq. (70), at $T = 0$ and T_c. The fact that there is very little change from $T = 0$ to T_c makes the important point that this momentum distribution function in a homogeneous system is not a good indicator of phase coherent pairing. For the PG case, this, in turn, derives from the fact that $\Delta(T)$ is nearly constant. For the BEC limit the excitation gap, which is dominated by μ, similarly, does not vary through T_c. In the BCS regime, $\Delta(T)$ is sufficiently small so as to be barely perceptible on the scale of the figure.

5.1.1. *Unitary limit and universality*

There has been considerable emphasis on the behavior of fermionic gases near the unitary limit where $a_s = \pm\infty$. Attention (Ho, 2004; Viverit et al., 2004) has concentrated on this limit in the absence of Feshbach bosons. We now want to explore the more general two-channel problem here. At unitarity we require that

$$\frac{4\pi a_s^*}{m} = U_0 + \frac{g_0^2}{2\mu - \nu_0} \tag{129}$$

diverges. This will be consistent, provided

$$v_0 = 2\mu \ . \tag{130}$$

It should be clear that the parameter U_0 is of no particular relevance in the unitary limit. This is to be contrasted with the one channel problem, where Feshbach bosons are absent and unitarity is achieved by tuning the direct inter-fermion interaction, U.

In the unitary limit, the $T = 0$ gap and number equations become

$$1 + U_c \sum_{\mathbf{k}} \frac{1}{2E_{\mathbf{k}}} = 0 \ , \tag{131}$$

and

$$n^{\mathrm{tot}} = 2n_b^0 + n = \frac{2\Delta_0^2}{g_0^2} + \sum_{\mathbf{k}} \left(1 - \frac{\varepsilon_{\mathbf{k}} - \mu}{E_{\mathbf{k}}}\right) \ , \tag{132}$$

where we have used the fact that at unitarity

$$n_b^0 = \frac{g^2\Delta_0^2}{[(2\mu - v)U + g^2]^2} = \frac{\Delta_0^2}{g_0^2} \ , \tag{133}$$

and we define $\Delta_0 \equiv \tilde{\Delta}_{\mathrm{sc}}(T = 0)$. Here U_c is the critical coupling, given in Eq. (17). From these equations it follows that in this limit the values of μ and Δ_0 in the ground state are entirely determined by the Feshbach coupling g_0.

Fig. 30 presents a plot of zero temperature properties showing their dependence on g_0. The two endpoints of the curves are of interest. For arbitrarily small but finite g_0 the unitary limit corresponds roughly to $\mu \approx 0$. Moreover, here the condensate consists exclusively of Feshbach bosons. At large g_0, (which appears to be appropriate to current experiments on ^{6}Li and ^{40}K), the behavior at unitarity is closer to that of the one channel problem (Ho, 2004). Here one finds the so-called universal behavior with parameters $\mu/E_{\mathrm{F}} = 0.59$, and $\Delta/E_{\mathrm{F}} = 0.69$ associated with the simple crossover ground state and a contact potential interaction.[8]

To what extent is the unitary limit of the two channel problem universal? It clearly is not in an absolute sense. However, there is a kind of universality implicit in these $T = 0$ calculations, as can be seen from Fig. 30 if we take into account the fact that there are a reduced number of fermions, as a result of the Bose condensate. We, thus, divide the two zero temperature energy scales by an effective Fermi energy defined by $E'_{\mathrm{F}} = E_{\mathrm{F}}(n/n^{\mathrm{tot}})^{2/3}$ with $n = n^{\mathrm{tot}} - 2n_b^0$. Fig. 30 shows that as g_0 decreases, the effective or rescaled Fermi energy E'_{F} decreases while the Bose condensate fraction increases. The rescaled quantities μ/E'_{F} and Δ/E'_{F} are universal, that is, they are essentially independent of g_0, as seen in the figure. A similar scaling can be done for the Cooper pair size ξ. With a reduced effective Fermi momentum $k'_{\mathrm{F}} = k_{\mathrm{F}}(n/n^{\mathrm{tot}})^{1/3}$, the dimensionless product $k'_{\mathrm{F}}\xi$ is also independent of g_0. We can arrive at some understanding of this modified universality, by referring back to Section 5.1. In summary, the breakdown of universality seen in Fig. 30 is to be associated with a reduced number of fermions, which, in turn derives from the Bose condensate n_b^0. Once n_b^0 is negligible, the distinction between one and two channel models disappears.

[8] In our plots we find small numerical corrections associated with our noninfinite cutoff.

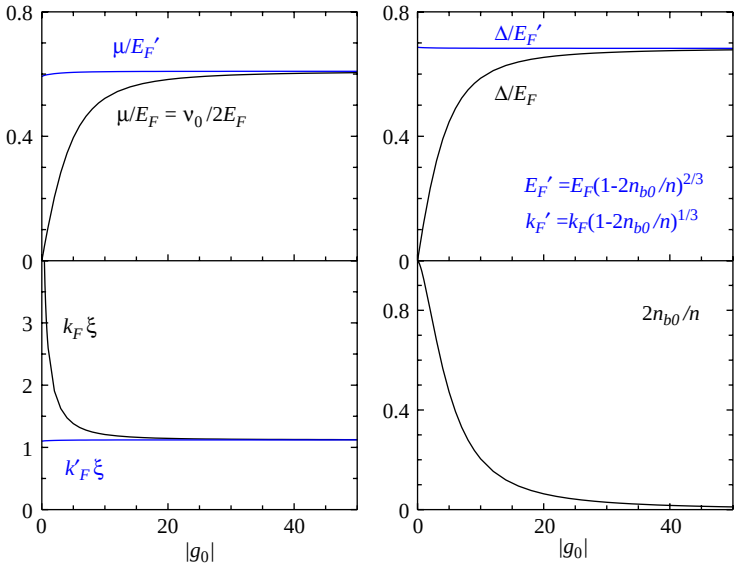

Fig. 30. (Color) Characteristics of the unitary limit at $T = 0$ as a function of $|g_0|$ in the two-channel problem. Here n_{b0} is the density of condensed Feshbach bosons. $E'_{\rm F} = k'^2_{\rm F}/2m$ defines an effective Fermi energy of the fermionic component with a density $n = n^{\rm tot} - 2n_{b0}$. After rescaling, $\mu/E'_{\rm F}$, $\Delta/E'_{\rm F}$, and $k'_{\rm F}\xi$ are essentially a constant in g_0. This indicates that at unitarity, the system can be treated effectively as a two-fluid model at $T = 0$. The units for g_0 are $E_{\rm F}/k_{\rm F}^{3/2}$.

Finite temperature properties, such as T_c and $\Delta(T_c)$ can also be calculated in the unitary limit, as a function of g_0. These are plotted in Fig. 31. Just as for the zero temperature energy scales, these parameters [along with $\mu(T_c)$] increase monotonically with g_0. However, at finite temperatures there are noncondensed Feshbach bosons as well as noncondensed fermion pairs, which interact strongly with each other. These noncondensed states are represented in the lower right inset. Plotted there is the fraction of noncondensed bosons $[n_b(T_c)]$ and sum of both noncondensed fermion pairs and noncondensed bosons $[n_p(T_c)]$ at T_c. These quantities correspond to the expressions shown in Eqs. (80) and (92), respectively.

These noncondensed particles are responsible for the fact that at T_c a simple rescaling will not yield the universality found at $T = 0$. Moreover, these noncondensed bosons and fermion pairs influence calculations of T_c, itself, via pseudogap effects which enter as $\Delta(T_c)$. These pseudogap effects, which are generally ignored in the literature, compete with superconductivity, so that T_c is bounded with its a maximum given by $\approx 0.25T_{\rm F}$, just as seen in Fig. 25, for the one channel problem. Despite the fact that there is no universality, even in the rescaled sense, at T_c one can associate the large g_0 limits with the behavior of the one channel system which has been rather extensively studied in the unitary limit (Ho, 2004). This large g_0 limit seems to be reasonably appropriate for the currently studied Feshbach resonances in ^{6}Li and ^{40}K. In this sense, these particular atomic resonances are well treated by a one channel problem, near the unitary limit.

In summary, comparison between Figs. 30 and 31 reveals that (i) at $T = 0$, all Feshbach bosons and pairs are condensed and the two (fermionic and bosonic) condensates are relatively independent of each other. (ii) By contrast, at $T = T_c$, fermionic quasiparticles, noncondensed fermion pairs and Feshbach bosons all coexist and interact strongly with each other. This destroys the simple scaling found at $T = 0$.

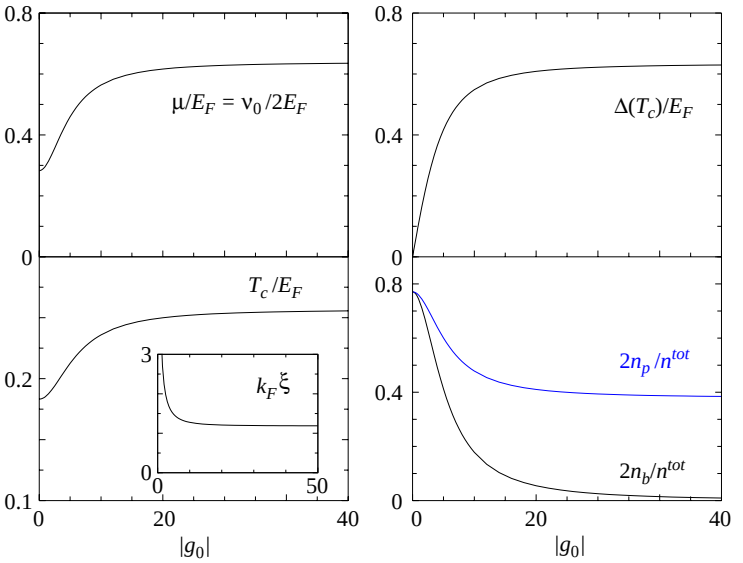

Fig. 31. (Color) Characteristics of the unitary limit at $T = T_c$ as a function of $|g_0|$ in the two channel problem. In contrast to the previous figure for $T = 0$, there is no rescaling which would lead to universal behavior of μ, Δ or ξ with respect to g_0. More than 20% of the system is composed of fermionic quasiparticles when $|g_0| \to 0$. Here n_b and n_p denote the density of noncondensed Feshbach bosons and of the sum of FB and fermion pairs, respectively. The units for g_0 are $E_F/k_F^{3/2}$.

5.1.2. *Weak Feshbach resonance regime:* $|g_0| = 0^+$

The effects of very small yet finite g_0 lead to a nearly bi-modal description of crossover phenomena. Fig. 32 presents the behavior for very narrow Feshbach resonances. It shows that there is a rather abrupt change as a function of magnetic field (via v_0) from a regime in which the condensate is composed only of Feshbach bosons, to one in which it contains only fermion pairs. Depending on the size of g_0, this transition point (taken for concreteness to be where $2n_b^0/n^{\rm tot} \approx 0.5$, for example) varies somewhat, but it seems to occur close to the unitary limit and, importantly, for negative scattering lengths i.e., on the BCS side. This should be contrasted with the large g_0 case). This small g_0 regime of parameter space was explored by Ohashi and Griffin (Ohashi and Griffin, 2002). Indeed the behavior shown in the figure is similar to the physical picture which Falco and Stoof (Falco and Stoof, 2004) presented.

This figure represents a natural evolution in the behavior already indicated by Figs. 23 and 24. Here, however, in contrast to these previous figures the behavior of T_c is essentially monotonic, and the weak maximum and minimum found earlier has disappeared. For this regime, the small pseudogap which can be seen in the upper right panel arises predominantly from the contribution of Feshbach bosons via Eqs. (84) and (91). At the same time it should be noted that the transition from mostly molecular bosons to mostly fermion pairs in the condensate is continuous. While it may look sharp particularly for a plot with a more extended range of v_0 than shown here, this closeup view gives a more precise picture of a smooth crossover transition.

We end by noting that in this small g_0 regime, the system is far from the one channel limit obtained when g_0 is identically 0, as shown in Fig. 25. It should be clear from the above discussion that *Feshbach bosons play a more important role in the regime of unitary scattering the smaller is* g_0, *provided that it does not strictly vanish*.

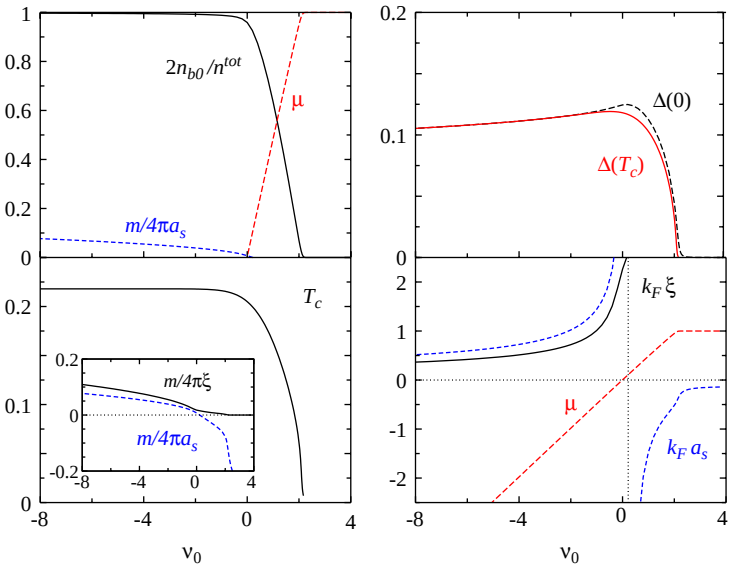

Fig. 32. (Color) Characteristics of the small g_0 limit as a function of ν_0 in the two-channel model. Unless indicated otherwise the plots correspond to $T = 0$. The molecular condensate fraction is very high and there is no maximum at unitarity. The gap Δ is very small ($\propto g_0$). Here we take $g_0 = -1E_F/k_F^{3/2}$ and $U_0 = -3E_F/k_F^3$. Note the very different scales for the abscissa when comparing with Figs. 23 and 24.

5.2. *Superfluidity in traps*

Most experiments on fermionic superfluids are done in the presence of a trap potential $V(r)$. For the most part, this is most readily included at the level of the local density approximation (LDA). In this section, we summarize the self consistent equations for spherical traps $V(r) = \frac{1}{2}m\omega^2 r^2$. T_c is defined as the highest temperature at which the self consistent equations are satisfied precisely at the center. At a temperature T lower than T_c the superfluid region extends to a finite radius R_{sc}. The particles outside this radius are in a normal state. Also important is the radius R_Δ beyond which the excitation gap is effectively zero, to a chosen level of numerical accuracy.

The self consistent equations (with simplified units $\hbar = 1$, fermion mass $m = \frac{1}{2}$, and Fermi energy $E_F = \hbar\omega(3N)^{\frac{1}{3}} = 1$, where ω is the trap frequency) are given in terms of the Feshbach coupling constant g and inter-fermion attractive interaction U by a gap equation

$$1 + \left[U + \frac{g^2}{2\mu - 2V(r) - \nu}\right] \sum_{\mathbf{k}} \frac{1 - 2f(E_{\mathbf{k}})}{2E_{\mathbf{k}}} = 0 \ . \tag{134}$$

which characterizes the excitation gap $\Delta(r)$ at positions r such that $\mu_{\text{pair}}(r) = 0$. Moreover, the pseudogap contribution to $\Delta^2(T) = \tilde{\Delta}_{sc}^2(T) + \Delta_{pg}^2(T)$ is given by

$$\Delta_{pg}^2 = \frac{1}{Z} \sum_{\mathbf{q}} b(\Omega_q - \mu_{\text{pair}}) \ . \tag{135}$$

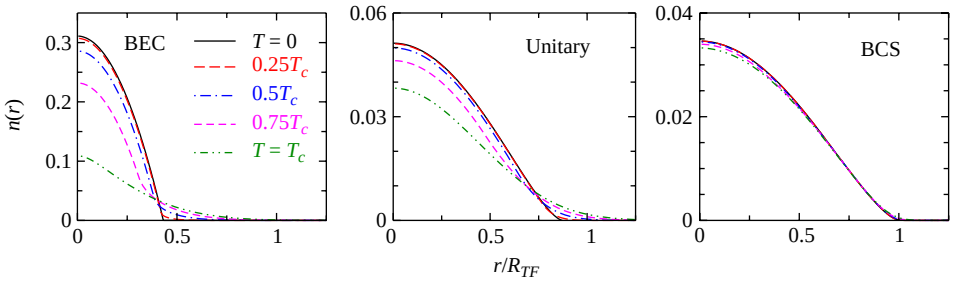

Fig. 33. (Color) Representative spatial profiles of fermions in a harmonic trap potential at various temperatures from T_c to $T = 0$ in the three indicated regimes. As the system evolves from the BCS to the deep BEC regime, the fermion cloud shrinks, and a bimodal distribution of the density develops below T_c. Note the different scales for the vertical axes.

Here b represents the usual Bose function. The density of particles at radius r:

$$n(r) = 2n_b^0 + \frac{2}{Z_b}\sum_{\mathbf{q}} b(\Omega_q - \mu_{\text{boson}}) + 2\sum_{\mathbf{k}}[v_{\mathbf{k}}^2(1 - f(E_{\mathbf{k}})) + u_{\mathbf{k}}^2 f(E_{\mathbf{k}})]\ . \tag{136}$$

The important quantity $\mu_{\text{pair}} = \mu_{\text{boson}}$ is identically zero in the superfluid region $r < R_{\text{sc}}$, and must be solved for self consistently at larger radii. Here M is the bare boson mass equal to $2m$, and the various residues, Z and Z_b and pair dispersion Ω_q are described in Section 2.3.

The transition temperature T_c is numerically determined as follows: (i) a chemical potential is assigned to the center of the trap $\mu(0)$. The chemical potential at radius r will then be $\mu(r) = \mu(0) - V(r)$. (ii) the gap equation [Eq. (134)] and pseudogap equation [Eq. (135)] are solved at the center (setting $\Delta_{pg} = \Delta$) to find T_c and $\Delta(0, T_c)$ (iii) next, the radius R_Δ is determined. (It can be defined as the point where the gap has a sufficiently small value, such as $\Delta(0, T_c)/1000$). (iv) Following this, the pseudogap equation [Eq. (135)] is solved for $\Delta(r, T_c)$ up to the radius R_Δ. Then $n(r)$ is determined using Eq. (136). (v) Finally, $n(r)$ is integrated over all space ($\int \mathrm{d}^3\mathbf{r}n(r)$) and compared with the given total number of fermions N. The procedure is repeated until the prescribed accuracy has been reached. To extend this algorithm below T_c a similar approach is used which now includes an additional step in which R_{sc} is computed.

Fig. 33 shows a plot of the density profiles obtained from solving the self consistent equations. Here the Thomas–Fermi radius, called R_{TF}, is calculated for the noninteracting case. In the BCS regime there is virtually no temperature dependence in the density profile as expected from the small values for Δ. In the unitary and BEC regimes as the system approaches T_c, $n(r)$ can be reasonably well fit to a Gaussian. A bi-modality in the distribution is evident in the BEC regime, thus providing a clear signature of the superfluid phase. However, in the PG or unitary case it is more difficult to establish superfluidity, since the profiles do not show a clear break at the position where the condensate first appears (Stajic et al., 2005a).

These observations differ somewhat from other theoretical predictions in the literature (Chiofalo et al., 2002; Ho, 2004). The differences between the present theory and this other work can be associated with the inclusion of noncondensed pairs or pseudogap effects. These noncondensed pairs smooth out the otherwise abrupt transition between the condensate and the fermionic excitations. In contrast to earlier work (Perali et al., 2004b) these studies, which are based on the standard crossover ground state (Leggett, 1980), yield only monotonic density distributions. Future experiments will be needed to look

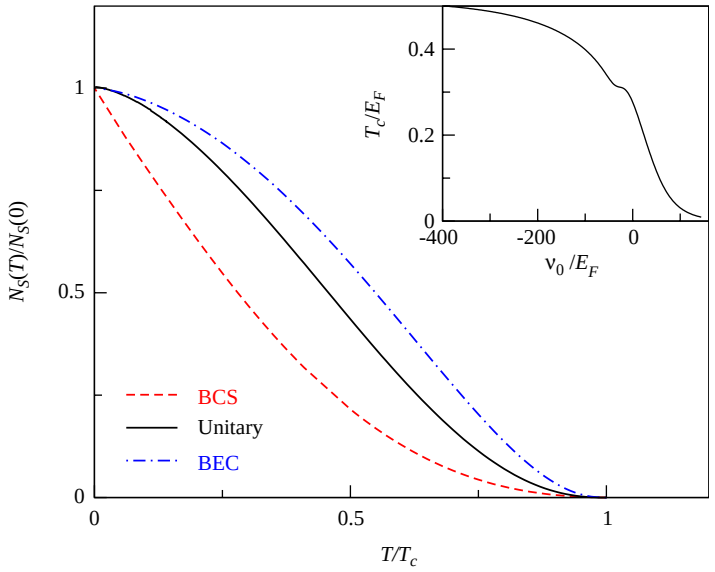

Fig. 34. Behavior of superfluid density N_s as a function of T in the three different regimes. Note that the negative curvatures at low T for the unitary and BEC cases are different from the linear behavior in the BCS case. In the BEC limit, $N - N_s \propto T^{3/2}$. In the inset we show T_c as a function of magnetic detuning ν_0 in a trap. We have taken $U_0 = -0.9E_F/k_F^3$ and $g_0 = -35E_F/k_F^{3/2}$, based on experimental data for ^{40}K.

for the secondary maxima predicted by Strinati and co-workers (Perali et al., 2004a) in the BEC and unitary regimes.

Finally, Fig. 34 shows the behavior of T_c (inset) in a trap, together with the superfluid density (main figure). The latter is computed following the discussion in Section 3. From the inset one can read off that $T_c/E_F \approx 0.3$ at resonance, which is very close to (Perali et al., 2004a), or slightly smaller than other estimates (Ohashi and Griffin, 2003) in the literature.

The structure seen in the plot of T_c for the trapped gas reflects the minimum and maximum found for the homogeneous solution (Fig. 23); these are related, respectively, to where $\mu \approx 0$ and where unitary scattering occurs. The T_c curve follows generally the decrease in the density at the center of the trap from BEC to BCS. The temperature dependences of the (integrated over r) superfluid density reflect the nature of excitations of the condensate. The BEC limit has only bosonic, while the BCS has only fermionic excitations. The unitary case is somewhere in between. The fermionic contributions are apparent in the BCS regime, where N_s decreases almost linearly at low T. For an s-wave superfluid this reflects the contributions from low $\Delta(r) \leqslant T$ regions, near the edge of the trap. These are present to a lesser degree in the unitary case. The bosonic contribution to N_s and to thermodynamics (in both the BEC and unitary regimes) is governed by the important constraint that $\mu_{\text{pair}}(r)$ vanishes at positions r where there is a co-existent superfluid. A similar constraint is imposed at the level of Hartree–Fock–Bogoliubov theory for true bosons (Shi and Griffin, 1998). These gapless pair excitations are responsible for a $T^{3/2}$ temperature dependence in N_s. In this way the low T power law dependences are similar to their analogues in the homogeneous case of Section 6.4, much as found for true Bose gases (Carr et al., 2004) in a trap.

As for the BEC regime there is an interesting observation to make about the contribution to the density profile associated with the condensate. Experimentalists generally assume a Gaussian form throughout the trap for the noncondensed pairs. In this way they estimate the condensate fraction. Here we find (Stajic et al., 2005a) that this Gaussian form is not correct in the superfluid region of the trap, and that this Gaussian approximation will underestimate (by $\approx$ a factor of 1.5) the condensate fraction in the BEC regime.

5.3. Comparison between theory and experiment: cold atoms

As time progresses it will be important to assess the assumed ground state wavefunction (Leggett, 1980) and its two channel variant (Milstein et al., 2002; Ohashi and Griffin, 2002; Stajic et al., 2005b) in more detail. A first generation set of measurements and theories have indicated an initial level of success in addressing four experiments: RF pairing gap spectroscopy and collective mode measurements, as well as more recently, the particle density profiles (Stajic et al., 2005a) and thermodynamics (Kinast et al., 2005) of Fermi gases in the unitary regime. The first of these experiments (Chin et al., 2004) seem to provide some support for the fact that the Bogoliubov excitations with dispersion, $E_{\mathbf{k}} \equiv \sqrt{(\varepsilon_{\mathbf{k}} - \mu)^2 + \Delta^2(T)}$ have a "gap parameter", $\Delta(T)$ which is in general different from the superconducting order parameter, as a consequence of noncondensed pairs at and above T_c. Torma and colleagues (Kinnunen et al., 2004b) have used the formalism outlined in Section 2.2, to address RF spectroscopy. Subsequently (Kinnunen et al., 2004a) they have combined this analysis with an approximate LDA treatment of the trap to make contact with RF experiments (Chin et al., 2004). Important to their work is the fact that the edges of a trap have a free atom character, where there is a vanishing $\Delta(r)$.

Additional support for the wavefunction comes from the collective mode behavior near $T = 0$. The mode frequencies can be connected to an equation of state (Stringari, 2004). Numerical studies (Heiselberg, 2004b; Hu et al., 2004) of this equation for the standard crossover ground state demonstrate a good fit to the measured breathing mode frequencies (Bartenstein et al., 2004a; Kinast et al., 2004). Importantly, in the near-BEC limit the frequencies decrease with increasing magnetic field; this is opposite to the behavior predicted for true bosons (Stringari, 2004), and appears to reenforce the notion that for the magnetic fields studied thus far, the "BEC" regime should be associated with composite rather than real bosons.

At $T = 0$, calculations of the collective mode frequencies are based on an equation of state. Moreover, the zero temperature equation of state associated with the mean field ground state can be computed analytically in the near-BEC limit

$$\mu = -\frac{1}{2ma_s^2} + \frac{\pi a_s n}{m} - \frac{3(\pi n a_s^3)^2}{4ma_s^2} + O(n^3) \ ,$$

where the first two terms on the right hand side were previously discussed following Eq. (55). Importantly, the third (negative) term is responsible for the observed agreement between theory and collective mode experiments, in the near-BEC regime.

A serious shortcoming of the wavefunction ansatz has been emphasized in the literature. This is associated with the ratio of the inter-boson to the fermionic scattering length near the unitary regime, but on the BEC side of the Feshbach resonance. Experimentally the numbers are considerably smaller (Bartenstein et al., 2004b; Zwierlein et al., 2004) (0.6) than the factor of 2 predicted for the one channel model discussed below Eq. (55). They are consistent, however, with more exact few body calculations (Petrov et

al., 2004). These few body calculations presumably apply to a regime of magnetic fields where $k_F a_s$ is around 0.3–0.4 or smaller. This seems to be close to the boundary for the "quasi-BEC" regime which can be accessed experimentally (Bartenstein et al., 2004b) in ^{6}Li.

It is interesting to repeat the $T = 0$ many body calculations now with the inclusion of FB, since (for ~ 40 K) these two channel effects begin to be important at $k_F a_s$ smaller than around 0.2–0.25. Here, one sees (Stajic et al., 2005b), that the factor of 2 found in the one channel calculations is no longer applicable, and the values of the ratio (of bosonic to fermionic scattering lengths) are considerably smaller, and, thus, tending in the direction which is more in line with experiment. This reflects the decrease in the number of fermionic states which mediate the interaction between molecular bosons.

In this way the mean field theory presented here looks promising. Nevertheless, uncertainties remain. Current theoretical work (Kinnunen et al., 2004a) on the RF experiments is limited to the intermediate coupling phase, while experiments are also available for the near-BEC and near-BCS regimes, and should be addressed theoretically. In addition, the predictions of alternative approaches (Perali et al., 2004b) which posit a different ground state will need to be compared with these RF data. The collective mode calculations (Heiselberg, 2004b; Hu et al., 2004) which have been performed have not yet considered the effects of Feshbach bosons, which may change the behavior in the deeper BEC regime.

It is, finally, quite possible that incomplete $T = 0$ condensation will become evident in future experiments. If so, an alternative wavefunction will have to be contemplated. Indeed, it has been argued (Holland et al., 2004) that the failure of the one channel model to match the calculations of Petrov and co-workers (Petrov et al., 2004) is evidence that there are serious weaknesses. At an experimental level, new pairing gap spectroscopies appear to be emerging at a fairly rapid pace (Bruun and Baym, 2004; Greiner et al., 2005) which will further test these and subsequent theories.

6. Physical implications: high T_c superconductivity

We begin with an important caveat that many of the experiments outlined in this section can alternatively be addressed from a Mott physics point of view (Lee et al., 2004). Here we summarize the interpretation of these experiments within BCS–BEC crossover theory with the hope that this discussion will be of value to the cold atom community, and that ultimately, it will help to establish precisely how relevant is the BCS–BEC crossover scenario for understanding high temperature superconductivity.

6.1. Phase diagram and superconductor–insulator transition: boson localization effects

The high T_c superconductors are different from the ultracold fermionic superfluids in one key respect; they are *d*-wave superconductors and their electronic dispersion is associated with a quasi-two dimensional tight binding lattice. In many ways this is not a profound difference from the perspective of BCS–BEC crossover. Fig. 35 shows a plot of the two important temperatures T_c and T^* as a function of increasing attractive coupling. On the left is BCS and the right is PG. The BEC regime is not apparent. This is because T_c disappears before it can be accessed. At the point where T_c vanishes, $\mu/E_F \approx 0.8$.

A competition between increasing T^* and T_c is also apparent in Fig. 35. This is a consequence of pseudogap effects. There are fewer low energy fermions around to pair, as T^* increases. It is interesting to compare Fig. 35 with the experimental phase diagram plotted as a function of x in Fig. 7. If one inverts the horizontal axis (and ignores the AFM region, which is not addressed here) the two are very similar. To

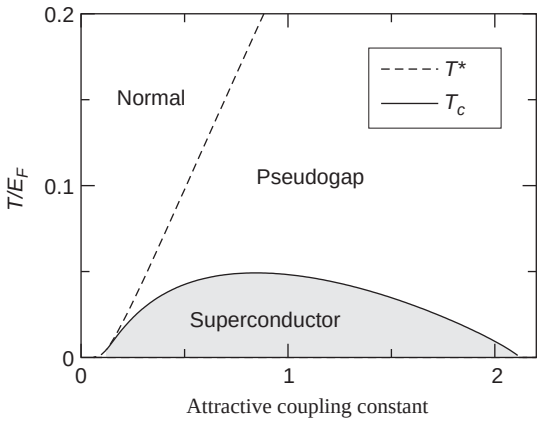

Fig. 35. Phase diagram for a quasi-two dimensional (2D) *d*-wave superconductor on a lattice. Here the horizontal axis corresponds to the strength of attractive interaction $-U/4t$, where t is the in-plane hopping matrix element.

make an association between the coupling U and the variable x, it is reasonable to simply fit $T^*(x)$. We do not dwell on this last step here, since we wish to emphasize crossover effects which are not complicated by "Mott physics".

Because of quasi-two dimensionality, the energy scales of the vertical axis in Fig. 35 are considerably smaller than their three dimensional analogues. Thus, pseudogap effects are intensified, just as conventional fluctuation effects are more apparent in low dimensional systems. This may be one of the reasons why the cuprates are among the first materials to clearly reveal pseudogap physics. Moreover, the present calculations show that in a strictly $2D$ material, T_c is driven to zero, by bosonic or fluctuation effects. This is a direct reflection of the fact that there is no Bose condensation in $2D$.

Fig. 36 presents a plot (Chen et al., 1999) of boson localization effects associated with *d*-wave pairing. A divergence in the effective mass m/M^* occurs when the coupling strength, or equivalently T^* becomes sufficiently large. Once the bosons localize the system can no longer support superconductivity and T_c vanishes. It is generally believed that a system of bosons with short range repulsion is either a superfluid or a Mott insulator in its ground state (Fisher et al., 1989). Moreover, the insulating phase is presumed to contain some type of long range order. Interestingly, there are recent reports of ordered phases (Fu et al., 2004; Vershinin et al., 2004) in the very underdoped cuprates. These appear on the insulating side and possibly penetrate across the superconductor-insulator boundary; they have been interpreted by some as Cooper pair density waves (Chen et al., 2004; Melikyan and Tešanović, 2004; Tešanović, 2004). The observation of boson localization appears to be a natural consequence of BCS–BEC theory; it should be stressed that it is associated with the *d*-wave lattice case. Because *d*-wave pairs are more spatially extended (than their *s*-wave counterparts) they experience stronger Pauli repulsion (Chen et al., 1999) and this inhibits their hopping.

6.2. Superconducting coherence effects

The presence of pseudogap effects raises an interesting set of issues surrounding the signatures of the transition which the high T_c community has wrestled with, much as the cold atom community is doing

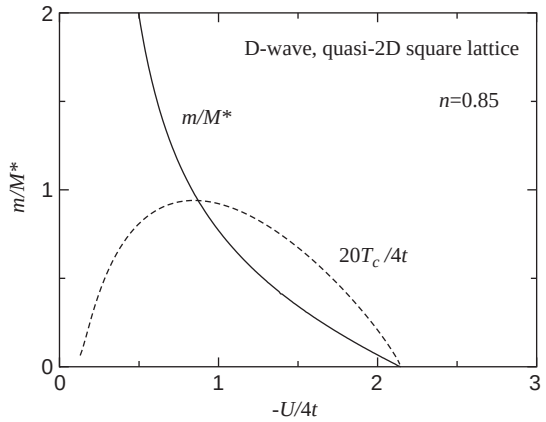

Fig. 36. Inverse pair mass (solid line) and T_c (dashed line) as a function of coupling strength $-U/4t$ for a d-wave superconductor on a quasi-2D square lattice, where t is the in-plane hopping matrix element. T_c vanishes when the pair mass diverges, before the bosonic regime is reached. The electron density is taken to be $n = 0.85$ per unit cell, corresponding to optimal hole doping in the cuprate superconductors.

today. For a charged superconductor there is no difficulty in measuring the superfluid density, through the electrodynamic response. Thus one knows with certainty where T_c is. Nevertheless, people have been concerned about precisely how the onset of phase coherence is reflected in thermodynamics, such as C_V or in the fermionic spectral function. One understands how phase coherence shows up in BCS theory, since the ordered state is always accompanied by the appearance of an excitation gap. When a gap is already well developed at T_c, how do these signatures emerge?

To address these coherence effects one has to introduce a distinction between the self energy (Chen et al., 2001) associated with noncondensed and condensed pairs. This distinction is blurred by the approximation of Eq. (89). Above, but near T_c, or at any temperature below we now use an improved approximation (Maly et al., 1999a, b)

$$\Sigma_{pg} \approx \frac{\Delta^2}{\omega + \xi_{\mathbf{k}} + \mathrm{i}\gamma} \,. \tag{137}$$

This is to be distinguished from Σ_{sc} where the condensed pairs are infinitely long-lived and there is no counterpart for γ. The value of this parameter, and even its T-dependence is not particularly important, as long as it is nonzero.

Fig. 37 plots the fermionic spectral function at $\xi_{\mathbf{k}} = 0$, called $A(\omega)$, as the system passes from above to below T_c. One can see in this figure that just below T_c, $A(\omega)$ is zero at a point $\omega = 0$, and that as temperature further decreases the spectral function evolves smoothly into approximately two slightly broadened delta functions, which are just like their counterparts in BCS. In this way there is a clear signature associated with superconducting coherence. To compare with experimental data is somewhat complicated, since measurements of the spectral function (Campuzano et al., 2004; Damascelli et al., 2003) in the cuprates also reveal other higher energy features ("dip, hump and kink"), not specifically associated with the effects of phase coherence. Nevertheless, this Figure, like its experimental counterpart, illustrates that sharp gap features can be seen in the spectral function, but only below T_c.

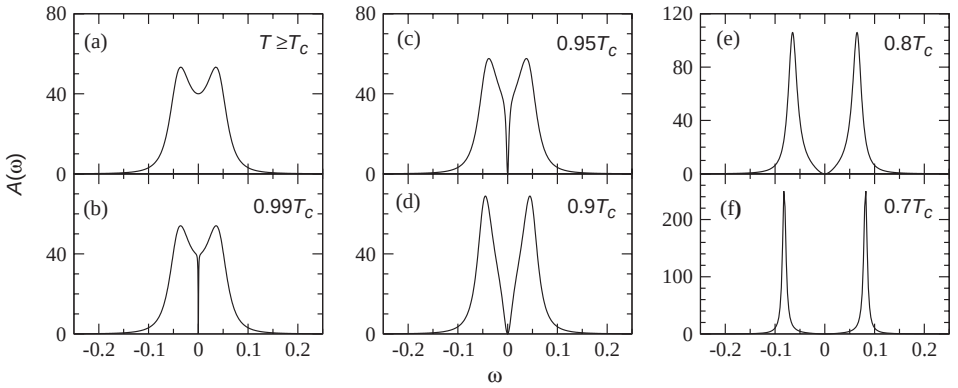

Fig. 37. Evolution of spectral functions of a pseudogapped superconductor with temperature. As soon as T drops below T_c, the spectral peaks split up rapidly, signalling the onset of phase coherence.

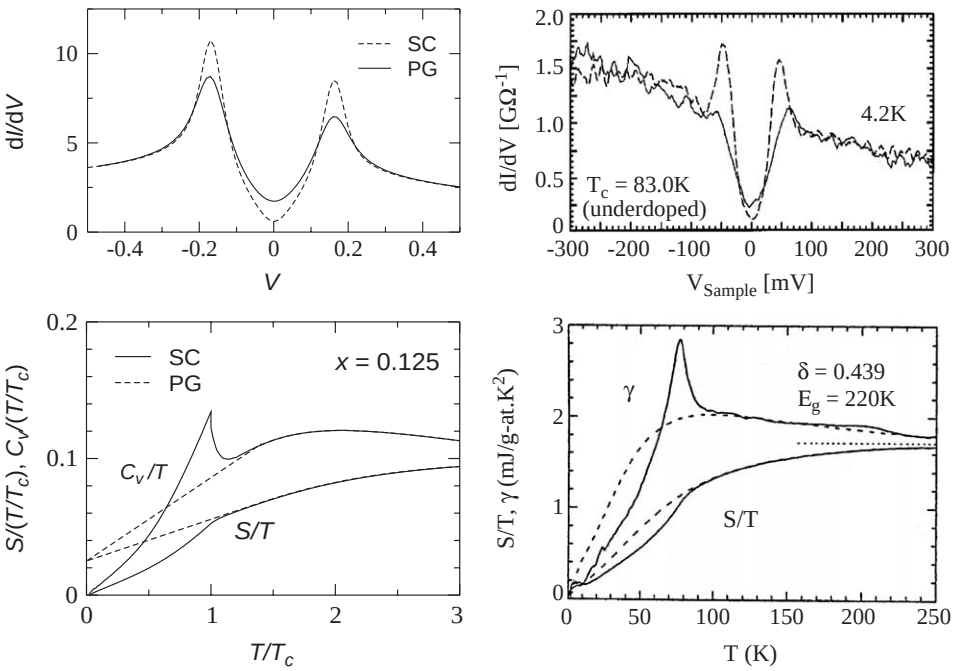

Fig. 38. Superconducting state (SC) and extrapolated normal state (PG) contributions to SIN tunneling characteristics $\mathrm{d}I/\mathrm{d}V$ (upper panels) and thermodynamics S/T and C_v/T (lower panels). We compare theoretical calculations (left) with experiments (right) on tunneling for BSCCO from (Renner et al., 1998) and on specific heat for $Y_{0.8}Ca_{0.2}Ba_2Cu_3O_{7-\delta}$ (YBCO) from Tallon and Loram (2001). The theoretical SIN curve is calculated for $T = T_c/2$, while the experimental curves are measured outside (dashed line) and inside (solid line) a vortex core. The *dashed and solid* curves in the upper left panel are for SC and PG state, respectively. In both lower panels, the *solid and dashed* curves indicate the SC and PG state, respectively.

Analogous plots of superconducting coherence effects are presented in Fig. 38 in the context of more direct comparison with experiment. Shown are the results of specific heat and tunneling calculations and their experimental counterparts (Renner et al., 1998; Tallon and Loram, 2001). The latter measures,

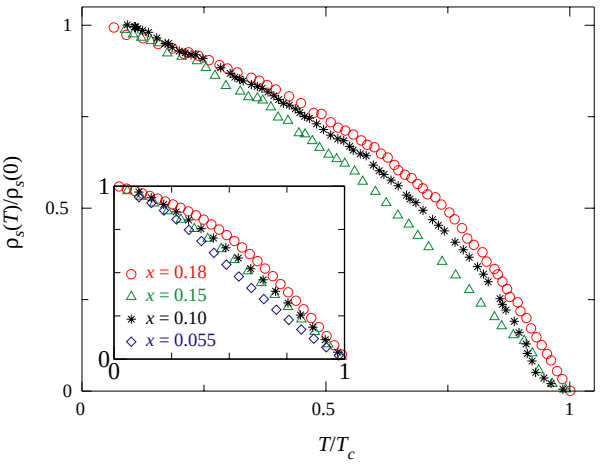

Fig. 39. Comparison of normalized superfluid density $\rho_s/\rho_s(0)$ versus T/T_c for experiment (main figure) and theory (inset) in high T_c superconductors with variable doping concentration x. Both experiment and theory show a quasi-universal behavior with respect to doping.

effectively, the density of fermionic states. Here the label "PG" corresponds to an extrapolated normal state in which we set the superconducting order parameter Δ_{SC} to zero, but maintain the total excitation gap Δ to be the same as in a phase coherent, superconducting state. Agreement between theory and experiment is satisfactory. We present this artificial normal state extrapolation in discussing thermodynamics in order to make contact with its experimental counterpart. However, it should be stressed that in zero magnetic field, there is no coexistent nonsuperconducting phase. BCS theory is a rather special case in which there are two possible phases below T_c, and one can, thereby, use this coexistence to make a reasonable estimate of the condensation energy. When Bose condensation needs to be accommodated, there seems to be no alternative "normal" phase below T_c.

6.3. *Electrodynamics and thermal conductivity*

In some ways the subtleties of phase coherent pairing are even more perplexing in the context of electrodynamics. Fig. 12 presents a paradox in which the excitation gap for fermions appears to have little to do with the behavior of the superfluid density. To address these data (Stajic et al., 2003b) one may use the formalism of Section 3.1. One has to introduce the variable x (which accounts for Mott physics) and this is done via a fit to $T^*(x)$ in the phase diagram. Here for Fig. 40 it is also necessary to fit $\rho_s(T=0,x)$ to experiment, although this is not important in Fig. 39. The figures show a reasonable correspondence (Stajic et al., 2003b) with experiment. The paradox raised by Fig. 12 is resolved by noting that there are bosonic excitations of the condensate, as in Eq. (113) and that these become more marked with underdoping, as pseudogap effects increase. In this way ρ_s does not exclusively reflect the fermionic gap, but rather vanishes "prematurely" before this gap is zero, as a result of pair excitations.

The optical conductivity $\sigma(\omega)$ is similarly modified (Iyengar et al., 2003; Timusk and Statt, 1999). Indeed, there is an intimate relation between ρ_s and $\sigma(\omega)$ known as the f-sum rule. Optical conductivity studies in the literature, both theory and experiment, have concentrated on the low ω, T regime and the

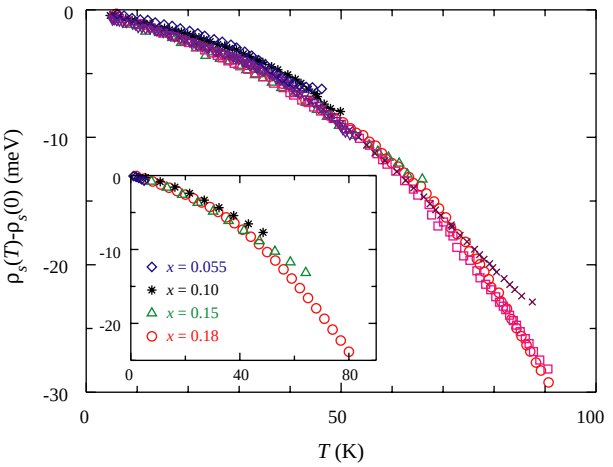

Fig. 40. Offset plot of superfluid density ρ_s comparing experiment (main figure) with theory (inset). Both experiment and theory show the same quasi-universal slope $\mathrm{d}\rho_s/\mathrm{d}T$ for different hole concentrations x.

interplay between impurity scattering and d wave superconductivity (Berlinsky et al., 2000). Also of interest are unusually high ω tails (Molegraaf et al., 2002; Santander-Syro et al., 2003) in the real part of $\sigma(\omega)$ which can be inferred from sum-rule arguments and experiment. Fig. 12 raises a third set of questions which pertain to the more global behavior of σ. In the strong PG regime, where Δ has virtually no T dependence below T_c, the BCS-computed $\sigma(\omega)$ will be similarly T-independent. This is in contrast to what is observed experimentally where $\sigma(\omega)$ reflects the same T dependence as in $\rho_s(T)$, as dictated by the f-sum rule.

One may deduce a consequence of this sum rule, based on Eq. (113). If we associate the fermionic contributions with the first term in square brackets in this equation, and the bosonic contributions with the second. Note that the fermionic transport terms reflect the full Δ just as do the single particle properties. (This may be seen by combining the superconducting and Maki Thompson or PG diagrams in Appendix B). We may infer a sum rule constraint on the bosonic contributions, which vanish as expected in the BCS regime where Δ_{pg} vanishes. We write

$$\frac{2}{\pi}\int_0^\infty \mathrm{d}\Omega\, \sigma^{\mathrm{bosons}}(\Omega, T) = \frac{\Delta_{pg}^2}{\Delta^2}\left(\frac{n_s}{m}\right)^{\mathrm{BCS}}(T)\ . \tag{138}$$

The bosonic contributions can be determined most readily from a framework such as time dependent Ginzburg–Landau theory, which represents rather well the contributions from the Aslamazov–Larkin diagrams, discussed in Appendix B. The bosons make a maximum contribution at T_c.

The resulting optical conductivity (Iyengar et al., 2003) in the superconducting state is plotted in Fig. 41 below. The key feature to note is the decrease in width of the so-called Drude peak with decreasing temperature. In the present picture this pseudogap effect can be understood as coming from the contribution of bosonic excitations of the condensate, which are present at T_c, but which disappear at low T. This behavior is reasonably consistent with what is reported experimentally (Timusk and Statt, 1999), where "the effect of the opening of a pseudogap is a narrowing of the coherent Drude peak at low frequency".

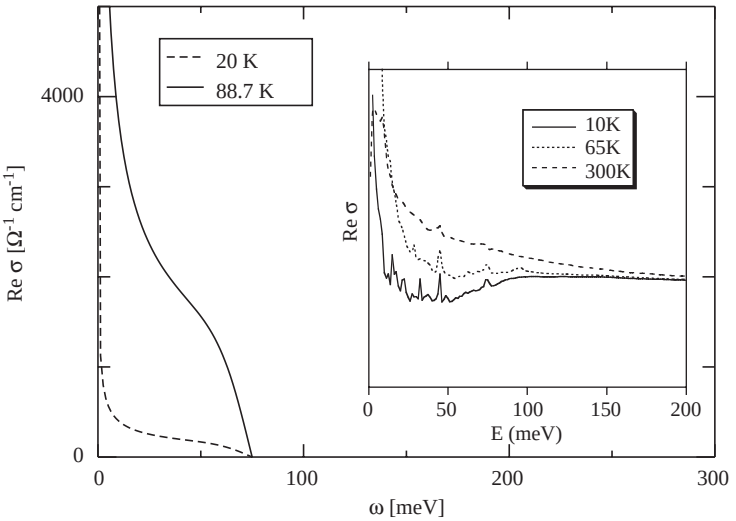

Fig. 41. Real part of ac conductivity at low and high T below T_c. Here pseudogap effects, which insure that $\Delta(T) \approx$ *constant* below T_c, require that one go beyond BCS theory to explain the data shown in the inset (Puchkov et al., 1996). In the theory, inelastic and other effects which presumably lead to the large constant background term observed in the data have been ignored.

The calculations leading to Fig. 41, indicate that by 20 K most of the conductivity is fermionic except for a high frequency tail associated with the bosons. This tail may be responsible in part for the anomalously high ω contributions to σ required to satisfy the sum rule (Molegraaf et al., 2002; Santander-Syro et al., 2003).

Although the normal state calculations have not been done in detail, once the temperature is less than T^*, pseudogap effects associated with the fermionic contribution will also lead to a progressive narrowing in the Drude peak with decreasing T, down to T_c, due to the opening of an excitation gap. This mechanism (which is widely ascribed to (Timusk and Statt, 1999) in the literature) reflects longer lived electronic states, associated with the opening of this gap. However, it cannot be applied to explain the progressive narrowing of the conductivity peaks, once $\Delta(T)$ becomes temperature independent, as is the case at low T. In this way, one can see that pseudogap effects show up in the optical conductivity of underdoped samples, both from the fermionic contributions (near and below T^*) and the bosonic contributions (below T_c) as a narrowing of the Drude peak.

The data shown in the inset of Fig. 41 reveal that the condensate is made from frequency contributions primarily up to ≈ 0.15 eV. These data pose a challenge for applying strict BCS theory to this problem, since one consequence of a temperature independent Δ in the underdoped phase is the absence of T dependence in the optical conductivity. This is the same challenge as posed by Fig. 12. Strikingly there is no explicit "gap feature" in the optical conductivity in the normal state. Such a gap feature, that is a near vanishing of σ for an extended range of frequencies, will occur in models where the pseudogap is unrelated to superconductivity; it is not seen experimentally, thus far.

By contrast with the electrical conductivity, the thermal conductivity is dominated by the fermionic contributions at essentially all T. This is because the bosonic contribution to the heat current (as in standard TDGL theory (Larkin and Varlamov, 2001)), is negligibly small, reflecting the low energy scales

of the bosons. Thermal conductivity, experiments (Sutherland et al., 2003) in the high T_c superconductors provide some of the best evidence for the presence of fermionic d-wave quasiparticles below T_c. In contrast to the ac conductivity, here one sees a universal low T limit (Lee, 1993), and there is little to suggest that something other than conventional d-wave BCS physics is going on here. This cannot quite be the case however, since in the pseudogap regime, the temperature dependence of the fermionic excitation gap is highly anomalous, as shown in Fig. 3, compared to the BCS analogue.

6.4. Thermodynamics and pair-breaking effects

The existence of noncondensed pair states below T_c affects thermodynamics, in the same way that electrodynamics is affected, as discussed above. Moreover, one can predict (Chen et al., 2000) that the q^2 dispersion will lead to ideal Bose gas power laws in thermodynamical and transport properties. These will be present in addition to the usual power laws or (for s-wave) exponential temperature dependences associated with the fermionic quasiparticles. Note that the q^2 dependence reflects the spatial extent ξ_{pg}, of the composite pairs, and this size effect has no natural counterpart in true Bose systems. It should be stressed that numerical calculations show that these pair masses, as well as the residue Z are roughly T independent constants at low T. As a result, Eq. (94) implies that $\Delta_{pg}^2 = \Delta^2(T) - \Delta_{\rm sc}^2(T) \propto T^{3/2}$.

The consequences of these observations can now be listed (Chen et al., 2000). For a quasi-two dimensional system, C_v/T will appear roughly constant at the lowest temperatures, although it vanishes strictly at $T = 0$ as $T^{1/2}$. The superfluid density $\rho_s(T)$ will acquire a $T^{3/2}$ contribution in addition to the usual fermionic terms. By contrast, for spin singlet states, there is no explicit pair contribution to the Knight shift. In this way the low T Knight shift reflects only the fermions and exhibits a scaling with $T/\Delta(0)$ at low temperatures. Experimentally, in the cuprates, one usually sees a finite low T contribution to C_v/T. A Knight shift scaling is seen. Finally, also observed is a deviation from the predicted d-wave linear in T power law in ρ_s. The new power laws in C_v and ρ_s are conventionally attributed to impurity effects, where $\rho_s \propto T^2$, and $C_v/T \propto const$. Experiments are not yet at a stage to clearly distinguish between these two alternative explanations.

Pair-breaking effects are viewed as providing important insight into the origin of the cuprate pseudogap. Indeed, the different pair-breaking sensitivities of T^* and T_c are usually proposed to support the notion that the pseudogap has nothing to do with superconductivity. To counter this inference, a detailed set of studies was conducted, (based on the BEC–BCS scenario), of pair-breaking in the presence of impurities (Chen and Schrieffer, 2002; see also Kao et al., 2002) and of magnetic fields (Kao et al., 2001). These studies make it clear that the superconducting coherence temperature T_c is far more sensitive to pair-breaking than is the pseudogap onset temperature T^*. Indeed, the phase diagram of Fig. 35 which mirrors its experimental counterpart, shows the very different, even competing nature of T^* and T_c, despite the fact that both arise from the same pairing correlations.

6.5. Anomalous normal state transport: Nernst and other precursor transport contributions

Much attention is given to the anomalous behavior of the Nernst coefficient in the cuprates (Xu et al., 2000). This coefficient is rather simply related to the transverse thermoelectric coefficient α_{xy} which is plotted in Fig. 13. In large part, the origin of the excitement in the literature stems from the fact that the Nernst coefficient behaves smoothly through the superconducting transition. Below T_c it is understood to be associated with superconducting vortices. Above T_c if the system were a Fermi liquid, there are

arguments to prove that the Nernst coefficient should be essentially zero. Hence the observation of a nonnegligible Nernst contribution has led to the picture of normal state vortices.

Another way to view these data is that there are bosonic degrees of freedom present in the normal state, as in the BCS–BEC crossover approach. To describe this dynamics we begin with the TDGL scheme outlined in Section 1.8.1. This formalism must be modified somewhat however. When "pre-formed" pairs are present at temperatures T^* high compared to T_c, the classical bosonic fields of conventional TDGL must be replaced by their quantum counterparts (Tan and Levin, 2004). We investigate this fairly straightforward extension of TDGL in the next sub-section, and subsequently explore the resulting implications for transport.

6.5.1. Quantum extension of TDGL

To make progress on the quantum analogue of TDGL we study a Hamiltonian describing bosons coupled to a particle reservoir of fermion pairs. The latter are addressed in a quantum mechanical fashion. Our treatment of the reservoir has strong similarities to the approach of Caldeira and Leggett (1983). These bosons are in the presence of an electromagnetic field, which interacts with the fermion pairs of the reservoir as well, since they have charge $e^* = 2e$. For simplicity we assume that the fermions are dispersionless. This Hamiltonian is given by

$$\begin{aligned} H = & \sum_{\mathbf{lm}} \varepsilon_{\mathbf{lm}} \psi_{\mathbf{l}}^{\dagger}(t) \exp(-\mathrm{i}e^* C_{\mathbf{lm}}(t)) \psi_{\mathbf{m}}(t) \\ & + \sum_{\mathbf{l}} e^* \phi \psi^{\dagger} \psi + \sum_{i\mathbf{l}} \{(a_i + e^* \phi) w_i^{\dagger} w_i + \eta_i \psi^{\dagger} w_i + \eta_i^* w_i^{\dagger} \psi\} \\ & + \sum_{i\mathbf{l}} \{(b_i - e^* \phi) v_i^{\dagger} v_i + \zeta_i \psi^{\dagger} v_i^{\dagger} + \zeta_i^* v_i \psi\} \ . \end{aligned} \tag{139}$$

Here $\varepsilon_{\mathbf{lm}}$ is the hopping matrix element for the bosons. $C_{\mathbf{lm}}(t)$ is the usual phase factor associated with the vector potential. Annihilation operators for the reservoir, w_i and v_i (with infinitesimal coupling constants η_i and ζ_i), represent positive and negative frequencies respectively and need to be treated separately. The energies a_i and b_i of the reservoir are both positive.

The bosonic propagator $T(\mathbf{k}, \omega)$ can be exactly computed from the equations of motion. Here $A(\mathbf{k}, \omega) = \mathrm{Re}2\mathrm{i}T(\mathbf{k}, \omega)$ is the boson spectral function, and

$$T(\mathbf{k}, \omega) \equiv \left(\omega - \varepsilon(\mathbf{k}) - \Sigma_1(\omega) + \frac{\mathrm{i}}{2} \Sigma_2(\omega) \right)^{-1} . \tag{140}$$

We have

$$\Sigma_2(\omega) \equiv 2\pi \sum_i |\eta_i|^2 \delta(\omega - a_i) - 2\pi \sum_i |\zeta_i|^2 \delta(\omega + b_i) \ , \tag{141}$$

with $\Sigma_1(\omega)$ defined by a Kramers Kronig transform.

The reservoir parameters a_i, b_i, η_i and ζ_i which are of no particular interest, are all subsumed into the boson self energy $\Sigma_2(\omega)$. From this point forward we may ignore these quantities in favor of the boson self energy. We reiterate that this theory makes an important simplification, that the reservoir pairs have no dispersion. *For this case one can solve for the exact transport coefficients*.

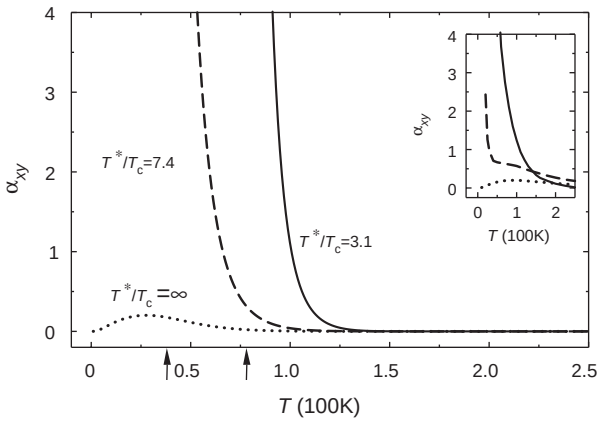

Fig. 42. Calculated transverse thermoelectric response, which appears in the Nernst coefficient. Inset plots experimental (Xu et al., 2000) data. Both the theoretical and experimental values of α_{xy} are normalized by the value of α_{xy} for an optimally doped sample at $2T_c$, $0.0232(B/\mathrm{T})$ V/(KΩm).

For small, but constant magnetic and electric fields and thermal gradients we obtain the linearized response. For notational convenience, we define $v_{ab}(\mathbf{k}) \equiv \partial^2/\partial k_a \partial k_b \varepsilon(\mathbf{k})$. Then we can write a few of the in-plane transport coefficients which appear in Eqs. (8) and (9) as

$$\sigma = -\frac{e^{*2}}{2} \int \frac{\mathrm{d}^3 k}{(2\pi)^3} \frac{\mathrm{d}\omega}{2\pi} \, v_x v_x A^2(\mathbf{k}, \omega) \frac{\partial b(\omega)}{\partial \omega} \tag{142}$$

and

$$\alpha_{xy} = -\frac{e^{*2} B_z}{6T} \int \frac{\mathrm{d}^3 k}{(2\pi)^3} \frac{\mathrm{d}\omega}{2\pi} \, v_x v_x v_{yy} \omega A^3(\mathbf{k}, \omega) \frac{\partial b(\omega)}{\partial \omega} \, . \tag{143}$$

These equations naturally correspond to their TDGL counterparts (except for different phenomenological coefficients) when $T \approx T_c$.

6.5.2. Comparison with transport data

The formalism of the previous sub-section and in particular, Eqs. (142) and (143),), can be used to address transport data within the framework of BCS–BEC crossover. The results for α_{xy}, which relates to the important Nernst effect, are plotted in Fig. 42 with a subset of the data plotted in the upper right inset. It can be seen that the agreement is reasonable. In this way a "pre-formed pair" picture is, at present, a viable alternative to "normal state vortices".

Within the crossover scenario, just as in TDGL, there are strong constraints on other precursor transport effects: paraconductivity, diamagnetism and optical conductivity are all indirectly or directly connected to the Nernst coefficient, in the sense that they all derive from the same dynamical equation of motion for the bosons. Analogous inferences have been made (Geshkenbein et al., 1997), based on similar bosonic generalizations of TDGL.

The calculated behavior of a number of these other properties is summarized (Tan and Levin, 2004) in Figs. 43 and 44 below, which indicate both quasi-two dimensional and more three dimensional behavior.

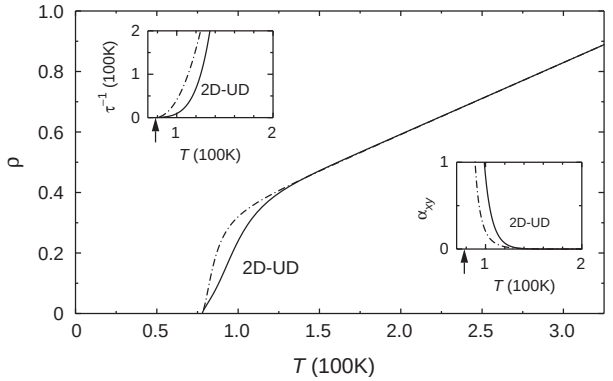

Fig. 43. dc resistivity ρ (normalized by $\rho_Q \equiv s/e^2$) vs. T, for quasi-2D underdoped (UD) samples with two different forms for μ_{pair}. These are shown plotted in the left inset as $\tau^{-1} \equiv -\mu_{\text{pair}}/\text{Im}\,\gamma$. The right inset shows corresponding α_{xy}, and arrows indicate T_c.

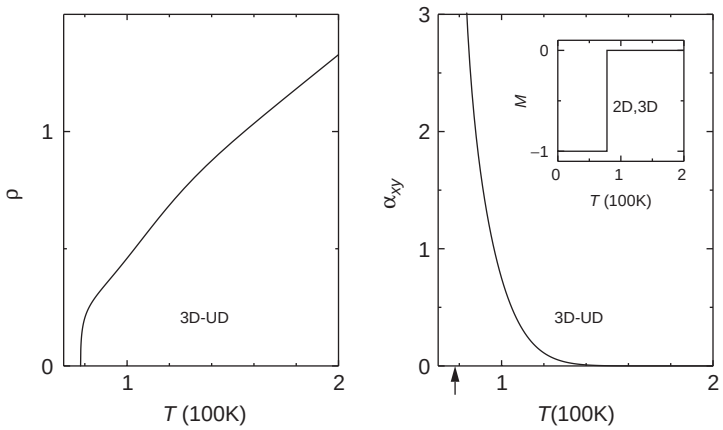

Fig. 44. dc resistivity and α_{xy}, for an underdoped, more three-dimensional, system like YBCO. The arrow indicates T_c. The magnetization M is plotted as the inset, and is independent of dimensionality.

In the plots for the resistivity, ρ, a fairly generic (Leridon et al., 2001) linear-in-T contribution[9] from the fermions has been added, as a background term. A central theme of concern in the literature is whether one can understand the behavior of ρ simultaneously with that of α_{xy}. Experiments (Leridon et al., 2001; Watanabe et al., 1997) indicate that there is a small feature corresponding to T^* at which ρ deviates from the background linear fermionic term, but that the deviation is not noticeably large except in the immediate vicinity of T_c. This is in contrast to the behavior of α_{xy} which shows a significant high temperature onset. A key observation from the theoretical calculations shown in the figures is that the onset temperatures for the Nernst coefficient and the resistivity are rather different with the former being considerably higher

[9] In reality, one should include an additional temperature dependence from pseudogapped fermions which presumably has a small upturn, relative to a linear curve, as T decreases.

than the latter. Moreover all onsets appear to be significantly less than T^*. Qualitative agreement with experiment is not unreasonable. However, a more quantitative comparison with experiment has not been established, since it depends in detail on a phenomenological input: the temperature dependence of the pair chemical potential $\mu_{\rm pair}$.

Another important feature of these plots is the fact that there is virtually no diamagnetic precursor, as was also found to be the case in simple TDGL. To see this, note that the magnetization can be written (Schmid, 1969; Tan and Levin, 2004)

$$\frac{\mu_0 M}{B} = -\frac{4}{3}\frac{\alpha k_{\rm B} T}{\hbar c}\frac{\xi_{ab}^2}{s\sqrt{1+(2\xi_c/s)^2}}\,,$$

where α is the fine structure constant, c is the speed of light, s is the interlayer spacing, and ξ_{ab} (ξ_c) are coherence lengths in the direction parallel (perpendicular) to the planes. From this result we can estimate the order of magnitude of the diamagnetic susceptibility due to preformed pairs. For a typical high T_c superconductor, $T \sim 50$K, so that $\lambda \equiv hc/k_{\rm B}T \sim 3\times 10^{-4}$m, and $\lambda/\alpha \sim 4\times 10^{-2}$m. Because the coherence lengths and the interlayer spacing are on the nanometer length scale, precursor effects in the diamagnetic susceptibility are of the order 10^{-6}, and thus extremely small, as is consistent with experiment (Wang et al., 2001).

In order to make the BCS–BEC scenario more convincing it will be necessary to take these transport calculations below T_c. This is a project for future research and in this context it will ultimately be important to establish in this picture how superconducting state vortices are affected by the persistent pseudogap. Magnetic field induced magnetic order which has been associated with vortices (Lake et al., 2002) will, moreover, need to be addressed. The analogous interplay of vortices and pseudogap will also be of interest in the neutral superfluids.

7. Conclusions

In this Review we have summarized a large body of work on the subject of the BCS–BEC crossover scenario. In this context, we have explored the intersection of two very different fields: high T_c superconductivity and cold atom superfluidity. Theories of cuprate superconductivity can be crudely classified as focusing on "Mott physics" which reflects the anomalously small zero temperature superfluid density and "crossover physics", which reflects the anomalously short coherence length. Both schools are currently very interested in explaining the origin of the mysterious pseudogap phase. In this Review we have presented a case for its origin in crossover physics. The pseudogap in the normal state can be associated with meta-stable pairs of fermions; a (pseudogap) energy must be supplied to break these pairs apart into their separate components. The pseudogap also persists below T_c in the sense that there are noncondensed fermion pair excitations of the condensate. These concepts have a natural analogue in self consistent theories of superconducting fluctuations, but for the crossover problem the width of the "critical region" is extremely large. This reflects the much stronger-than-BCS attractive interaction.

It was not our intent to shortchange the role of Mott physics which will obviously be of importance in our ultimate understanding of the superconducting cuprates. There is, however, much in this regard which is still uncertain associated with establishing the simultaneous relevance and existence of spin-charge separation (Anderson, 1997), stripes (Kivelson et al., 2003), and hidden order parameters (Chakravarty

et al., 2001). What we do have in hand, though, is a very clear experimental picture of an extremely unusual superconductor in which superconductivity seems to evolve gradually from above T_c to below. We have in this Review tried to emphasize the common ground between high T_c superconductors and ultracold superfluids. These Mott issues may nevertheless, set the agenda for future cold atom studies of fermions in optical lattices (Hofstetter et al., 2002).

The recent discovery of superfluidity in cold fermion gases opens the door to a new set of fascinating problems in condensed matter physics. Unlike the bosonic system, there is no ready-made counterpart of Gross Pitaevskii theory. A new mean field theory which goes beyond BCS and encompasses BEC in some form or another will have to be developed in concert with experiment. *As of this writing, there are four experiments where the simple mean field theory discussed in this review is in reasonable agreement with the data*. These are the collective mode studies over the entire range of accessible magnetic fields (Heiselberg, 2004b; Hu et al., 2004). In addition in the unitary regime, RF spectroscopy-based pairing gap studies (Kinnunen et al., 2004a), as well as density profile (Stajic et al., 2005a) and thermodynamic studies (Kinast et al., 2005) all appear to be compatible with this theory.

The material in this Review is viewed as the first of many steps in a long process. It was felt, however, that some continuity should be provided from another community which has addressed and helped to develop the BCS–BEC crossover, since the early 1990s when the early signs of the cuprate pseudogap were beginning to appear. As of this writing, it appears likely that the latest experiments on cold atoms probe a counterpart to this pseudogap regime. That is, on both sides, but near the resonance, fermions form in long lived metastable pair states at higher temperatures than those at which they Bose condense.

Acknowledgements

We gratefully acknowledge the help of our many close collaborators over the years: J. Maly, B. Jankó, I. Kosztin, Y.-J. Kao and A. Iyengar. We also thank our colleagues T.R. Lemberger, B.R. Boyce, J.N. Milstein, M.L. Chiofalo and M.J. Holland, and most recently, J.E. Thomas, J. Kinast, and A. Turlapov. This work was supported by NSF-MRSEC Grant No. DMR-0213765 (JS,ST and KL), NSF Grant No. DMR0094981 and JHU-TIPAC (QC).

Appendix A. Derivation of the $T = 0$ variational conditions

The ground state wavefunction is given by

$$\bar{\Psi}^0 = \mathrm{e}^{-\lambda^2/2+\lambda b_0^\dagger}|0\rangle \otimes \Pi_{\mathbf{k}}(u_{\mathbf{k}} + v_{\mathbf{k}} a_{\mathbf{k}}^\dagger a_{-\mathbf{k}}^\dagger)|0\rangle \ . \tag{A.1}$$

Thus one has three variational parameters λ, $u_{\mathbf{k}}$, $v_{\mathbf{k}}$ with normalization condition $u_{\mathbf{k}}^2 + v_{\mathbf{k}}^2 = 1$. We can define $\theta_{\mathbf{k}}$ such that $u_{\mathbf{k}} = \sin\theta_{\mathbf{k}}$ and $v_{\mathbf{k}} = \cos\theta_{\mathbf{k}}$, so that we have only two variational parameters, λ and $\theta_{\mathbf{k}}$.

We then have

$$\langle\bar{\Psi}^0|H - \mu N|\bar{\Psi}^0\rangle = (v - 2\mu)\lambda^2 + 2\sum_{\mathbf{k}}(\varepsilon_{\mathbf{k}} - \mu)v_{\mathbf{k}}^2 + 2U\sum_{\mathbf{k},\mathbf{k}'} u_{\mathbf{k}} v_{\mathbf{k}} u_{\mathbf{k}'} v_{\mathbf{k}'} + 2g\lambda\sum_{\mathbf{k}} u_{\mathbf{k}} v_{\mathbf{k}} \ ,$$

where we have chosen $\varphi_{\mathbf{k}} = 1$ in Eq. (11) for simplicity.

Let us define

$$\Delta_{\rm sc} = -2U \sum_{\mathbf{k}} u_{\mathbf{k}} v_{\mathbf{k}} \ . \tag{A.2}$$

The variational conditions are

$$\frac{\delta\langle H-\mu N\rangle}{\delta\lambda} = 0 \tag{A.3}$$

and

$$\frac{\delta\langle H-\mu N\rangle}{\delta\theta_{\mathbf{k}}} = 0 \tag{A.4}$$

These conditions yield two equations: a relationship between the two condensates

$$\frac{g\lambda}{\Delta_{\rm sc}} = \frac{1}{U}\,\frac{g^2}{\nu - 2\mu} \tag{A.5}$$

and the $T=0$ gap equation:

$$1 + \left(U + \frac{g^2}{2\mu-\nu}\right)\sum_{\mathbf{k}} \frac{1}{2E_{\mathbf{k}}} = 0 \ . \tag{A.6}$$

Similarly, we can write an equation for the total number of fermions

$$n^{\rm tot} = \left\langle \bar{\Psi}^0 | 2\sum_{\mathbf{k}} b^\dagger_{\mathbf{k}} b_{\mathbf{k}} + 2\sum_{\mathbf{k}} a^\dagger_{\mathbf{k}} a_{\mathbf{k}} | \bar{\Psi}^0 \right\rangle = 2\lambda^2 + \sum_{\mathbf{k}} \left[1 - \frac{\varepsilon_{\mathbf{k}} - \mu}{E_{\mathbf{k}}}\right] \ ,$$

where

$$E_{\mathbf{k}} = \sqrt{(\varepsilon_{\mathbf{k}} - \mu)^2 + \tilde{\Delta}^2_{\rm sc}} \ , \tag{A.7}$$

with $\tilde{\Delta}_{\rm sc} = \Delta_{\rm sc} - g\lambda$. Thus we have obtained the three equations which characterize the system at $T=0$. It should be clear that the variational parameter λ is the same as the condensate weight so that $\lambda = \phi_m \equiv \langle b_{\mathbf{q}=0}\rangle$.

Appendix B. Proof of Ward identity below T_c

We now want to establish that the generalized Ward identity in Eq. (106) is correct for the superconducting state as well. The vertex $\delta\mathbf{\Lambda}_{pg}$ may be decomposed into Maki–Thompson (MT) and two types of Aslamazov–Larkin (AL_1, AL_2) diagrams, whose contribution to the response is shown here in Fig. 45b. We write

$$\delta\mathbf{\Lambda}_{pg} \equiv \delta\mathbf{\Lambda}_{\rm MT} + \delta\mathbf{\Lambda}^1_{\rm AL} + \delta\mathbf{\Lambda}^2_{\rm AL}(\mathbf{\Lambda}) \ . \tag{B.1}$$

Using conventional diagrammatic rules one can see that the *MT* term has the same sign reversal as the anomalous superconducting self energy diagram. This provides insight into Eq. (107). Here, however,

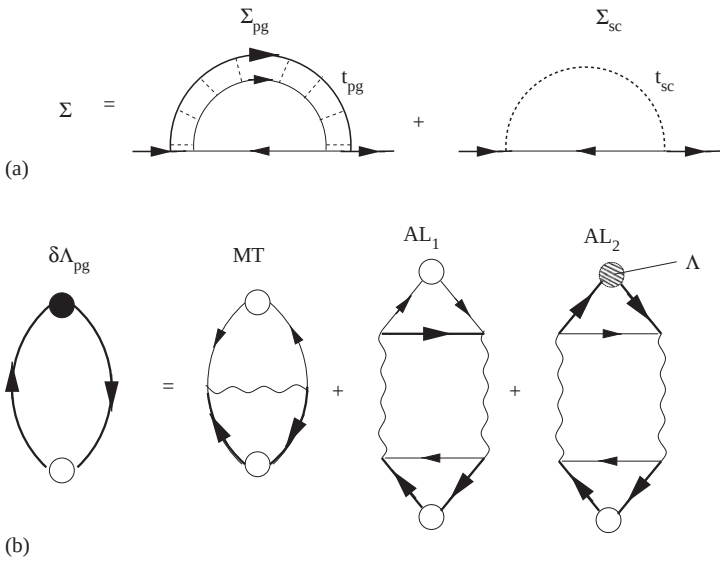

Fig. 45. Self energy contributions (a) and response diagrams for the vertex correction corresponding to Σ_{pg} (b). Heavy lines are for dressed, while light lines are for bare Green's functions. Wavy lines indicate t_{pg}. See text for details.

the pairs in question are noncondensed and their internal dynamics (via t_{pg} as distinguished from $t_{\rm sc}$) requires additional AL_1 and AL_2 terms as well, which will ultimately be responsible for the absence of a Meissner contribution from this normal state self energy effect.

Note that the AL_2 diagram is specific to our GG_0 scheme, in which the field couples to the full G appearing in the T-matrix through a vertex $\mathbf{\Lambda}$. It is important to distinguish the vertex $\boldsymbol{\Lambda}$ which appears in the AL_2 diagram from the full EM vertex $\Lambda^{\rm EM}$.

In particular, we have

$$\boldsymbol{\Lambda} = \boldsymbol{\lambda} + \delta\boldsymbol{\Lambda}_{pg} - \delta\boldsymbol{\Lambda}_{\rm sc} \ , \tag{B.2}$$

where the sign change of the superconducting term (relative to $\mathbf{\Lambda}^{\rm EM}$) is a direct reflection of the sign in Eq. (107).

We now show that there is a precise cancellation between the MT and AL_1 pseudogap diagrams at $Q = 0$. This cancellation follows directly from the normal state Ward identity

$$Q \cdot \lambda(K, K+Q) = G_0^{-1}(K) - G_0^{-1}(K+Q) \ , \tag{B.3}$$

which implies

$$Q \cdot [\delta\Lambda^1_{\rm AL}(K, K+Q) + \delta\Lambda_{\rm MT}(K, K+Q)] = 0 \tag{B.4}$$

so that $\delta\boldsymbol{\Lambda}^1_{\rm AL}(K, K) = -\delta\boldsymbol{\Lambda}_{\rm MT}(K, K)$ is obtained exactly from the $Q \to 0$ limit.

Similarly, it can be shown that

$$Q \cdot \Lambda(K, K+Q) = G^{-1}(K) - G^{-1}(K+Q) \ . \tag{B.5}$$

The above result can be used to infer a relation analogous to Eq. (B.4) for the AL_2 diagram, leading to

$$\delta\Lambda_{pg}(K, K) = -\delta\Lambda_{\rm MT}(K, K) \ , \tag{B.6}$$

which expresses this pseudogap contribution to the vertex entirely in terms of the Maki–Thompson diagram shown in Fig. 45b. It is evident that $\delta\Lambda_{\rm MT}$ is simply the pseudogap counterpart of $\delta\Lambda_{\rm sc}$, satisfying

$$-\delta\Lambda_{\rm MT}(K, K) = \frac{\partial\Sigma_{pg}(K)}{\partial\mathbf{k}} \ . \tag{B.7}$$

Therefore, one observes that for $T \leqslant T_c$

$$\delta\Lambda_{pg}(K, K) = \frac{\partial\Sigma_{pg}(K)}{\partial\mathbf{k}} \ , \tag{B.8}$$

which establishes that Eq. (106) applies to the superconducting phase as well. As expected, there is no direct Meissner contribution associated with the pseudogap self-energy.

Appendix C. Quantitative relation between BCS–BEC crossover and Hartree-TDGL

In this appendix we make more precise the relation between Hartree-approximated TDGL theory and the T-matrix of our GG_0 theory. The Ginzburg–Landau (GL) free energy functional in momentum space is given by (Hassing and Wilkins, 1973)

$$F[\Psi] = N(0) \sum_{\mathbf{q}} |\Psi_{\mathbf{q}}|^2(\varepsilon + \xi_1^2 q^2) + \frac{b_0}{2} \sum_{\mathbf{q}_i} \Psi^*_{\mathbf{q}_1} \Psi^*_{\mathbf{q}_2} \Psi_{\mathbf{q}_3} \Psi_{\mathbf{q}_1+\mathbf{q}_2-\mathbf{q}_3} \ , \tag{C.1}$$

where $\Psi_{\mathbf{q}}$ are the Fourier components of the order parameter $\Psi(\mathbf{r}, t)$, $\varepsilon = (T - T^*)/T^*$, ξ_1 is the GL coherence length, $b_0 = [1/T^2\pi^2]\frac{7}{8}\zeta(3)$, T^* is the critical temperature when feedback effects from the quartic term are neglected, and $N(0)$ is the density of states at the Fermi level in the normal state. The quantity $\langle|\Psi_{\mathbf{q}}|^2\rangle$ is determined self-consistently via

$$\langle|\Psi_{\mathbf{q}}|^2\rangle = \frac{\int D\Psi \mathrm{e}^{-\beta F[\Psi]}|\Psi_{\mathbf{q}}|^2}{\int D\Psi \mathrm{e}^{-\beta F[\Psi]}} \ , \tag{C.2}$$

where $F[\Psi]$ is evaluated in the Hartree approximation (Stajic et al., 2003b). Our self consistency condition can be then written as

$$\langle|\Psi_{\mathbf{q}}|^2\rangle = \frac{T}{N(0)} \left[\varepsilon + b_0 \sum_{\mathbf{q}'} \langle|\Psi_{\mathbf{q}'0}|^2\rangle + \xi_1^2 q^2 \right]^{-1} \ . \tag{C.3}$$

If we sum Eq. (C.3) over $\mathbf{q}$ and identify $\sum_{\mathbf{q}} \langle |\Psi_{\mathbf{q}0}|^2 \rangle$ with Δ^2, we obtain a self-consistency equation for the energy "gap" (or pseudogap) Δ above T_c

$$\Delta^2 = \sum_{\mathbf{q}} \frac{T}{N(0)} [\varepsilon + b_0 \Delta^2 + \xi_1^2 q^2]^{-1} , \tag{C.4}$$

$$\Delta^2 = \sum_{\mathbf{q}} \frac{T}{N(0)} \frac{1}{-\bar{\mu}_{\text{pair}}(T) + \xi_1^2 q^2} , \tag{C.5}$$

where

$$\bar{\mu}_{\text{pair}}(T) = -\varepsilon - b_0 \Delta^2 . \tag{C.6}$$

Note that the critical temperature is renormalized downward with respect to T^* and satisfies

$$\bar{\mu}_{\text{pair}}(T_c) = 0 . \tag{C.7}$$

To compare with GL theory we expand our T-matrix equations to first order in the self energy correction. The T-matrix can be written in terms of the attractive coupling constant U as

$$t(Q) = \frac{U}{1 + U\chi_0(Q) + U\delta\chi(Q)} , \tag{C.8}$$

where

$$\chi_0(Q) = \sum_K G_0(Q - K) G_0(K) . \tag{C.9}$$

Defining

$$\Delta^2 = -\sum_Q t(Q) , \tag{C.10}$$

we arrive at the same equation as was derived in Section 2.3

$$\Sigma(K) \approx -G_0(-K)\Delta^2 , \tag{C.11}$$

where one can derive a self consistency condition on Δ^2 in terms of the quantity $\delta\chi(0)$ (which is first order in Σ), which satisfies

$$\delta\chi(0) = -b_0 N(0) \Delta^2 , \tag{C.12}$$

implying that

$$\delta\chi(0) = -b_0 T \sum_{\mathbf{q}} \frac{1}{\varepsilon + \xi_1^2 q^2 - \delta\chi(0)/N(0)} , \tag{C.13}$$

which coincides with the condition derived earlier in Eq. (C.4).

Appendix D. Convention and notation

D.1. Notation

We follow standard notations as much as possible. They are summarized below.

E_{F}	Fermi energy
k_{F}	Fermi momentum
$\hbar$	Planck constant
k_{B}	Boltzmann constant
c	speed of light
e	electron charge
T_c	critical temperature for (superfluid/superconducting) phase transition
T^*	pair formation or pseudogap onset temperature
T	temperature
μ, μ_{pair}, μ_{B}	Fermionic, pair and bosonic chemical potential, respectively
Δ	Fermionic excitation gap
Δ_{sc}	superconducting/superfluid order parameter
Δ_{pg}	pseudogap

Four vector $K \equiv (\mathrm{i}\omega_n, \mathbf{k})$, $\sum_K \equiv T\sum_n \sum_{\mathbf{k}}$, where $\omega_n = (2n+1)\pi T$ is the odd (fermionic) Matsubara frequency.

Four vector $Q \equiv (\mathrm{i}\Omega_n, \mathbf{q})$, $\sum_Q \equiv T\sum_n \sum_{\mathbf{q}}$, where $\Omega_n = 2n\pi T$ is the even (bosonic) Matsubara frequency.

$f(x) = 1/(\mathrm{e}^{x/k_{\mathrm{B}}T} + 1)$	Fermi distribution function
$b(x) = 1/(\mathrm{e}^{x/k_{\mathrm{B}}T} - 1)$	Bose distribution function
$G(K)$, $G_0(K)$	full and bare Green's functions for fermions
$D(Q)$, $D_0(Q)$	full and bare Green's functions for Feshbach bosons
$\Sigma(K)$,$\Sigma_B(Q)$	self energy of fermions and bosons, respectively
$\chi(Q)$	pair susceptibility
$t(Q)$	T-matrix
$\boldsymbol{\lambda}$, $\boldsymbol{\Lambda}$	bare and full vertex, respectively
ν, ν_0	magnetic detuning parameter
a_s, a_s^*	S-wave inter-fermion scattering length
U, U_0	renormalized and bare strength of the attractive interaction between fermions in the open-channel. $U_0 \propto a_s(\nu = +\infty)$
U_c	critical coupling strength at which the two-body scattering length diverges
$A = (\phi, \mathbf{A})$	four vector potential
$J = (\rho, \mathbf{J})$	four current
$K^{\mu\nu}(Q)$	electromagnetic response kernel

$\varepsilon_{\mathbf{k}} = k^2/2m$	bare fermion dispersion in free space
$\xi_{\mathbf{k}} = \varepsilon_{\mathbf{k}} - \mu$	bare fermion dispersion measured from chemical potential
$E_{\mathbf{k}}$	Bogoliubov quasiparticle dispersion
$u^2_{\mathbf{k}} = \frac{1}{2}(1 + \xi_{\mathbf{k}}/E_{\mathbf{k}})$, $v^2_{\mathbf{k}} = \frac{1}{2}(1 - \xi_{\mathbf{k}}/E_{\mathbf{k}})$	coherence factor as given in BCS theory
$n^{\mathrm{tot}} = n + 2(n_b + n_{b0})$	total, fermion, finite momentum boson, condensed boson density, respectively
$V(r) = \frac{1}{2}m\omega^2 r^2$	harmonic trap potential

We use alphabetic ordering when multiple authors appear together.

We always refer to the absolute value when we refer to the interaction parameters U, U_0, g, g_0 as increasing or decreasing.

D.2. Convention for units

Throughout this Review, we use the convention for units where it is not explicitly spelled out:

$$\hbar = k_{\mathrm{B}} = c = 1 \ .$$

$$E_{\mathrm{F}} = T_{\mathrm{F}} = k_{\mathrm{F}} = 2m = 1 \ .$$

In a harmonic trap, E_{F}, T_{F} and k_{F} are defined by the noninteracting Fermi gas with the same total particle number N. $E_{\mathrm{F}} = \hbar\omega(3N)^{1/3}$. We further take the Thomas–Fermi radius $R_{\mathrm{TF}} = 1$.

In this convention, the fermion density in a homogeneous gas in three dimensions is $n = 1/3\pi^2$, the harmonic trap frequency $\omega = 2$, and the total fermion number in a trap is $N = 1/24$.

In the two-channel model, the units are $E_{\mathrm{F}}/k_{\mathrm{F}}^3$ for U and U_0, and $E_{\mathrm{F}}/k_{\mathrm{F}}^{3/2}$ for g and g_0.

Our fermionic chemical potential μ is measured with respect to the bottom of the energy band, which leads to (i) $\mu = E_{\mathrm{F}}$ in the noninteracting limit at $T = 0$, and (ii) μ changes sign when the system crosses the boundary between fermionic and bosonic regimes.

D.3. Abbreviations

BCS	Bardeen–Cooper–Schrieffer (theory)
BEC	Bose–Einstein condensation
pg	pseudogap
sc	superconductor
AFM	antiferromagnet
LSCO	$La_{1-x}Sr_xCuO_4$
BSCCO	$Bi_2Sr_2CaCu_2O_{8+\delta}$
YBCO	$YBa_2Cu_3O_{7-\delta}$
ARPES	angle-resolved photoemission spectroscopy
STM	scan tunneling microscopy
SIN	superconductor–insulator–normal metal (tunnelling junction)
TDGL	time-dependent Ginzburg–Landau theory

FB	Feshbach boson
FLEX	fluctuation exchange
NSR	Noziéres and Schmitt-Rink
AB	Anderson–Bogoliubov
TF	Thomas–Fermi
3D	three dimensions
RPA	Random phase approximation
LDA	Local density approximation
GP	Gross–Pitaevskii (theory)
RF	Radio frequency (spectroscopy)
SI	Superconductor–insulator (transition)

References

Aeppli, G., Mason, T.E., Hayden, S.M., Mook, H.A., Kulda, J., 1997a. Science 278 (5342), 1432.
Aeppli, G., Mason, T.E., Mook, H.A., Schroeder, A., Hayden, S.M., 1997b. Physica C 231, 282–287.
Anderson, P.W., 1997. The Theory of Superconductivity in the High-T_c Cuprate Superconductors. Princeton University Press, Princeton.
Anderson, P.W., Brinkman, W.F., 1973. Phys. Rev. Lett. 30 (1), 1108.
Anderson, P.W., Lee, P.A., Randeria, M., Rice, T.M., Trivedi, N., Zhang, F.C., 2004. J. Phys.: Condens. Matter. 16, R755.
Ando, Y.G.S., Boebinger, P.A., Kimura, T., Kishio, K., 1995. Phys. Rev. Lett. 75 (25), 4662.
Andrenacci, N., Perali, A., Pieri, P., Strinati, G.C., 1999. Phys. Rev. B 60, 12410.
Baker, J.G.A., 1999. Phys. Rev. C 60, 054311.
Baldo, M., Lombardo, U., Schuck, P., 1995. Phys. Rev. C 52, 975.
Bartenstein, M., Altmeyer, A., Riedl, S., Jochim, S., Chin, C., Denschlag, J., Grimm, R., 2004a. Phys. Rev. Lett. 92, 203201.
Bartenstein, M., Altmeyer, A., Riedl, S., Jochim, S., Chin, C., Hecke, D., G.R., 2004b. Phys. Rev. Lett. 92, 120401.
Baym, G., 1962. Phys. Rev. 127 (4), 1391.
Belkhir, L., Randeria, M., 1992. Phys. Rev. B 45 (1), 5087.
Benard, P., Chen, L., Tremblay, A.M.S., 1993. Phys. Rev. B 47 (22), 15217.
Berlinsky, A., Bonn, D., Harris, R., Kallin, C., 2000. Phys. Rev. B 61 (13), 9088.
Bourdel, T., Khaykovich, L., Cubizolles, J., Zhang, J., Chevy, F., Teichmann, M., Tarruell, L., Kokkelmans, S.J., Salomon, C., 2004. Phys. Rev. Lett. 93, 050401.
Bruun, G.M., Baym, G., 2004. Phys. Rev. Lett. 93, 150403.
Bruun, G.M., Pethick, C.J., 2004. Phys. Rev. Lett. 92, 140404.
Caldeira, A., Leggett, A., 1983. Physica 121A (4), 587.
Campuzano, J.C., Norman, M.R., Randeria, M., 2004. Physics of Superconductors, vol. II, Chapter-Photoemission in the High Tc Superconductors, Springer-Verlag, Springer, Berlin, pp. 167–273.
Carlson, E.W., Emery, V.J., Kivelson, S.A., Orgad, D., 2002. Concepts in high temperature superconductivity, preprint; cond-mat/0206217.
Carlson, E.W., Kivelson, S.A., Emery, V.J., Manousakis, E., 1999. Phys. Rev. Lett. 83 (3), 612.
Carr, L.D., Shlyapnikov, G.V., Castin, Y., 2004. Phys. Rev. Lett. 92 (15), 150404.
Castellani, C., DiCastro, C., Grilli, M., 1995. Phys. Rev. Lett. 75 (25), 4650.
Chakravarty, S., Laughlin, R.B., Morr, D.K., Nayak, C., 2001. Phys. Rev. B 63 (10), 094503.
Chen, H.-D., Vafek, O., Yazdani, A., Zhang, S.C., 2004. Phys. Rev. Lett. 93, 187002.
Chen, Q.J., 2000. Generalization of BCS theory to short coherence length superconductors: A BCS–Bose–Einstein crossover scenario, Ph.D. Thesis, University of Chicago, unpublished.
Chen, Q.J., Kosztin, I., Jankó, B., Levin, K., 1998. Phys. Rev. Lett. 81 (21), 4708.
Chen, Q.J., Kosztin, I., Jankó, B., Levin, K., 1999. Phys. Rev. B 59 (10), 7083.
Chen, Q.J., Kosztin, I., Levin, K., 2000. Phys. Rev. Lett. 85 (14), 2801.

Chen, Q.J., Levin, K., Kosztin, I., 2001. Phys. Rev. B 63, 184519.
Chen, Q.J., Schrieffer, J.R., 2002. Phys. Rev. B 66, 014512.
Cheong, S.W., Aeppli, G., Mason, T.E., Mook, H.A., Hayden, S.M., Canfield, P.C., Fisk, Z., Clausen, K.N., Martinez, J.L., 1991. Phys. Rev. Lett. 67, 1791.
Chin, C., Bartenstein, M., Altmeyer, A., Riedl, S., Jochim, S., Hecker-Denschlag, J., Grimm, R., 2004. Science 305, 1128.
Chiofalo, M.L., Kokkelmans, S.J.J.M.F., Milstein, J.N., Holland, M.J., 2002. Phys. Rev. Lett. 88, 090402.
Chubukov, A.V., Pines, D., Stojkovic, B.P., 1996. J. Phys. Cond. Matt. 8, 10017.
Cohen, R.W., Abeles, B., Fuselier, C.R., 1969. Phys. Rev. Lett. 23, 377.
Corson, J., Mallozzi, R., Orenstein, J., Eckstein, J.N., Bozovic, I., 1999. Nature 398, 221.
Cote, R., Griffin, A., 1993. Phys. Rev. B 48 (14), 10404.
Cubizolles, J., Bourdel, T., Kokkelmans, S., Shlyapnikov, G., Salomon, C., 2003. Phys. Rev. Lett. 91 (24), 240401.
Dalfovo, F., Giorgini, S., Pitaevskii, L.P., Stringari, S., 1999. Rev. Mod. Phys. 71, 463.
Damascelli, R., Hussain, Z., Shen, Z.-X., 2003. Rev. Mod. Phys. 75 (2), 473.
Deisz, J.J., Hess, D.W., Serene, J.W., 1998. Phys. Rev. Lett. 80 (2), 373.
DeMarco, B., Jin, D.S., 1999. Science 285, 1703.
Demler, E., Zhang, S.-C., 1995. Phys. Rev. Lett. 75 (22), 4126.
Deutscher, G., 1999. Nature 397 (20), 410.
Ding, H., Yokoya, T., Campuzano, J.C., Takahashi, T., Randeria, M., Norman, M.R., Mochiku, T., Hadowaki, K., Giapintzakis, J., 1996. Nature 382 (6586), 51.
Domanski, T., Ranninger, J., 2003. Phys. Rev. Lett. 91 (25), 255301.
Eagles, D.M., 1969. Phys. Rev. 186 (2), 456.
Emery, V.J., Kivelson, S.A., 1995. Nature 374 (6521), 434.
Falco, G.M., Stoof, H.T.C., 2004. Phys. Rev. Lett. 92, 130401.
Fisher, M., Weichman, P.B., Grinstein, G., Fisher, D.S., 1989. Phys. Rev. B 40, 546.
Fong, H.F., Keimer, B., Anderson, P.W., Reznik, D., Dogan, F., Aksay, I.A., 1995. Phys. Rev. Lett. 75 (2), 316.
Friedberg, R., Lee, T.D., 1989a. Phys. Lett. A 138 (8), 423.
Friedberg, T., Lee, T.D., 1989b. Phys. Rev. B 40 (10), 6745.
Fu, H.C., Davis, J.C., Lee, D.-H., 2004. On the charge ordering observed by recent STM experiments, preprint, cond-mat/0403001.
Geshkenbein, V., Ioffe, L., Larkin, A., 1997. Phys. Rev. B 55 (5), 3173.
Giovannini, B., Berthod, C., 2001. Phys. Rev. B 63 (2), 144516.
Greiner, M., Regal, C.A., Jin, D.S., 2003. Nature 426, 537.
Greiner, M., Regal, C.A., Jin, D.S., 2005. Phys. Rev. Lett. 94, 070403.
Griffin, A., Ohashi, Y., 2003. Phys. Rev. A 67, 063612.
Hassing, R.F., Wilkins, J.W., 1973. Phys. Rev. B 7, 1890.
Haussmann, R., 1993. Z. Phys. B 91 (3), 291.
Heiselberg, H., 2001. Phys. Rev. A 63, 043606.
Heiselberg, H., 2004a. J. Phys. B 37, 141.
Heiselberg, H., 2004b. Phys. Rev. Lett. 93, 040402.
den Hertog, B., 1999. Phys. Rev. B 60, 559.
Ho, T.-L., 2004. Phys. Rev. Lett. 92 (9), 090402.
Ho, T.-L., Zahariev, N., 2004. High temperature universal properties of atomic gases near feshbach resonance with non-zero orbital angular momentum, preprint cond-mat/0408469.
Hofstetter, W., Cirac, J.I., Zoller, P., Demler, E., Lukin, M.D., 2002. Phys. Rev. Lett. 89 (22), 220407.
Holland, M., Kokkelmans, S.J.J.M.F., Chiofalo, M.L., Walser, R., 2001. Phys. Rev. Lett. 87, 120406.
Holland, M.J., Menotti, C., Viverit, L., 2004. The role of boson-fermion correlations in the resonance theory of superfluids, preprint, cond-mat/0404234.
Houbiers, M., Ferwerda, R., Stoof, H.T.C., McAlexander, W., Sackett, C.A., Hulet, R.G., 1997. Phys. Rev. A 56, 4864.
Hu, H., Minguzzi, A., Liu, X.-J., Tosi, M.P., 2004. Phys. Rev. Lett. 93, 190403.
Ioffe, L.B., Millis, A.J., 1999. Science 285, 1241.
Itakura, K., 2003. Nucl. Phys A 715, 859.
Iyengar, A., Stajic, J., Kao, Y.-J., Levin, K., 2003. Phys. Rev. Lett. 90, 187003.
Jankó, B., Maly, J., Levin, K., 1997. Phys. Rev. B 56 (18), R11407.

Jochim, S., Bartenstein, M., Altmeyer, A., Hendl, G., Chin, C., Denschlag, J.H., Grimm, R., 2003a. Phys. Rev. Lett. 91 (24), 240402.
Jochim, S., Bartenstein, M., Altmeyer, A., Hendl, G., Riedl, S., Chin, C., Denschlag, J.H., Grimm, R., 2003b. Science 302, 2101.
Junod, A., Erb, A., Renner, C., 1999. Physica C 317–318 (20), 333.
Kadanoff, L.P., Martin, P.C., 1961. Phys. Rev. 124 (3), 670.
Kao, Y.-J., Iyengar, A., Chen, Q.J., Levin, K., 2001. Phys. Rev. B 64 (14), 140505.
Kao, Y.-J., Iyengar, A., Stajic, J., Levin, K., 2002. Phys. Rev. B 68, 214519.
Kao, Y.-J., Si, Q.M., Levin, K., 2000. Phys. Rev. B 61 (18), R118980.
Kastner, M.A., Birgeneau, R.J., Shirane, G., Endoh, Y., 1998. Rev. Mod. Phys. 70, 897.
Kinast, J., Hemmer, S.L., Gehm, M.E., Turlapov, A., Thomas, J.E., 2004. Phys. Rev. Lett. 92, 150402.
Kinast, J., Turlapov, A., Thomas, J.E., Chen, Q.J., Stajic, J., Levin, K., 2005. Science 307, 1296, published online 27 January 2005; doi:10.1126/science.1109220.
Kinnunen, J., Rodriguez, M., Törmä, P., 2004a. Science 305, 1131.
Kinnunen, J., Rodriguez, M., Törmä, P., 2004b. Phys. Rev. Lett. 92 (23), 230403.
Kivelson, S.A., Bindloss, I.P., Fradkin, E., Oganesyan, V., Tranquada, J.M., Kapitulnik, A., H.C., 2003. Rev. Mod. Phys. 75 (4), 1201.
Klinkhamer, F.R., Volovik, G.E., 2004. Emergent cpt violation from the splitting of fermi points, preprint hep-th/0403037.
Kokkelmans, S.J.J.M.F., et al., 2002. Phys. Rev. A 65, 053617.
Kolb, P.F., Heinz, U., 2003. Hydrodynamic description of ultrarelativistic heavy ion collisions, preprint nucl-th/0305084.
Kostyrko, T., Ranninger, J., 1996. Phys. Rev. B 54, 13105.
Kosztin, I., Chen, Q.J., Jankó, B., Levin, K., 1998. Phys. Rev. B 58 (10), R5936.
Kosztin, I., Chen, Q.J., Kao, Y.-J., Levin, K., 2000. Phys. Rev. B 61 (17), 11662.
Kugler, M., Fischer, O., Renner, C., Ono, S., Ando, Y., 2001. Phys. Rev. Lett. 86 (21), 4911.
Kulik, I.O., Entin-Wohlman, O., Orbach, R., 1981. J. Low Temp. Phys. 43 (20), 591.
Kwon, H.-J., Dorsey, A., 1999. Phys. Rev. B 59 (9), 6438.
Lai, C.W., Gossard, Z.J.A.C., Chemla, D.S., 2004. Science 303 (5273), 503.
Lake, B., Ronnow, H.M., Christensen, N.B., Aeppli, G., Lefmann, K., McMorrow, D.F., Vorderwisch, P., Smeibidl, P., Mangkorntong, N., Sasagawa, T., Nohara, M., Takagi, H., et al., 2002. Nature 415, 299.
Larkin, A., Varlamov, A., 2001. Fluctuation phenomena in superconductors., cond-mat/0109177.
Lee, P.A., 1993. Phys. Rev. Lett. 71, 1887.
Lee, P.A., 2004. Physica C 408-10, 5.
Lee, P.A., Nagaosa, N., Wen, X.-G., 2004. Doping a mott insulator: Physics of high temperature superconductivity, preprint, cond-mat/0410445.
Leggett, A.J., 1980. In: Modern Trends in the Theory of Condensed Matter, Springer-Verlag, Berlin, pp. 13–27.
Leggett, A.J., 1999. Phys. Rev. Lett. 83 (2), 392.
Leridon, B., Defossez, A., Dumont, J., Lesueur, J., 2001. Phys. Rev. Lett. 87 (19), 197007.
Levin, K., Valls, O.T., 1983. Phys. Rep. 98 (1), 1.
Liu, D.Z., Levin, K., 1997. Physica C 275, 81.
Liu, D.Z., Zha, Y., Levin, K., 1995. Phys. Rev. Lett. 75 (22), 4130.
Loram, J.W., Mirza, K., Cooper, J., Liang, W., Wade, J., 1994. J. Supercond. 7 (1), 243.
Maly, J., Jankó, B., Levin, K., 1999a. Physica C 321, 113.
Maly, J., Jankó, B., Levin, K., 1999b. Phys. Rev. B 59 (2), 1354.
Mathai, A., Gim, Y., Black, R.C., Amar, A., Wellstood, F.C., 1995. Phys. Rev. Lett. 74 (22), 4523.
Melikyan, A., Tešanović, Z., 2004. A model of phase fluctuations in a lattice *d*-wave superconductor: application to the Cooper pair charge-density-wave in underdoped cuprates, preprint cond-mat/0408344.
Sá de Melo, C.A.R., Randeria, M., Engelbrecht, J.R., 1993. Phys. Rev. Lett. 71 (19), 3202.
Micnas, R., Pedersen, M.H., Schafroth, S., Schneider, T., Rodriguez-Nunez, J., Beck, H., 1995. Phys. Rev. B 52 (22), 16223.
Micnas, R., Ranninger, J., Robaszkiewicz, S., 1990. Rev. Mod. Phys. 62 (1), 113.
Micnas, R., Robaszkiewicz, S., 1998. Cond. Matt. Phys. 1, 89.
Millis, A.J., Monien, H., Pines, D., 1990. Phys. Rev. B 42 (1), 167.
Milstein, J.N., Kokkelmans, S.J.J.M.F., Holland, M.J., 2002. Phys. Rev. A 66, 043604.
Molegraaf, H.J., Presura, C., van der Marel, D., Kes, P.H., Li, M., 2002. Science 295, 2239.

Mook, H.A., Dai, P., Hayden, S.M., Aeppli, G., Perring, T.G., Dogan, F., 1998. Nature 395 (6702), 580.
Norman, M.R., Pepin, C., 2003. Rep. Prog. Phys. 66, 1547.
Nozieres, P., Pistolesi, F., 1999. Eur. Phys. J. B 10, 649.
Nozières, P., Schmitt-Rink, S., 1985. J. Low Temp. Phys. 59, 195.
Oda, M., Hoya, K., Kubota, R., Manabe, C., Momono, N., Nakano, T., Ido, M., 1997. Physica C 281 (1), 135.
O'Hara, K.M., Hemmer, S.L., Gehm, M.E., Granade, S.R., Thomas, J.E., 2002. Science 298 (1), 2179.
Ohashi, Y., Griffin, A., 2002. Phys. Rev. Lett. 89 (13), 130402.
Ohashi, Y., Griffin, A., 2003. Phys. Rev. A 67, 033603.
Patton, B.R., 1971a. The effect of fluctuations in superconducting alloys above the transition temperature. Ph.D. Thesis, Cornell University, (unpublished).
Patton, B.R., 1971b. Phys. Rev. Lett. 27 (19), 1273.
Perali, A., Pieri, P., Pisani, L., Strinati, G.C., 2004a. Phys. Rev. Lett. 92 (22), 220404.
Perali, A., Pieri, P., Strinati, G.C., 2003. Phys. Rev. A 68 (3), 031601R.
Perali, A., Pieri, P., Strinati, G.C., 2004b. Phys. Rev. Lett. 93 (10), 100404.
Petrov, D.S., Salomon, C., Shlyapnikov, G.V., 2004. Phys. Rev. Lett. 93, 090404.
Pieri, P., Pisani, L., Strinati, G.C., 2004. Phys. Rev. Lett. 92, 110401.
Pieri, P., Strinati, G.C., 2000. Phys. Rev. B 61 (22), 15370.
Pines, D., 1997. Physica C 273, 282–287.
Puchkov, A.V., B.D.N., T.T., 1996. J. Phys.: Condens. Matter 8 (48), 10049.
Quintanilla, J., Gyorffy, B.L., Arnett, J.F., Wallington, J.P., 2002. Phys. Rev. B 66, 214526.
Randeria, M., 1995. In: Griffin, A., Snoke, D., Stringari, S. (Eds.), Bose–Einstein Condensation. Cambridge University Press, Cambridge, pp. 355–392.
Ranninger, J., Robaszkiewicz, S., 1985. Physica B 135 (2), 468.
Ranninger, J., Robin, J.M., 1996. Phys. Rev. B 53 (18), R11961.
Regal, C.A., Greiner, M., Jin, D.S., 2004. Phys. Rev. Lett. 92 (1), 040403.
Regal, C.A., Ticknor, C., Bohn, J.L., Jin, D.S., 2003. Nature 424 (1), 47.
Renner, C., Revaz, B., Kadowaki, K., Maggio-Aprile, I., Fischer, O., 1998. Phys. Rev. Lett. 80 (16), 3606.
Rojo, A., Levin, K., 1993. Phys. Rev. B 48 (22), 16861.
Rossat-Mignod, J., Regnault, L.P., Vettier, C., Bourges, P., Burlet, P., Bossy, J., Henry, J.Y., Lapertot, G., 1991. Physica C 185, 86.
Santander-Syro, A.F., Lobo, R.P.S.M., Bontemps, N., Konstantinovic, Z., Li, A.A., Raffy, H., 2003. Europhys. Lett. 62 (4), 568.
Scalapino, D.J., Loh, J.E., H.J.E., 1986. Phys. Rev. B 34 (2), 8190.
Schmid, A., 1969. Phys. Rev. 180 (2), 527.
Serene, J.W., 1989. Phys. Rev. B 40 (16), 10873.
Shi, H., Griffin, A., 1998. Phys. Rep. 304, 1.
Si, Q.M., Lu, J.P., Levin, K., 1992. Phys. Rev. B 45, 4930.
Si, Q.M., Zha, Y.Y., Levin, K., Lu, J.P., 1993. Phys. Rev. B 47 (14), 9055.
Sofo, J.O., Balseiro, C.A., 1992. Phys. Rev. B 45 (14), 8197.
Stajic, J., Chen, Q.J., Levin, K., 2005a. Phys. Rev. Lett. 94, 060401.
Stajic, J., Chen, Q.J., Levin, K., 2005b. Phys. Rev. A 71, 033601.
Stajic, J., Iyengar, A., Chen, Q.J., Levin, K., 2003a. Phys. Rev. B 68, 174517.
Stajic, J., Iyengar, A., Levin, K., Boyce, B.R., Lemberger, T.R., 2003b. Phys. Rev. B 68 (9), 024520.
Stajic, J., Milstein, J.N., Chen, Q.J., Chiofalo, M.L., Holland, M.J., Levin, K., 2004. Phys. Rev. A 69, 063610.
Strecker, K.E., Partridge, G.B., Hulet, R., 2003. Phys. Rev. Lett. 91 (8), 080406.
Stringari, S., 2004. Europhys. Lett. 65, 749.
Sutherland, M., Hawthorn, D.G., Hill, R.W., Ronning, F., Wakimoto, S., Zhang, H., Proust, C., Boaknin, E., Lupien, C., Taillefer, L., 2003. Phys. Rev. B 67 (17), 174520.
Tallon, J.L., Bernhard, C., Williams, G.V.M., Loram, J.W., 1997. Phys. Rev. Lett. 79, 5294.
Tallon, J.L., Loram, J.W., 2001. Physica C 349, 53.
Tan, S., Levin, K., 2004. Phys. Rev. B 69 (1), 064510(1).
Tchernyshyov, O., 1997. Phys. Rev. B 56 (6), 3372.
Tešanović, Z., 2004. Phys. Rev. Lett. 93, 217004.

Timmermans, E., Furuya, K., Milonni, P.W., Kerman, A.K., 2001. Phys. Lett. A 285, 228.
Timusk, T., Statt, B., 1999. Rep. Prog. Phys. 62 (20), 61.
Tranquada, J.M., Gehring, P.M., Shirane, G., Shamoto, S., Sato, M., 1992. Phys. Rev. B 46 (9), 5561.
Tsuei, C.C., Kirtley, J.R., Chi, C.C., Yu-Jahnes, L.S., Gupta, A., Shaw, T., Sun, J.Z., Ketchen, M.B., 1994. Phys. Rev. Lett. 73 (4), 593.
Tucker, J.R., Halperin, B.I., 1971. Phys. Rev. B 3 (1), 3768.
Uemura, Y.J., 1997. Physica C 194, 282–287.
Ussishkin, I., Sondhi, S., Huse, D., 2002. Phys. Rev. Lett. 89 (28), 287001.
Varma, C., 1999. Phys. Rev. Lett. 83 (17), 3538.
Vershinin, M., Misra, S., Ono, S., Abe, Y., Yoichi, A., Yazdani, A., 2004. Science 303, 1995.
Viverit, L., Giorgini, S., Pitaevskii, L.P., Stringari, S., 2004. Phys. Rev. A 69 (1), 013607.
Vojta, M., Zhang, Y., Sachdev, S., 2000. Phys. Rev. Lett. 85 (23), 4940.
Wang, Q.-H., Lee, D.-H., 2003. Phys. Rev. B 67 (2), 020511.
Wang, Y., Xu, Z.A., Kakeshita, T., Uchida, S., Ong, N.P., 2001. Phys. Rev. B 64 (22), 224519.
Watanabe, T., Fujii, T., Matsuda, A., 1997. Phys. Rev. Lett. 79 (11), 2113.
Wollman, D.A., Van, D.J., Harlingen, Giapintzakis, J., Ginsberg, D.M., 1995. Phys. Rev. Lett. 74 (5), 797.
Xu, Z., Ong, N., Want, Y., Kakeshita, T., Uchida, S., 2000. Nature 406 (5), 486.
Yanase, Y., Takanobu, J., Nomura, T., Ikeda, H., Hotta, T., Yamada, K., 2003. Phys. Rep. 387 (1–4), 1.
Zachar, O., Kivelson, S.A., Emery, V.J., 1997. J. Supercond. 10 (4), 373.
Zha, Y., Levin, K., Si, Q.M., 1993. Phys. Rev. B 47 (14), 9124.
Zhao, Y., Liu, H., Yang, G., Dou, S., 1993. J. Phys. Condens. Matter 5 (20), 3623.
Zwierlein, C.A., andStan, M.W., Schunck, C.H., Raupach, S.M.F., Gupta, S., Hadzibabic, Z., Ketterle, W., 2003. Phys. Rev. Lett. 91, 250401.
Zwierlein, M.W., Stan, C.A., Schunck, C.H., Raupach, S.M.F., Kerman, A.J., Ketterle, W., 2004. Phys. Rev. Lett. 92, 120403.